Journal of the Institute of Petroleum

VOL. 47 JUNE 1961 No. 450

CONTENTS

175 **Pre-flame Reactions in Diesel Engines. Part V. A Study of Temperature, Pressure, and Ignition Delay**
By F. H. Garner, O.B.E., Frank Morton, and J. B. Saunby

201 **Mechanism of Oxidation of Transformer Oils**
By V. Prabhashankar and D. J. Badkas

212 **A Laboratory-Scale High Efficiency Vacuum Fractionation Unit**
By A. A. Mohajer

219 **Foam Compounds for Use against Fires in Water Miscible Solvents**
By P. Nash and R. J. French

222 **Obituary: Robert Blythman Kerr, M.B.E.**

Abstracts 670–779

PRICE 10s 0D A COPY OR £4-14-6 YEARLY *POST FREE*

Published by the Institute of Petroleum 61 New Cavendish Street London W1

Printed in Great Britain by Richard Clay and Company Ltd Bungay Suffolk

COUNCIL AND OFFICERS, 1961–62

President

Julian M. Leonard, M.I.Chem.E.

Immediate Past-President

C. M. Vignoles, C.B.E., M.A.

Vice-Presidents

C. Chilvers, B.Sc., F.R.I.C.

J. S. Parker, M.A., B.Sc.

Members of Council

J. G. Annan, B.Sc.
W. S. Ault, B.A.
F. N. Beaumont, B.Sc.(Eng.), M.I.Mech.E., M.I.E.E.
G. Chandler, M.A.
J. M. Dougary, B.Sc., F.R.I.C., A.M.I.Chem.E.
A. J. Foster
T. F. Gaskell, M.A., Ph.D., F.R.A.S.
Sir Stephen Gibson, C.B.E., M.A., M.I.Mech.E.
R. H. W. Hamilton, M.A.
L. L. Hosking, B.E., M.I.C.E., A.M.N.Z.I.E.
M. E. Hubbard, B.A., M.I.Mech.E.
H. Hyams
W. E. Madden, A.R.S.M.
D. L. Samuel, B.Sc., A.R.I.C.
W. H. Thomas, A.R.S.M., F.R.I.C.

Representing the Branches Committee

J. H. M. Clark, T.D., A.C.A.
H. Kaye, B.Sc., A.M.I.Chem.E.
W. B. Peutherer, Ph.D., F.H-W.C., F.R.I.C.

Honorary Treasurer

O. F. Thompson, O.B.E.

Honorary Secretary

G. A. Dickins, B.Sc.(Hons.), F.R.I.C., M.Am.Chem.Soc.

Honorary Editor

E. B. Evans, M.Sc., Ph.D., F.R.I.C.

Honorary Associate Editor

D. L. Samuel, B.Sc., A.R.I.C.

General Secretary

D. A. Hough, T.D., F.I.A.C.

Editor

M. J. Wells

Honorary Secretaries of Branches

Bahrain Branch: M. B. Runeckles, P.O. Box 745, Awali, Bahrain, Persian Gulf.

Essex Branch: D. Rawlinson, F.R.I.C., c/o Shell Refining Co. Ltd., Shell Haven, Essex.

Fawley Branch: C. W. Banyard, B.Sc.(Eng.), c/o Esso Petroleum Co. Ltd., Fawley, Southampton.

Kuwait Branch: C. J. Edgerton, 4/10th Avenue, Ahmadi 1, Kuwait.

London Branch: D. M. Watson, Standard Vacuum Service & Supply Ltd., Africa House, Kingsway, London, W.C.2.

Northern Branch: H. Kaye, B.Sc., A.M.I.Chem.E., c/o Manchester Oil Refinery Ltd., Twining Road, Trafford Park, Manchester 17.

Scottish Branch: W. M. Stirling, A.H-W.C., A.M.I.E.E., Scottish Oils Ltd., Middleton Hall, Uphall, Broxburn, W. Lothian.

South-Eastern Branch: D. K. L. Morgan, B.Sc., c/o BP Refinery (Kent) Ltd., Isle of Grain, Rochester, Kent.

South Wales Branch: G. L. Jenkins, BP Refinery (Llandarcy) Ltd., Llandarcy, Glam.

Stanlow Branch: A. S. Brooman, B.Sc., 11 Grange Crescent, Hooton, Wirral, Cheshire.

Trinidad Branch: W. G. Poole, B.Sc., A.R.S.M., F.G.S., c/o Texaco Trinidad Inc., Forest Reserve, Fyzabad, Trinidad, B.W.I.

Yorkshire Branch: A. Furness, c/o J. W. Miller and Son Ltd., Hillside Oil Works, Brighouse, Yorks.

THE INSTITUTE OF PETROLEUM

AN Ordinary General Meeting of the Institute of Petroleum was held at 61 New Cavendish Street, London, W.1, on 4 January 1961, the Chair being taken by Julian M. Leonard, President of the Institute.

The General Secretary read the minutes of the previous meeting, which were confirmed and signed as a correct record.

The President then introduced Professor Frank Morton, who presented the following paper in summary.

PRE-FLAME REACTIONS IN DIESEL ENGINES

PART V. A STUDY OF TEMPERATURE, PRESSURE, AND IGNITION DELAY*

By F. H. GARNER,† O.B.E. (Fellow), FRANK MORTON‡ (Fellow), and J. B. SAUNBY§ (Associate Fellow)

SUMMARY

An electro-optical pyrometer has been used to measure the rapidly fluctuating temperatures occurring during combustion in a diesel engine. Simultaneous measurements of the variations of pressure have been made using a capacitance type pressure pick-up. The effect of compression ratio, injection timing, and fuel characteristics upon temperature and pressure variations throughout the firing stroke have been investigated. The temperature measurements show the occurrence of two distinct peaks in the temperature–time curve. The first rapid rise in temperature occurs immediately after ignition. The temperature then falls, rises to a second maximum, and thereafter gradually falls as the expansion stroke is entered. The intermediate fall in temperature is not accompanied by any measurable change in the rate of pressure rise, and varies markedly with variations in compression ratio, injection setting, and fuel characteristics. This fall in temperature is least apparent at operating conditions giving minimum delay periods.

A thermodynamic analysis of the pressure measurements has shown that the pre-flame energy release is constant for a given fuel. At high compression ratios this energy is derived mainly from the compression of the charge, the energy released by the fuel being directly proportional to the delay period.

INTRODUCTION

THE phenomena of ignition delay have been observed and studied since the diesel engine first assumed its role as one of the primary sources of power. That these studies have been helpful is shown by the constant improvements in efficiency and flexibility of diesel engines. Nevertheless, a complete understanding of the phenomena that occur during the ignition delay period has still to be achieved.[6] Studies of combustion reactions in spark ignition engines by a variety of methods have established that pre-flame oxidation reactions occur during the compression of the fuel–air mixture and in the "end gases" of the enflamed mixture, leading to pre-ignition and "knock" respectively, and that these reactions are affected by the chemical nature of the fuel as well as by the engine operating conditions. Similar studies of combustion in a diesel engine are complicated by the heterogenous nature of the fuel–air system following the start of injection of the fuel.

The reactions occurring during the ignition delay period in an operating engine have been examined by two different methods, namely:

1. Analysis of the reactants and products at varying stages during the cycle.
2. Thermodynamic analysis of the pressure and temperature variations occurring during the cycle to establish the energy released in the pre-flame period.

In the first method samples of gas are withdrawn from the engine chamber and analysed by chemical means. This method has been used by several workers, but limitations are imposed by the time required for the collection of samples. Unstable intermediates are liable to decompose before analysis can be completed, and it is extremely difficult to detect and measure small concentrations of organic peroxides.[1] When pre-flames occur they are often irregular in both intensity and duration,[2] and with sampling methods these cyclic variations cannot be taken into consideration. Spectrographic methods have been used to examine the reactants *in situ*. This method has been useful in the study of combustion in the spark-ignition engine, but it is not applicable to diesel combustion, the normal flame spectrum being

* MS received 31 August 1960.

† Department of Chemical Engineering, University of Birmingham.

‡ Department of Chemical Engineering, Manchester College of Science and Technology.

§ Now at Development Department, Union Carbide Chemicals Company, South Charleston, West Virginia, U.S.A.

COUNCIL AND OFFICERS, 1961–62

President
Julian M. Leonard, M.I.Chem.E.

Immediate Past-President
C. M. Vignoles, C.B.E., M.A.

Vice-Presidents
C. Chilvers, B.Sc., F.R.I.C. — J. S. Parker, M.A., B.Sc.

Members of Council

J. G. Annan, B.Sc.
W. S. Ault, B.A.
F. N. Beaumont, B.Sc.(Eng.), M.I.Mech.E., M.I.E.E.
G. Chandler, M.A.
J. M. Dougary, B.Sc., F.R.I.C., A.M.I.Chem.E.
A. J. Foster
T. F. Gaskell, M.A., Ph.D., F.R.A.S.
Sir Stephen Gibson, C.B.E., M.A., M.I.Mech.E.
R. H. W. Hamilton, M.A.
L. L. Hosking, B.E., M.I.C.E., A.M.N.Z.I.E.
M. E. Hubbard, B.A., M.I.Mech.E.
H. Hyams
W. E. Madden, A.R.S.M.
D. L. Samuel, B.Sc., A.R.I.C.
W. H. Thomas, A.R.S.M., F.R.I.C.

Representing the Branches Committee
J. H. M. Clark, T.D., A.C.A. — H. Kaye, B.Sc., A.M.I.Chem.E.
W. B. Peutherer, Ph.D., F.H-W.C., F.R.I.C.

Honorary Treasurer
O. F. Thompson, O.B.E.

Honorary Secretary
G. A. Dickins, B.Sc.(Hons.), F.R.I.C., M.Am.Chem.Soc.

Honorary Editor
E. B. Evans, M.Sc., Ph.D., F.R.I.C.

Honorary Associate Editor
D. L. Samuel, B.Sc., A.R.I.C.

General Secretary
D. A. Hough, T.D., F.I.A.C.

Editor
M. J. Wells

Honorary Secretaries of Branches

Bahrain Branch: M. B. Runeckles, P.O. Box 745, Awali, Bahrain, Persian Gulf.

Essex Branch: D. Rawlinson, F.R.I.C., c/o Shell Refining Co. Ltd., Shell Haven, Essex.

Fawley Branch: C. W. Banyard, B.Sc.(Eng.), c/o Esso Petroleum Co. Ltd., Fawley, Southampton.

Kuwait Branch: C. J. Edgerton, 4/10th Avenue, Ahmadi 3, Kuwait.

London Branch: D. M. Watson, Standard Vacuum Service & Supply Ltd., Africa House, Kingsway, London, W.C.2.

Northern Branch: H. Kaye, B.Sc., A.M.I.Chem.E., c/o Manchester Oil Refinery Ltd., Twining Road, Trafford Park, Manchester 17.

Scottish Branch: W. M. Stirling, A.H.W.C., A.M.I.E.E., Scottish Oils Ltd., Middleton Hall, Uphall, Broxburn, W. Lothian.

South-Eastern Branch: D. K. L. Morgan, B.Sc., c/o BP Refinery (Kent) Ltd., Isle of Grain, Rochester, Kent.

South Wales Branch: G. L. Jenkins, BP Refinery (Llandarcy) Ltd., Llandarcy, Glam.

Stanlow Branch: A. S. Broomhall, B.Sc., 11 Grange Crescent, Hooton, Wirral, Cheshire.

Trinidad Branch: W. G. Poole, B.Sc., A.R.S.M., F.G.S., c/o Texaco Trinidad Inc., Forest Reserve, Fyzabad, Trinidad, B.W.I.

Yorkshire Branch: A. Furness, c/o J. W. Miller and Son Ltd., Hillside Oil Works, Brighouse, Yorks.

VOL. 47 NO. 450 JUNE 1961

THE INSTITUTE OF PETROLEUM

AN Ordinary General Meeting of the Institute of Petroleum was held at 61 New Cavendish Street, London, W.1, on 4 January 1961, the Chair being taken by Julian M. Leonard, President of the Institute.

The General Secretary read the minutes of the previous meeting, which were confirmed and signed as a correct record.

The President then introduced Professor Frank Morton, who presented the following paper in summary.

PRE-FLAME REACTIONS IN DIESEL ENGINES

PART V. A STUDY OF TEMPERATURE, PRESSURE, AND IGNITION DELAY*

By F. H. GARNER,† O.B.E. (Fellow), FRANK MORTON‡ (Fellow), and J. B. SAUNBY§ (Associate Fellow)

SUMMARY

An electro-optical pyrometer has been used to measure the rapidly fluctuating temperatures occurring during combustion in a diesel engine. Simultaneous measurements of the variations of pressure have been made using a capacitance type pressure pick-up. The effect of compression ratio, injection timing, and fuel characteristics upon temperature and pressure variations throughout the firing stroke have been investigated. The temperature measurements show the occurrence of two distinct peaks in the temperature–time curve. The first rapid rise in temperature occurs immediately after ignition. The temperature then falls, rises to a second maximum, and thereafter gradually falls as the expansion stroke is entered. The intermediate fall in temperature is not accompanied by any measurable change in the rate of pressure rise, and varies markedly with variations in compression ratio, injection setting, and fuel characteristics. This fall in temperature is least apparent at operating conditions giving minimum delay periods.

A thermodynamic analysis of the pressure measurements has shown that the pre-flame energy release is constant for a given fuel. At high compression ratios this energy is derived mainly from the compression of the charge, the energy released by the fuel being directly proportional to the delay period.

INTRODUCTION

THE phenomena of ignition delay have been observed and studied since the diesel engine first assumed its role as one of the primary sources of power. That these studies have been helpful is shown by the constant improvements in efficiency and flexibility of diesel engines. Nevertheless, a complete understanding of the phenomena that occur during the ignition delay period has still to be achieved.[6] Studies of combustion reactions in spark ignition engines by a variety of methods have established that pre-flame oxidation reactions occur during the compression of the fuel–air mixture and in the "end gases" of the enflamed mixture, leading to pre-ignition and "knock" respectively, and that these reactions are affected by the chemical nature of the fuel as well as by the engine operating conditions. Similar studies of combustion in a diesel engine are complicated by the heterogenous nature of the fuel–air system following the start of injection of the fuel.

The reactions occurring during the ignition delay period in an operating engine have been examined by two different methods, namely:

1. Analysis of the reactants and products at varying stages during the cycle.
2. Thermodynamic analysis of the pressure and temperature variations occurring during the cycle to establish the energy released in the pre-flame period.

In the first method samples of gas are withdrawn from the engine chamber and analysed by chemical means. This method has been used by several workers, but limitations are imposed by the time required for the collection of samples. Unstable intermediates are liable to decompose before analysis can be completed, and it is extremely difficult to detect and measure small concentrations of organic peroxides.[1] When pre-flames occur they are often irregular in both intensity and duration,[2] and with sampling methods these cyclic variations cannot be taken into consideration. Spectrographic methods have been used to examine the reactants *in situ*. This method has been useful in the study of combustion in the spark-ignition engine, but it is not applicable to diesel combustion, the normal flame spectrum being

* MS received 31 August 1960.

† Department of Chemical Engineering, University of Birmingham.

‡ Department of Chemical Engineering, Manchester College of Science and Technology.

§ Now at Development Department, Union Carbide Chemicals Company, South Charleston, West Virginia, U.S.A.

obscured by continuous radiation from incandescent carbon particles.[3]

Pressure and temperature measurements in firing and motoring engines have been used to give some insight into the pre-combustion reactions, and this method seems to offer a more rigorous solution to the problem.[4-6]

The effect of compression ratio on pre-flame reactions in a diesel engine was investigated in previous work.[2] The nature of the delay period and the effect of temperature and pressure on ignition lag were examined and compared with results obtained on rapid compression machines. Using a photomultiplier unit, pre-flames of varying intensity and duration were observed, mainly at high compression ratios and early injection settings. In the absence of temperature measurements, the exact nature of the pre-flames and their effect upon the ignition temperature could not be determined.

In order to clarify this point an attempt was made to determine flame temperatures in a firing diesel cycle using a spectral line reversal method. Despite the use of a high candlepower source and the addition of sodium to the flame, insufficient light was received by the spectrometer to permit flame temperatures to be calculated. Apparently the light was absorbed not only by carbon particles in the combustion chamber but also by the fuel droplets present and the carbon deposited on the inspection window, the combined effect allowing insufficient radiation from the source to be received by the spectrometer.[7]

Further study was then made of methods depending solely on the emission from the flame, and these have led to the development of a two-colour optical pyrometer capable of recording rapidly fluctuating temperatures. This has been used to study the variation in temperature throughout the firing cycle using two fuels of different cetane number at a variety of injection settings and compression ratios. Because the diesel engine is particularly susceptible to cyclic variations, pressure records were obtained simultaneously with the temperature records, a capacitance type pressure pick-up being used to give direct pressure–time records.

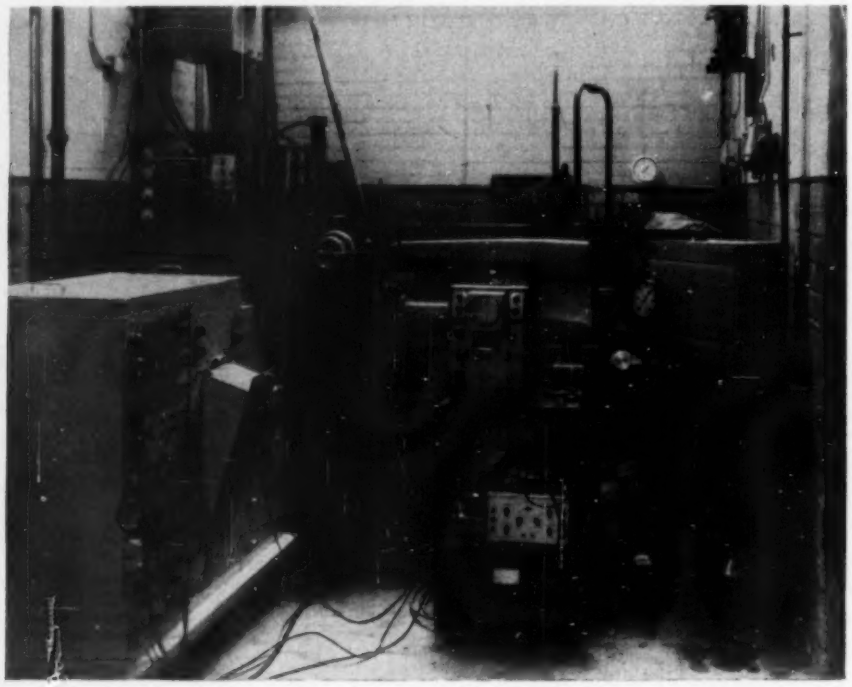

Fig 1

CFR–ASTM ENGINE WITH ANCILLARY EQUIPMENT

DESCRIPTION OF ENGINE AND INSTRUMENTATION

The engine used in this work was the standard CFR–ASTM diesel testing unit fitted with ancillary equipment for the measurement of temperature and pressure, illustrated in Fig 1. Except where otherwise stated, the engine was operated under the recommended operating conditions described previously.[2]

Initially a Standard–Sunbury time sweep and degree marker unit coupled to the engine crankshaft triggered the time base of a Cossor double beam oscilloscope and supplied the signal for the horizontal degree scale on one of the two beams. Standard–Sunbury equipment was also used to measure the point of injection, an electro-magnetic pick-up being fitted to the injector. In order that three traces could be displayed on the oscilloscope simultaneously,

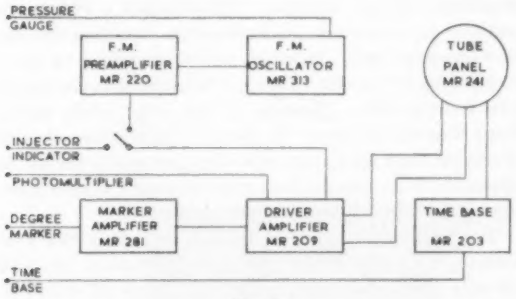

FIG 2

BLOCK DIAGRAM OF ELECTRICAL CIRCUIT

a Furzehill type S–500 beam switch was introduced before the input to the A1 amplifier of the oscilloscope, the A2 circuit being used for the display and triggering of the time base. With the switching frequency set at its fastest rate of 3500 cycles/sec, a satisfactory trace was obtained on the oscilloscope when using all the required time base frequencies.

Subsequent work using a capacitance type pressure pick-up necessitated the use of a direct coupled amplifier in conjunction with the oscilloscope. A Southern Instruments engine indicator was used for this purpose. This had available a frequency modulated pre-amplifier and oscillator, for use with the capacitance type pressure pick-up, and a driver amplifier, direct coupled with stepped sensitivity and direct shift with a maximum gain of 800 times.

The output from the degree marker unit was fed to a marker amplifier which converted the signal into a sharp pulse to define accurately the crank angle degrees. Using the Standard–Sunbury marker unit, a pulse was obtained every two degrees and top dead centre was defined by removing the preceding pulse. As the time base could be superimposed on either of the two oscilloscope traces without interfering with the shape of the trace, two beams were adequate. Each beam had independent brightness and focusing controls. The time base was triggered by contacts on the engine crankshaft. A block diagram of the electrical circuit is shown in Fig 2.

The variations in temperature and pressure during the engine cycle were recorded photographically using a drum camera. The drum speed was adjusted so that at least one complete engine cycle was recorded on the film, the exposure being made by rapidly switching the oscilloscope beams on and off with the drum rotating, the beams being deflected in a vertical direction only.

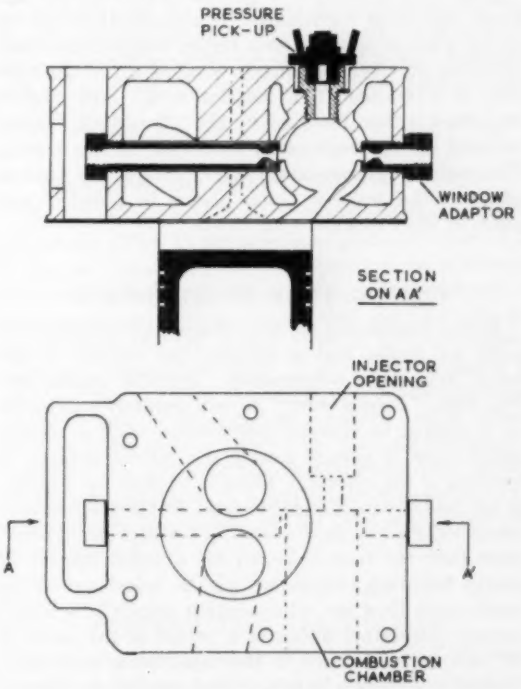

FIG 3

DIAGRAMMATIC REPRESENTATION OF CFR CYLINDER HEAD

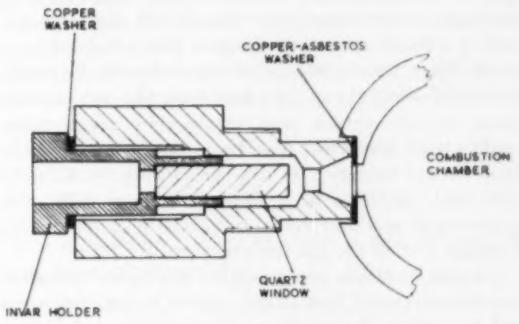

FIG 4

WINDOW HOLDER AND ADAPTOR

To enable the possibility of using spectral absorption methods to be investigated, windows opposite each other were fitted in the combustion chamber, as shown in Fig 3. The flat quartz windows used in previous work did not keep sufficiently clear with continuous operation in these positions. This was overcome by using the windows and window holders shown in Fig 4. The window holder was made of

"Invar" high nickel steel, which has approximately the same coefficient of expansion as quartz. This is necessary to prevent breaking of the glycerine and litharge cement used to hold the window in the holder.

This type of window kept clear under all but the worst operating conditions. It appears that the tip of the window operates at a higher temperature than with the previous flat quartz window, since the heat flow is restricted to a smaller area. Soft carbon deposited is then removed by the "breathing" effect induced by the restriction machined in the holder. The engine was warmed up with a plug in the window adaptor, the window being placed in position just prior to observations being made.

TEMPERATURE MEASUREMENT

Before considering methods of temperature measurement for flames and in engines, the validity of the term "true flame temperature" must be established. The term "temperature" is only properly applicable to a system in thermal equilibrium with a certain distribution of energy among the various degrees of freedom of the system. There is no such equilibrium in the case of flames or explosions. At the temperature levels attained in these cases, Hottel and Broughton[8] state that the time required for a redistribution of energy following combustion may be calculated on the assumption that the equipartition principle is valid. Such a calculation indicates a period of the order of 10^{-7} sec. The fraction of the total flame body containing molecules which have had insufficient time to allow redistribution of energy to take place is therefore exceedingly small. Temperature, therefore, as applied to a flame may be used with a high degree of exactness as to its meaning. Practically, the temperature of a flame may be defined as that attained by a small object, large compared to the molecular diameter, but small enough to acquire heat from the surrounding gases by convection and conduction much more readily than it can lose heat by radiation through the flame to the outside. It has been shown by Schack[9] that soot particles in a luminous flame fulfil this requirement and that the temperature of such particles is within 1° C of the gas temperature.

Various methods are available for flame temperature measurement, but all are subject to both practical and theoretical limitations. The choice of the most convenient and reliable method is often a compromise, and depends largely on the type of flame being studied. Optical methods are best suited to engine flame temperature measurement, and these methods are advantageous in that they do not disturb the hot gas. Point temperatures cannot be determined, an average value for the temperature in the optical path being obtained.

Preliminary investigations showed that any satisfactory method for measuring flame temperatures during diesel combustion must depend on emission from the flame. Attempts to use a modified spectral line reversal technique, in which the absorption of light from a continuous spectral source by the hot gases is measured, were not successful. Insufficient light was transmitted through the flame, even with a 1000 candlepower tungsten arc source.

Methods based on the emission from the engine flame at a single wavelength were also unsuitable because of the random manner in which carbon was deposited on the window. This caused a change in window transmission characteristics between successive observations. It was decided, therefore, to use a method based on the relative intensity of radiation at two wavelengths. Because of the large cyclic variations known to occur in diesel combustion, it was desirable that these two radiation intensity traces be available from one engine cycle, together with a pressure record for the same cycle.

To eliminate any uncertainty regarding the performance of amplifiers, etc., the radiation at both wavelengths was received by the same photomultiplier. As this was known to have a peak spectral response at about 4000 Å, it was first calibrated as follows: Light from a tungsten arc lamp was focused on the entrance slit of a Hilger D246 spectrometer. With the photomultiplier replacing the normal spectrometer eyepiece, the deflection at known wavelength intervals was measured on the oscilloscope. The characteristics of the source correspond to the emission of tungsten and from a knowledge of the variation of spectral emissivity of tungsten with wavelength and the operating temperature of the lamp, the intensity of radiation at any wavelength can be calculated from Wien's Law

$$I_\lambda = C_1 A \lambda^{-5} E_\lambda e^{-\frac{C_2}{\lambda T}} \quad . \quad . \quad . \quad . \quad (1)$$

where I_λ = intensity at wavelength λ, C_1 = first radiation constant, A = area of source, E_λ = spectral emissivity of the radiating body at wavelength λ, C_2 = second radiation constant, T = true absolute temperature of radiating body. Maker's information gave the lamp temperature as 2950° K and the variation of spectral emissivity with wavelength for tungsten has been reported recently by de Vos.[10]

As only the relative intensity at any wavelength is required, Wien's Law can be used in the comparative form,

$$\frac{I_{\lambda_1}}{I_{\lambda_2}} = \frac{(\lambda_2)^5}{(\lambda_1)^5} \cdot \frac{E_{\lambda_1}}{E_{\lambda_2}} e^{-\frac{C_2}{T}\left(\frac{1}{\lambda_1} - \frac{1}{\lambda_2}\right)} \quad . \quad . \quad (2)$$

Assuming the intensity at 3000 Å to be one unit, values were obtained for the intensity at the required wavelengths. Putting the oscilloscope deflection at 3000 Å, also equal to one unit, enabled a correction curve to be constructed.

The pyrometer used in this work is shown in Fig 5.

Light from the combustion chamber was focused on the entrance slit S_1 of a Hilger E498 wide dispersion glass prism spectrometer. Two slits, S_2 and S_3, received light at about 5000 Å and 6000 Å and were of such a width that a wavelength range of 50 Å was

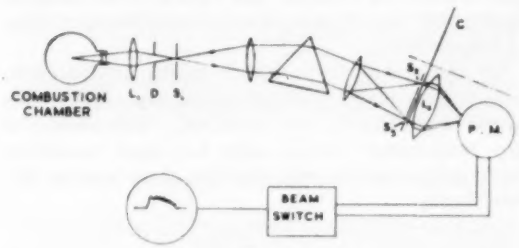

FIG 5

SCHEMATIC LAYOUT OF APPARATUS

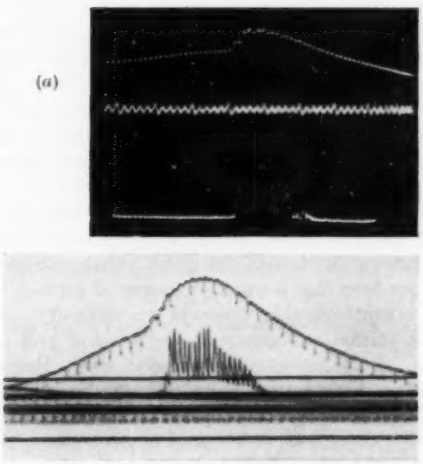

FIG 6

(*a*) TRACE OBTAINED USING BEAM SWITCH
(*b*) TRACE OBTAINED USING SOUTHERN INSTRUMENTS OSCILLOSCOPE
(*c*) ENVELOPES CONSTRUCTED FROM (*b*)

allowed to pass. The light from these slits was then interrupted alternately by a mechanical chopper, C, consisting of a disk with 60 radial slots driven through a 2 : 1 pulley arrangement by a balanced armature motor. The chopping frequency was about 10,000 cycles/sec. The light from each slit, when not interrupted by the chopper, was focused on to the photomultiplier, $P.M.$, by the lens L_2. The output from the photomultiplier was fed, initially, through a beam switch to the Cossor double beam oscilloscope, and in the later work directly to the driver amplifier of the Southern Instruments oscilloscope unit. Typical records obtained are shown in Fig 6 (*a*), using the beam switch, and Fig 6 (*b*), the Southern Instruments apparatus.

LOCATION OF SPECTROSCOPIC SLITS

These were initially located visually at the mercury yellow line (5780 Å) and a sodium green line (4985 Å). Following adjustments to the apparatus, the positions were checked using the Hilger D246 spectrometer as a monochromator. It was found that the slits were in fact located at 5970 Å and 5100 Å, the first transmitting a wavelength range of 70 Å and the latter a range of 50 Å. This resolution was considered adequate in view of the constant emissivity from diesel flames established by Lyn,[3] over this range of wavelength. The width of the entrance slit was varied during the investigation, being widest when carbon was deposited on the window, but for most of the work the width was 0·125 mm.

TEMPERATURE CALCULATION

From the oscillographs (Figs 6 (*a*) and (*b*)) two envelopes can be constructed as shown in Fig 6 (*c*), the top one, d_1, corresponding to the radiation intensity at 5970 Å (λ_1) and the lower one, d_2, to the radiation intensity at 5100 Å (λ_2). These deflections must be corrected for the non-linear response of the photomultiplier by the use of correction factors. Application of Wien's Law to these two relative deflections enables the temperature at any point to be determined as follows:

Applying Wien's Law and assuming $E_{\lambda_1} = E_{\lambda_2}$

$$\frac{I_{\lambda_1}}{I_{\lambda_2}} = \frac{(\lambda_2)^5}{(\lambda_1)^5}\, e^{-\frac{C_2}{T}\left(\frac{1}{\lambda_1}-\frac{1}{\lambda_2}\right)} \quad . \quad . \quad . \quad (3)$$

The correction factors at 5100 Å are 2·5 and 4·0 respectively; therefore

$$\frac{d_1 \,.\, 4{\cdot}0}{d_2 \,.\, 2{\cdot}5} = \frac{I_{\lambda_1}}{I_{\lambda_2}} \quad . \quad . \quad . \quad . \quad (4)$$

The value of the second radiation constant, C_2, is given by DuMond and Cohen [17] as 1·438 cm ° K.

$$\text{Hence, } \frac{d_2 \times 0{\cdot}625}{d_1} = \left(\frac{5970}{5100}\right)^5 \times e^{-\frac{1{\cdot}438}{T}\left(\frac{10^8}{5{\cdot}100}-\frac{10^8}{5{\cdot}970}\right)}$$

This reduces to

$$T = \frac{2005}{0{\cdot}3404 - \log_{10}\dfrac{d_2 \times 0{\cdot}625}{d_1}}$$

The temperature for any ratio of $\frac{d_2}{d_1}$ can then be obtained from a plot of $\frac{1}{T}$ *v.* $\log_{10}\frac{d_2}{d_1}$, allowance being made in the plot for the correction factors. This plot is shown in Fig 7.

The accuracy of the pyrometer was determined using a " Pointlite " source which operates at a known temperature. The emissivity at the two wavelengths is also known. With this source the maximum spread in the readings did not exceed 50° K, an error

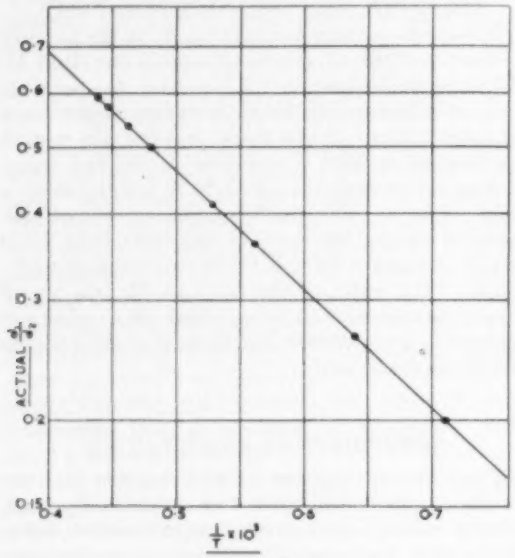

FIG 7
THEORETICAL PLOT

of 1·4 per cent. This was attributable in part to the thickness of the oscilloscope trace, which made exact visual reading difficult.

Consistent results were obtained using the pyrometer to measure the temperature of a diesel fuel diffusion flame. The absolute accuracy of these results could not however be checked with the apparatus available.

LIMITATIONS OF TEMPERATURE MEASUREMENTS

This method of temperature measurement depends upon radiation from the combustion chamber and so necessarily records an average temperature. This is the average temperature over all the degrees of freedom of the gas and can be influenced by any cool regions through which the radiation passes. It is also the temperature of that part of the gas which lies in the optical path of the window in the combustion chamber and is focused on the spectrometer slit.

The receiving slits of the pyrometer are located at 5100 Å and 5970 Å, which means that only radiation from hot flames is transmitted. The absence of pre-flames on the temperature records does not mean that they do not occur. If they do occur then they do not emit continuous radiation and radiate at wavelengths below 5100 Å. It is known that cool flames radiate at about 4000 Å.

In previous work[2] a photomultiplier unit had been used to measure total radiation intensity. Pre-flames of varying intensity were observed. The absence of any temperature traces under the same conditions using the pyrometer indicates that these were in fact cool flames.

SCALING ACCURACY

The measurement of deflections at the two wavelengths can be a source of error in the temperature determinations. The thickness of the trace on the oscillogram should be as fine as possible. This is controlled by the size of the oscilloscope beam, which is in turn controlled by the brightness required. Although high-speed blue-sensitive recording paper was used in the drum camera, the high drum speeds required to give adequate resolution with an engine speed of 900 rev/min needed a relatively high intensity beam, which led to rather coarse traces being obtained.

The determination of the exact position of the temperature base line is another source of error. Under good conditions this presents no difficulty. When carbon formation occurs on the window and a high degree of amplification is needed from the driver amplifier, background light pick-up by the photomultiplier and the microphonic effect of engine noise on the photomultiplier causes a broadening of the temperature base line. Although this does not cause any appreciable error when large oscilloscope deflections occur, when it is allied with small deflections, under three or four millimetres on the oscillogram, it can lead to serious errors. The possibility of inaccuracies in measurement also increases where rapid vertical deflections occur, giving rise to steep slopes.

Most of the scaling errors arise when high amplification is required because of carbon formation on the window. Under normal conditions, when large oscilloscope deflections occur, scaling errors are negligible.

REPEATABILITY

Fig 8 (*a*) shows three successive engine cycles recorded on a single drum camera record. In each case a similar temperature trace is obtained, the start of combustion occurring at −13° CA. The peak pressure varies by less than 5 psi and the pressure at the start of visible radiation is constant at 565 psia.

Temperatures calculated from the three diagrams are plotted against crank angle in Fig 8 (*b*). In each

case the rise of temperature is the same and the first peak occurs at −1° CA. Following the slight fall in temperature at about +3° CA there is another peak, and in this later stage some divergence between the three curves occurs. This is attributable in part to the difficulty of measuring the small deflections which occur later in the cycle.

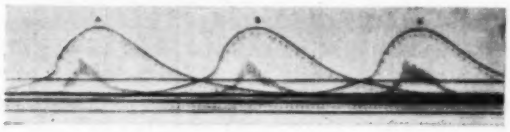

FIG 8 (*a*)
RECORD OF THREE SUCCESSIVE ENGINE CYCLES

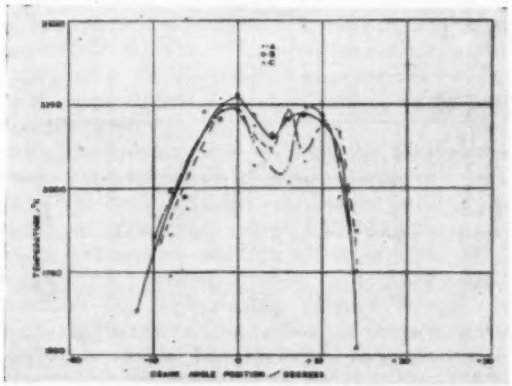

FIG 8 (*b*)
TEMPERATURE TRACES FROM THREE SUCCESSIVE ENGINE CYCLES

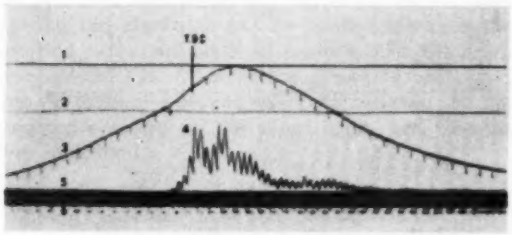

FIG 9
TYPICAL DRUM CAMERA RECORD

Traces 1 and 2	Pressure calibration lines
,, 3	Pressure
,, 4	Temperature
,, 5	Temperature base line
,, 6	Pressure base line

PRESSURE MEASUREMENTS

A Southern Instruments capacitance type pressure pick-up was used, together with the necessary oscillator and direct coupled frequency modulated amplifier. The pick-up was a G204 water-cooled unit with a nominal range of 0–2000 psi, with an incremental capacitance of 20 pf for this pressure range. The maximum working temperature was 300° C, with a temperature coefficient of 1 per cent of sensitivity per 20° C rise. Being direct coupled, the pick-up could be calibrated in a static test rig prior to use in the engine. Pressure calibration lines were then superimposed on each drum camera record after the engine pressure diagram had been obtained.

EXPERIMENTAL RESULTS

Temperature and Pressure Measurements

Experiments were carried out at the standard fuel rate of 13·0 ml/min with two fuels, D_1, cetane number 70, and D_6, cetane number 32. (Inspection data for these fuels has been reported.[1, 2]) The operating variables were injection timing and compression ratio. Injection timing was varied between −10° and −35° CA with fuel D_1, but it was only possible to cover the range −10° to −20° CA with fuel D_6, because of heavy knock at earlier settings. Compression ratio was nominally continuously variable between 10 : 1 and 30 : 1, but this range was also limited at lower values by knock.

A typical drum camera record obtained using the two-colour pyrometer and capacitance type pressure pick-up is shown in Fig 9. In this diagram traces 1 and 2 are pressure calibration lines. These were placed at a known pressure, usually 400 psi, apart and hence the pressure per centimetre of deflection on the oscillogram can be determined. Trace 3 is the pressure record with timing marks superimposed every two degrees crank angle, top dead centre being identified by the preceding gap. Trace 4 is the temperature record, the envelope obtained by joining the upper points being the radiation intensity at 5970 Å and that by joining the lower points the radiation intensity at 5100 Å. Trace 5 is the base line for temperature measurements and corresponds to zero radiation. Trace 6 is the pressure datum and corresponds to atmospheric pressure.

Pressure and temperature variations in the engine were recorded for a wide range of injection settings and compression ratios for both fuels.[7] A study of these results indicated certain definite trends, which are illustrated in the present communication by consideration of the following selected series of experiments:

1. Fuels D_1 and D_6 at an injection setting of −15° CA with varying compression ratio;
2. Fuel D_1 at constant compression ratio of 20 : 1 with varying injection setting;
3. Fuel D_1 at an injection setting of −30° CA with varying compression ratio;
4. Fuels D_1 and D_6 at constant compression ratio 20 : 1 with varying injection settings.

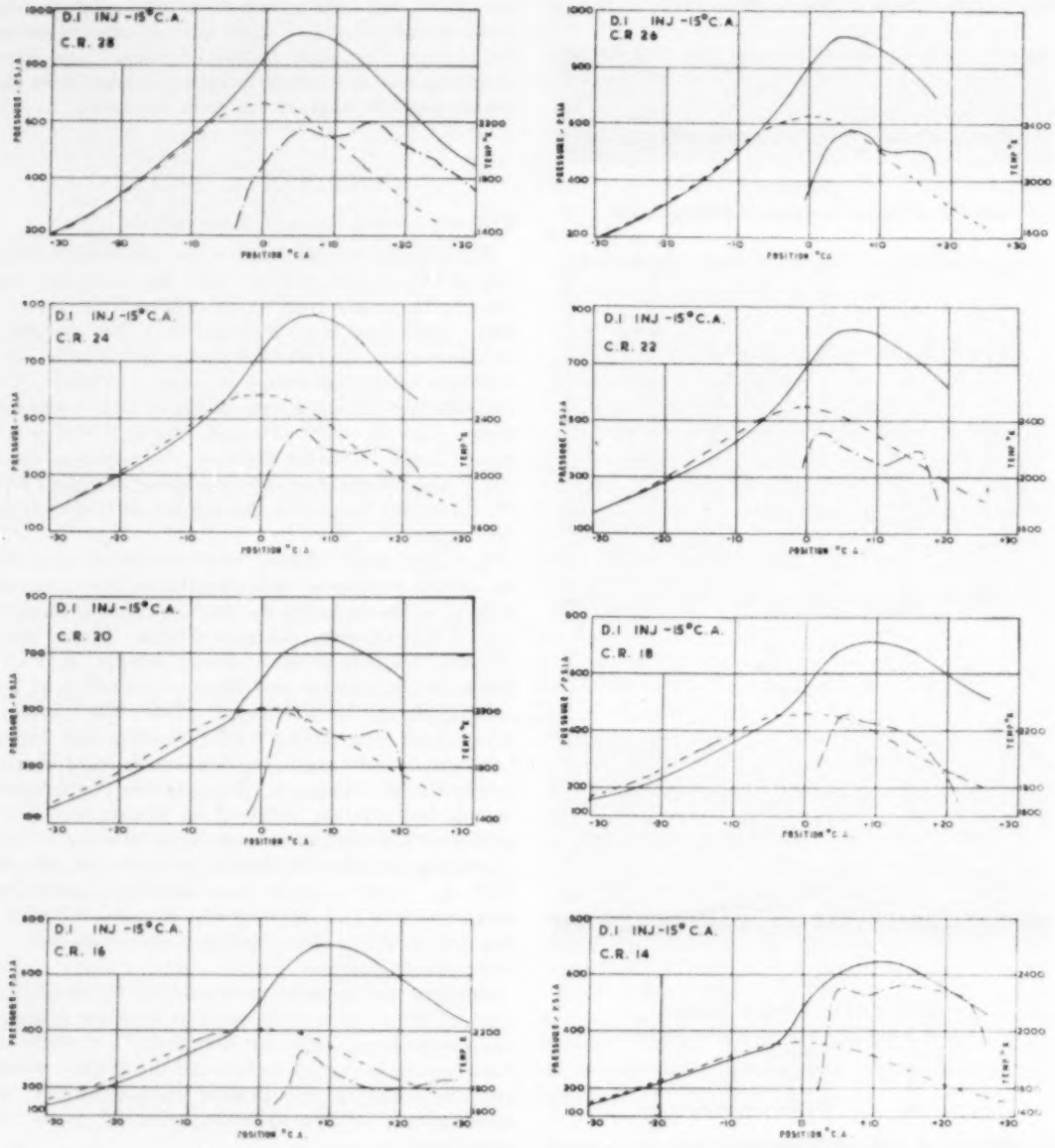

FIGS 10–17

PRESSURE AND TEMPERATURE RECORDS

CR from 28 : 1 to 14 : 1

———— Engine pressure firing - - - - - - Engine pressure motoring —·—·—·— Temperature, ° K

Fuel D_1, Injection −15° CA, Varying Compression Ratio

Figs 10–17 show the observed temperatures and pressures at compression ratios from 28 : 1 to 14 : 1. Also shown is a motoring pressure record obtained at the same compression ratio and the same inlet air temperature.

The mean flame temperature at all compression ratios is about 2200° K with a peak temperature of nearly 2350° K. As the compression ratio is lowered, the rate of temperature rise increases. At a compression ratio of 28 : 1 the rate of temperature rise, calculated from the start of visible radiation to the first temperature peak, is about 60° K/° CA, at a compression ratio of 20 : 1 it is 125°K/°CA, while at 14 : 1 it has risen to 350° K/° CA. This accounts for the engine running hot at the lower compression ratios, the rapid rate of temperature rise allowing less time for the heat to be dissipated.

At a compression ratio of 28 : 1 the temperature rises to a steady value with some evidence of a peak late in the cycle. As the compression ratio is decreased an initial peak occurs, followed by a slight drop in temperature and then a further peak. This may be a true temperature effect, but it is not accompanied by any corresponding pressure change. It may be due to two successive flame fronts passing the observation window, but this will be considered later.

The motoring pressure curves would be expected to follow the firing pressure curves before reactions take place. The vertical displacement which is apparent in some cases is due to a difference in engine temperature between the firing and motoring cycles. An approximate allowance can be made for this if the motoring curves are made to coincide with the firing cycle at −30° CA. Combustion pressures, calculated from the difference between the peak pressure and the motoring pressure at the same point, are then as given in Table I.

TABLE I

Effect of Compression Ratio upon Maximum Combustion Pressure and Maximum Temperature

(Fuel D_1, Injection Setting −15° CA)

Compression ratio	Peak pressure, psi	Compression pressure, psi	Maximum combustion pressure, psi	Maximum temp, °K
28	915	655	260	2200
26	905	615	290	2340
24	863	593	270	2330
22	820	510	310	2320
20	755	445	310	2250
18	715	415	300	2300
16	704	370	334	1960
14	650	320	330	2330

The maximum combustion pressure does not vary greatly, but shows a slight increase as the compression ratio is lowered. The rate of pressure rise increases as the compression ratio is decreased, corresponding to a similar temperature effect.

The low value for the maximum temperature at a compression ratio of 16 : 1 is thought to be due to experimental error.

Fuel D_6, Injection −15° CA, Varying Compression Ratio

The results for fuel D_6 are given in Figs 18–24. The temperature records show two distinct peaks, the first occurring 3° to 4° CA after the onset of visible radiation and the second 6° to 8° CA after the first. Between these peaks there is an apparent drop in temperature of 100° to 150° K. No corresponding pressure fluctuation occurs. The temperatures are lower than those observed with fuel D_1, being in the range 1700° to 1800° K at the higher compression ratios and rising to 2100° to 2200° K at compression ratios 20 : 1 and 18 : 1. The rate of temperature rise and the rate of pressure rise is greater with fuel D_6 than at the corresponding settings with fuel D_1.

Longer ignition delay periods cause the peak pressure to occur later in the cycle, the maximum combustion pressure being greater than with fuel D_1.

Fuel D_1, Injection −30° CA, Varying Compression Ratio

Figs 25–32 show the results obtained with fuel D_1 at compression ratios from 30 : 1 to 14 : 1 with ignition at −30° CA.

The phenomena observed with fuel D_6 at an injection timing of −15° CA of two temperature peaks is even more pronounced with fuel D_1 under these conditions. At the higher compression ratios the two peaks are well separated with a temperature drop of nearly 400° K between. No corresponding pressure fluctuation occurs. Neither of the peaks nor the large drop in temperature coincide with the peak pressure difference between the motoring and firing curves. As the compression ratio is lowered the temperature drop, after a first peak temperature, becomes less distinct and after a compression ratio of 20 : 1 is no more apparent than at an injection setting of −15° CA with the same fuel. The maximum temperature, as with the later injection setting of −15° CA, is in the range 2200° to 2300° K.

At compression ratios above 24 : 1 where two peaks occur, a high rate of temperature rise of 130° K/CA occurs. This falls to a minimum of 60° K/°CA at a compression ratio of 20 : 1, again increases as the compression ratio is lowered, and is 200° K/°CA at 14 : 1.

The motoring pressure curves do not coincide with the firing curves, in this case lying below them. This is due to the high operating temperature at this early injection setting. Higher combustion pressures also occur, and the rate of pressure rise is considerably

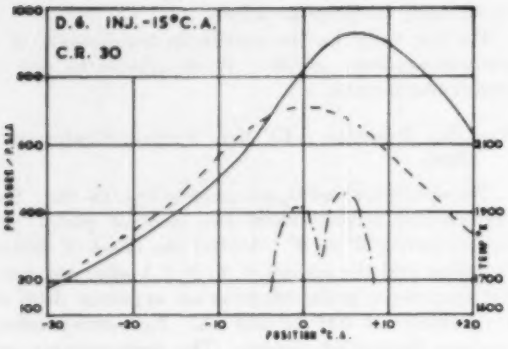

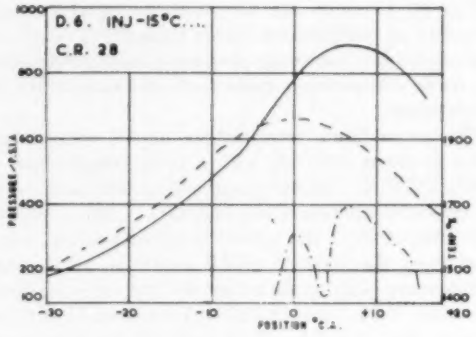

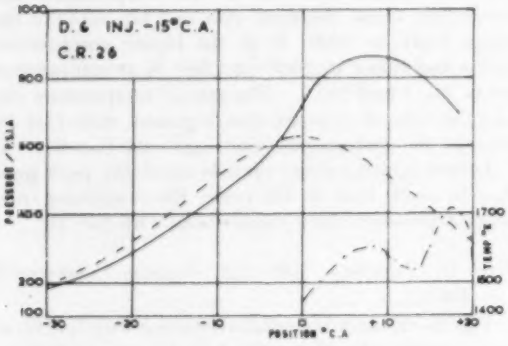

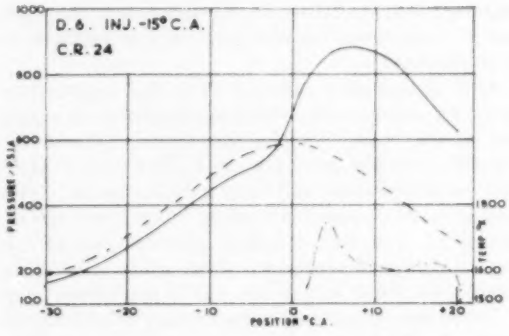

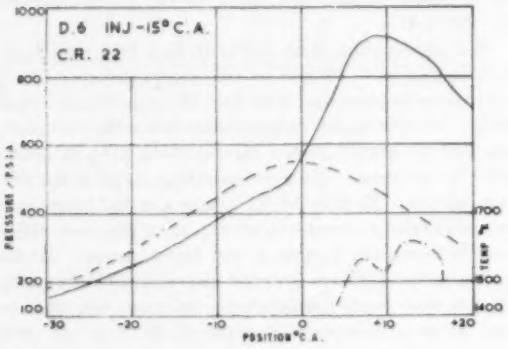

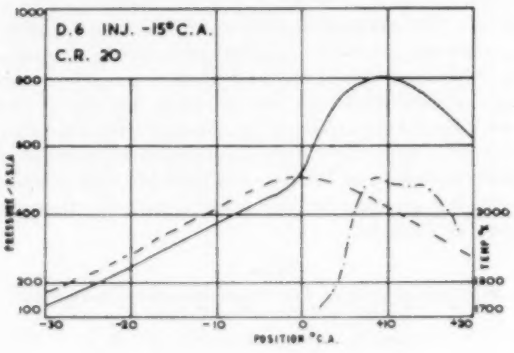

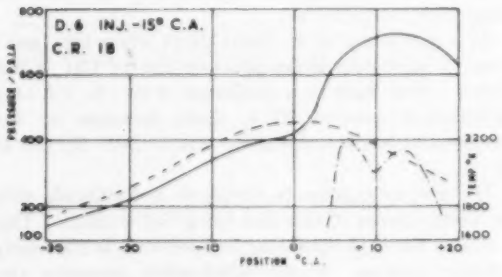

FIGS 18–24

PRESSURE AND TEMPERATURE RECORDS

CR from 30 : 1 to 18 : 1

——— Engine pressure firing

– – – – – – – Engine pressure motoring

—·—·—·— Temperature, ° K

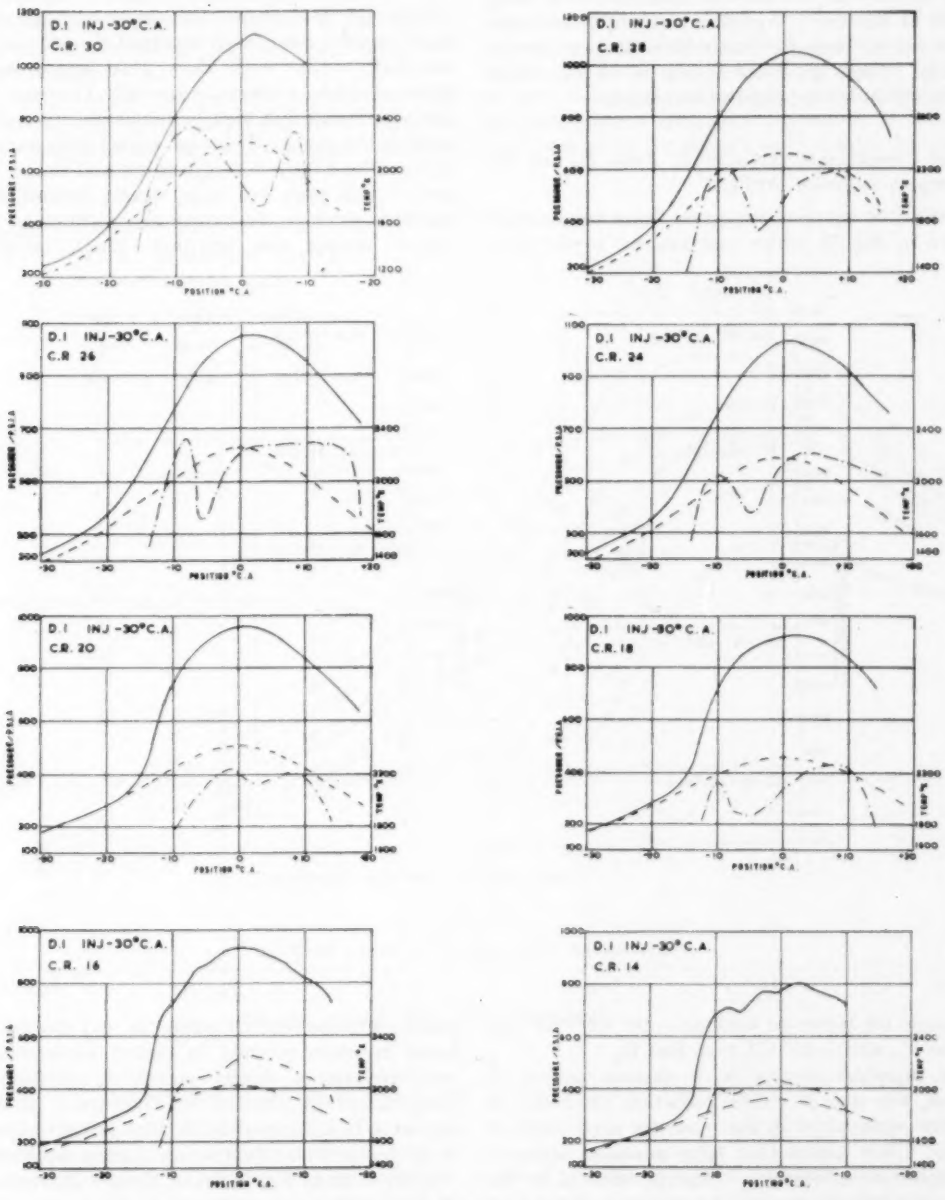

FIGS 25–32

PRESSURE AND TEMPERATURE RECORDS

CR from 30 : 1 to 14 : 1

———— Engine pressure firing — — — — Engine pressure motoring —·—·—·— Temperature, ° K

higher than with the same fuel and later injection. The oscillograms from which the pressure curves in Figs 29–32 were derived show the marked knock which occurred at this early injection with the lower compression ratios, pressure fluctuations of over 100 psi occurring. There does not appear to be any corresponding effect on the temperature record.

Constant Compression Ratio 20 : 1, Fuels D_1 and D_6, Varying Injection Settings

The effect of injection timing on flame temperature is shown in Fig 33, where temperature is plotted *v.* crank angle for injection settings −10° to −35° CA with fuel D_1, and −15° CA with fuel D_6.

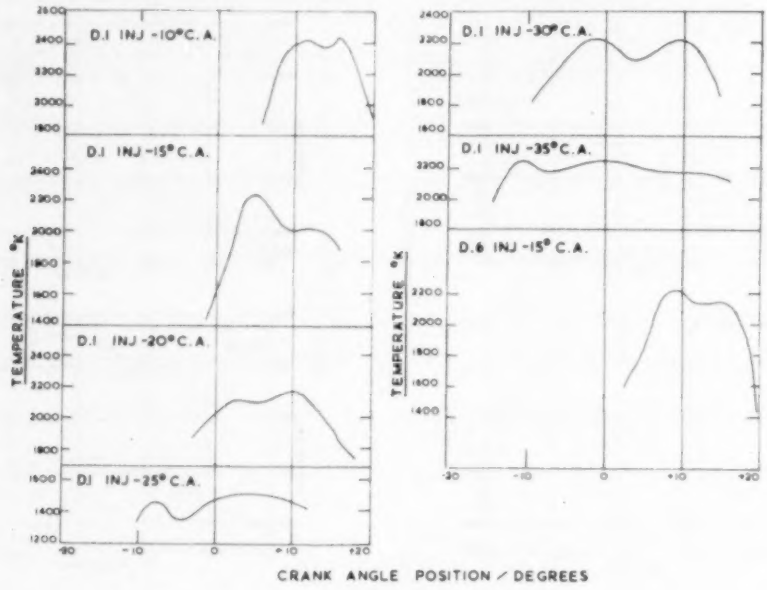

FIG 33

TEMPERATURE VARIATION AT CONSTANT CR 20 : 1

Later injection results in a shorter period of radiation, the end of visible radiation occurring at nearly the same point in the cycle for each point of injection. This means that later injection causes a more rapid rate of burning. This is reflected in the maximum temperature, which decreases from over 2400° K at an injection timing of −10° CA with fuel D_1 to under 1600° K with the same fuel at −25° CA. As the injection is further advanced, however, the flame temperature again increases to nearly 2300° K at −35° CA.

At all points of injection there is a peak temperature early in the cycle, followed by a trough of varying depth, followed by another less defined peak.

DISCUSSION OF RESULTS

Temperature Measurements

Although few results for flame temperatures in diesel engines have been reported, the temperatures recorded in this work show good agreement with those of other workers, especially Uyehara *et al*,[11] who also found that high temperatures were obtained early in the cycle. This high initial temperature was followed by a drop in temperature and then a further peak. This peak was most clearly defined at early injection settings, becoming less distinct as the injection timing was retarded. Small temperature peaks also occurred just before the end of combustion. Later injection resulted in higher combustion temperatures and a shorter period of radiation. The pressure curves reported by Uyehara *et al* did not appear to be influenced by the high initial temperature or the temperature fluctuations during combustion.

Later work by Uyehara and Myers[12] did not confirm the high initial temperatures but did show that a peak temperature occurred early in the cycle, followed by a drop in temperature and usually a second peak just before the end of radiation. This is in agreement with the present work, as shown in Fig 33.

Lyn[3] also observed a dip in the temperature curve, and this coincided with a peak value in the number of moles in the combustion chamber calculated from the measured temperature and pressure. It was suggested

that this effect was due to the injection characteristics of the engine, a lean mixture corresponding to the drop in temperature. This does not appear to be the case with the results from the CFR engine, as the drop in temperature is affected by the injection timing and compression ratio.

The presence of two temperature peaks of varying magnitude depending on the conditions of compression ratio and injection timing does appear to be a true temperature effect. Carbon particles have been shown to be present at the onset of visible radiation, and it is the temperature of these particles which is measured. As the window in the cylinder head has a restricted field of view, this temperature effect could be caused by the flame front being carried round the combustion chamber by the " swirl " which exists in the pre-combustion chamber. Passage of radiation through the cooler layers of gas would then cause a decrease in the measured temperature. This cannot be the sole cause of the drop in temperature, since the same effect does not obtain under all conditions.

The initial rapid rise in temperature immediately following ignition is due to the burning of the fuel molecules at the fuel air interface, the heat supplied by the pre-flame reactions and the compression heat release raising the temperature of the gas mixture to the spontaneous ignition temperature of fuel. The heat released by the flame is used to raise the temperature of the reacting gases, to supply the endothermic heat of the cracking reactions in the fuel rich vapour zone, and to vaporize the incoming fuel spray. If the heat absorbed by the pyrolysis of the fuel exceeds the heat released by the flame, then a fall in temperature of the mass of gas will result, unaccompanied by a corresponding pressure variation because of the rapid increase in the number of molecules present. Under conditions of minimum delay period, the quantity of fuel in the engine at the point of ignition is small and

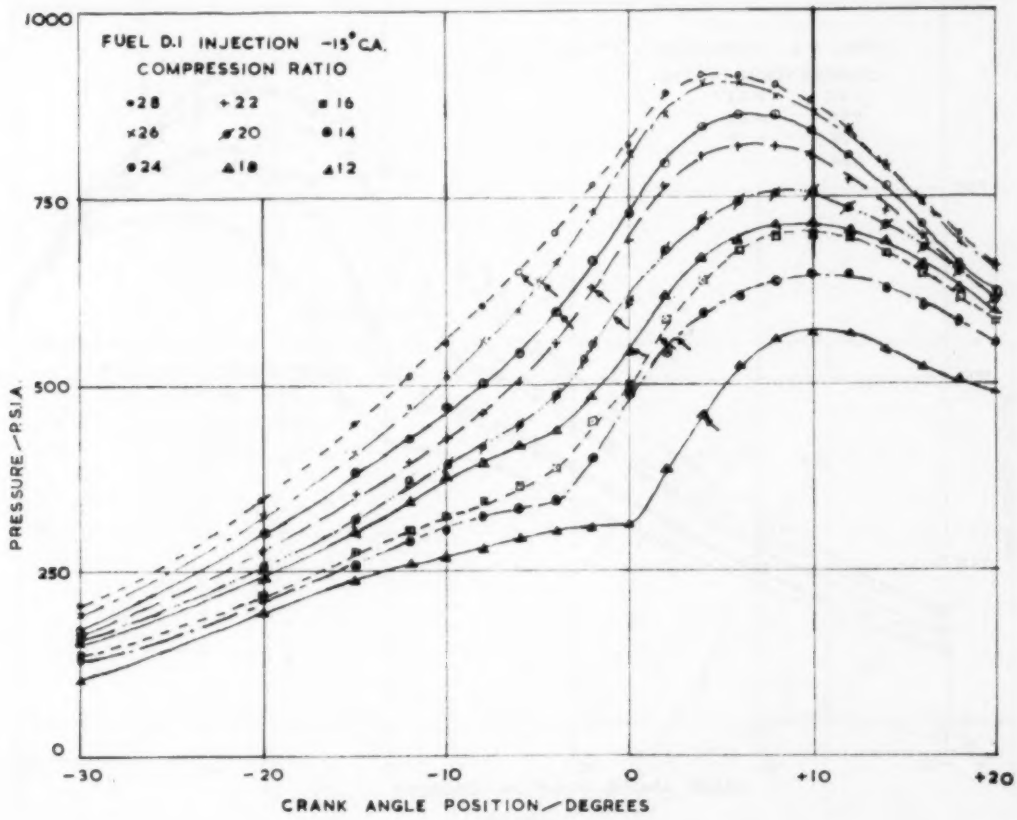

Fig 34

VARIATION OF ENGINE PRESSURE WITH CR FOR CONSTANT INJECTION SETTING

the heat release from the flame is sufficient to maintain the cracking reactions without a noticeable fall in temperature. Under conditions of long delay periods, the amount of fuel in the engine is large, the cracking reactions are excessive, and the heat absorbed is sufficient to cause the observed temperature fall. The combustion of the pyrolysed fuel fragments then follows, the heat of combustion causing the final observed increase in temperature.

motoring without fuel injection. Intake air temperature and jacket temperature were maintained near to the operating conditions (jacket temperature varies with injection timing, fuel, etc.)

The effect of compression ratio on pressure at an injection setting of −15° CA with fuel D_1 is shown in Fig 34. The point of flame arrival, derived from the temperature record, is also shown. A smooth family of curves is obtained in which the rate of pressure rise,

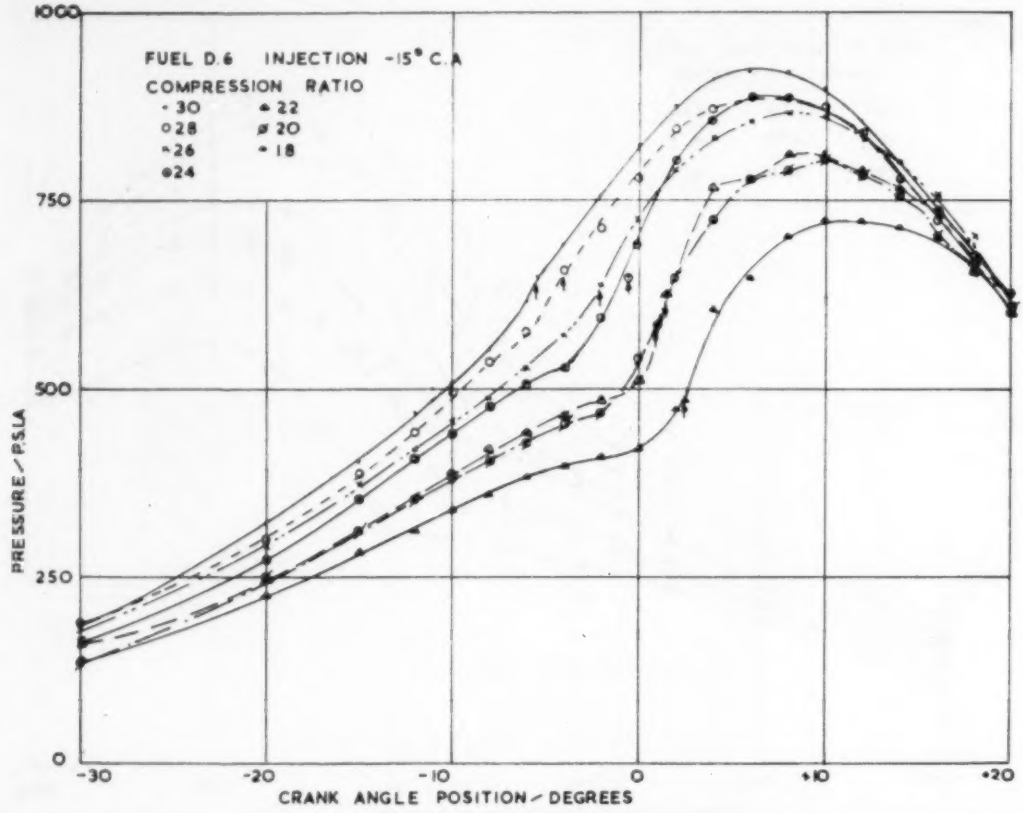

FIG 35

VARIATION OF ENGINE PRESSURE WITH CR FOR CONSTANT INJECTION SETTING

Total radiation intensity measurements[2] had shown that pre-flames occur at high compression ratios. Temperature records, obtained under the same conditions of injection timing and compression ratio as the earlier total radiation measurements, show no signs of pre-flames. This means that the pre-flames did not radiate at the wavelengths associated with hot radiation and it is concluded that they were in fact cool flames.

Pressure Measurements

For calibration and reference purposes a series of pressure records was obtained with the engine

calculated from the slope of the curve after ignition, gradually increases as the compression ratio is decreased. At the higher compression ratios the change in slope of the pressure curve after ignition is not clearly discernible, but as the compression ratio is lowered this break becomes increasingly obvious. It does not, however, coincide with the point of flame arrival. It can be seen that the point of flame arrival occurs in the pressure range 500 to 600 psia, and it seems probable that the gas has to be heated to the temperature corresponding to this pressure before radiation commences. It is apparent that the delay

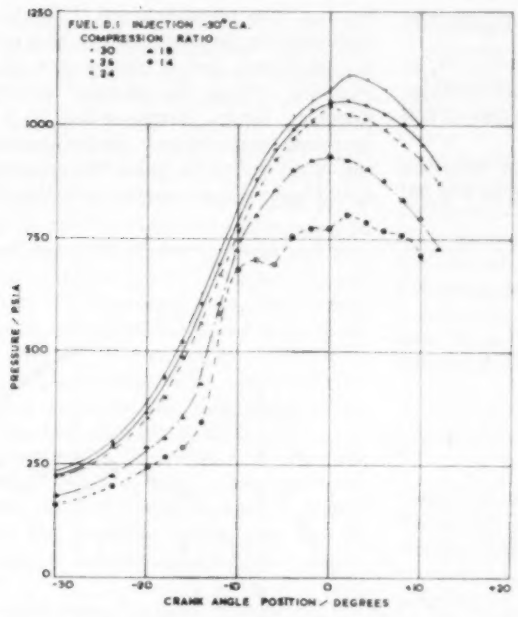

FIG 36

VARIATION OF ENGINE PRESSURE WITH CR FOR CONSTANT INJECTION SETTING

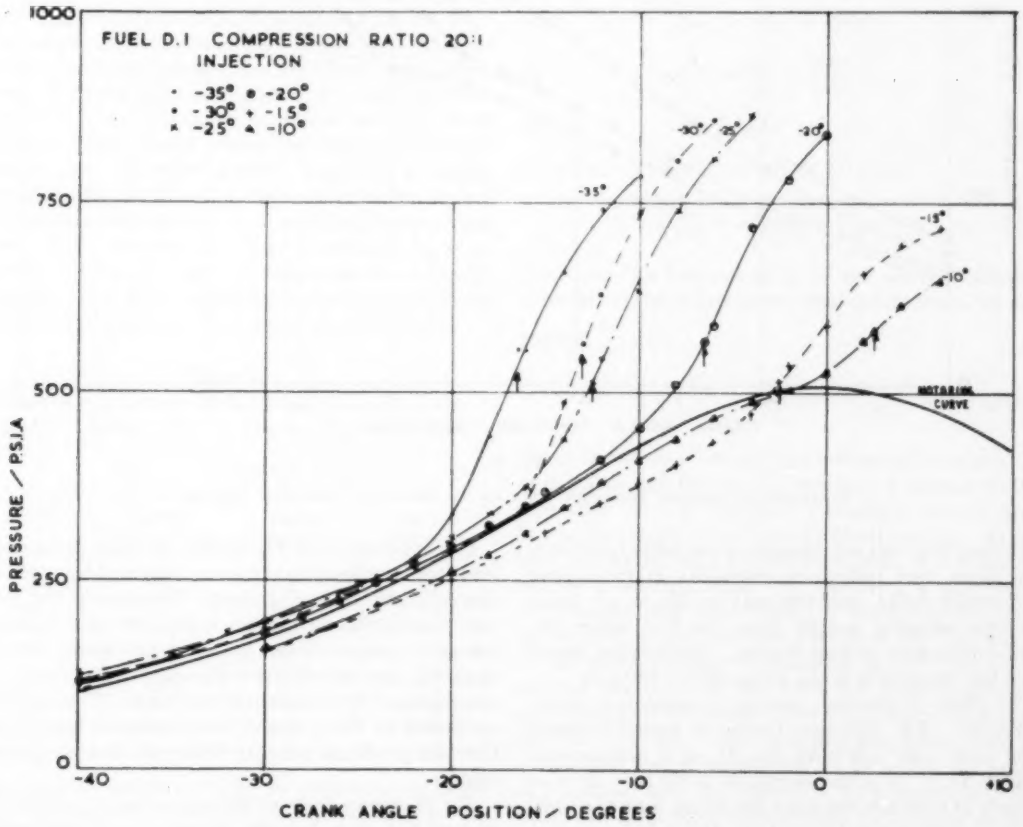

FIG 37

VARIATION OF ENGINE PRESSURE WITH INJECTION TIMING AT CONSTANT CR

between injection and flame arrival is no criterion of ignition quality if this is true.

Fig 35 gives a similar series of curves for fuel D_6 at an injection setting of −15° CA. The point of flame arrival with this fuel occurs in the range 550 to 650 psia.

The effect of compression ratio at an injection setting of −30° CA with fuel D_1 is shown in Fig 36. lies in a close pressure range of 500 to 600 psig. The motoring compression curve at this compression ratio is also shown, and it can be seen that at the early injection settings the pressure curves lie above this motoring curve, corresponding to a higher engine operating temperature. At the lower injection setting the firing curves lie below the motoring curve, corresponding to a lower engine operating temperature.

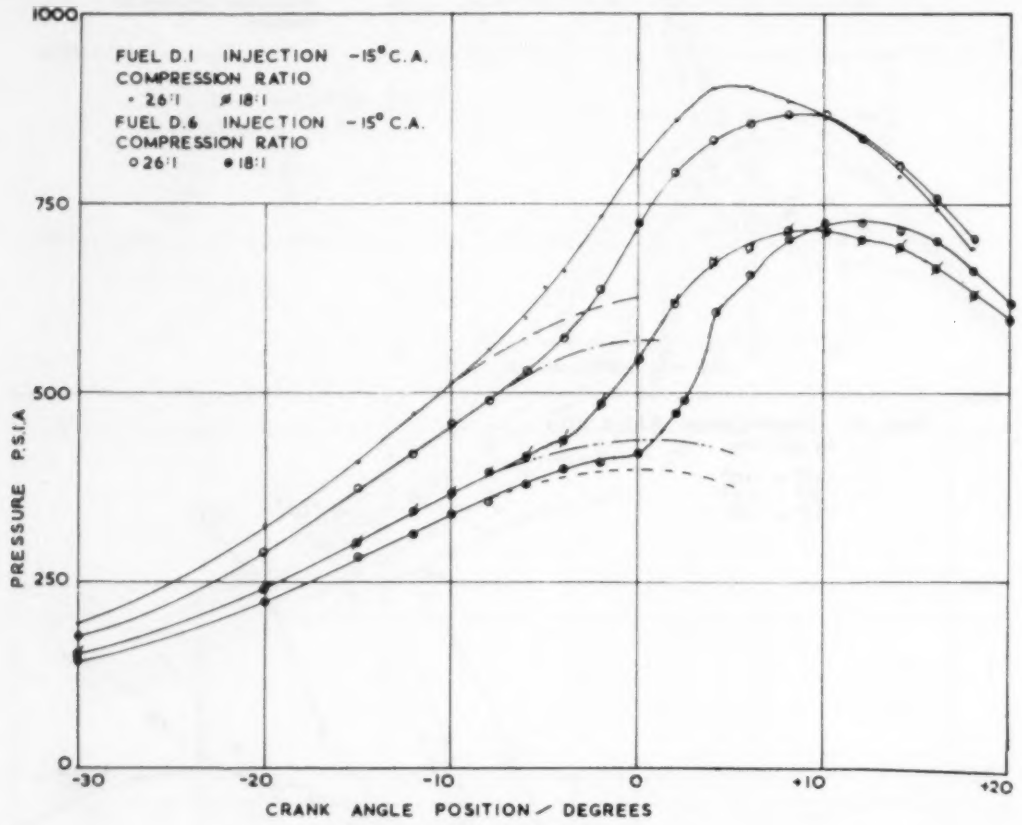

Fig 38

VARIATION OF ENGINE PRESSURE WITH CR AT CONSTANT INJECTION SETTING

The break from the compression curve after ignition is once again very indistinct, especially at the higher compression ratios, and this may be due to pre-flame reactions releasing energy from the fuel before the main combustion process begins. Combustion starts when the pressure is in the range 450 to 550 psia.

The effect of injection timing on pressure is shown in Fig 37. The injection timing is varied between −10° and −35° CA with fuel D_1 at a compression ratio of 20 : 1. For the curves at −35° to −20° CA, the rate of pressure rise after the break from the compression curve is nearly constant, but at later settings the rate decreases steadily. The point of flame arrival

It is apparent from Fig 34 that the start of reactions leading to combustion is not accompanied by radiation characteristic of hot ignition. Comparing the pressure records obtained in this work with total radiation intensity measurements obtained previously,[1,2] it is apparent that in most cases the start of reaction is not accompanied by radiation of any kind. This has been confirmed by Olson *et al*,[13] who measured total radiation and pre-flame pressure release in an auto-igniting engine.

Fig 34 shows that as the compression ratio is decreased the time between injection and combustion increases. The time between the break of the pressure

curve from the smooth compression curve and the point of combustion also increases during this period. This is best shown by comparing two compression ratios, as in Fig 38. The corresponding motoring curves are also shown. At the higher compression ratio the firing pressure curve shows no distinct break from the motoring curve, either before or after the point of flame arrival, for either fuel. The lower compression ratio of 18 : 1 shows two distinct stages in the pre-flame reactions. The first is accompanied by a small energy release extending 4° CA with fuel D_1 and 6° CA with fuel D_6. In the second, energy is released at a more rapid rate, extending up to and beyond the point of flame arrival. This effect probably does occur at the higher compression ratio, but is masked both by the higher pressures and the shorter delay period between injection and combustion.

The sampling curves for aldehydes and peroxides obtained by Grigg[1] showed that aldehydes were present before the start of visible radiation, and it seems likely that the reactions which give rise to these intermediates are accompanied by the pressure effects observed.

The term " ignition delay " is used extensively, but its precise meaning is difficult to define from the foregoing results. In previous work it has been taken as the time between injection and first visible radiation, except when pre-flames occurred. It could be measured to the point of hot flame arrival, but this would lead to a delay period which included considerable pressure rise. A better method would be to define ignition delay as the time between injection and a given pressure rise above the theoretical compression curve. For a pressure rise of 10 lb with fuel D_1 at an injection timing of −15° CA, the delay is shown in Table II. The delay measured to the point of flame arrival and to the start of radiation is also shown.

TABLE II

Comparison of Methods of Calculating " Delay Period "
(Fuel D_1, Injection −15° CA, Varying Compression Ratio)

Compression ratio	Ignition delay		
	10 lb pressure rise	Flame arrival	Start of radiation
30	6·7	7	8
28	8·2	9	7·5
26	8·3	10	7·5
24	9·3	11	7·0
22	8·8	13	8·0
20	9·7	12·5	8·0
18	10·2	15	8·5
16	10·5	15	9·0
14	11·3	15	11·0

The results based on a 10 lb pressure rise show reasonable agreement with those measured from the start of radiation, especially as these two sets of results were obtained some months apart.

Thermodynamic Analysis of the Pressure Developed during the Pre-flame Period

Pressure measurements showed that a pressure rise of varying magnitude occurred before the onset of hot radiation. This rise can best be investigated by calculating the energy supplied by compression of the gas and the energy released by the fuel during this period. Rifkin and Walcutt[6] made several simplifying assumptions regarding the behaviour and properties of the fuel–air mixture in the cylinder and then used the following approach to evaluate the energy released.

Assuming the fuel–air mixture obeys the perfect gas laws, from the first law of thermodynamics, for a differential compression or expansion

$$dq = de + dw \quad . \quad . \quad . \quad . \quad . \quad (5)$$

also
$$de = c_v dT \quad . \quad . \quad . \quad . \quad . \quad (6)$$

where c_v = heat capacity at constant volume. From the gas law $pv = nRT$, if the number of molecules is constant (fuel is less than 2 mol per cent of total and complete combustion would yield a maximum of 5 mol per cent)

then
$$pdv + vdp = nRdT$$

or
$$dT = \frac{pdv}{nR} + \frac{vdp}{nR} \quad . \quad . \quad . \quad . \quad (7)$$

also
$$dw = pdv \quad . \quad . \quad . \quad . \quad . \quad . \quad (8)$$

Substituting (6), (7), and (8) in (5) gives

$$dq = \left(\frac{c_v}{nR} + 1\right) pdv + \frac{c_v}{nR} \cdot vdp \quad . \quad (9)$$

Assuming the heat capacity of the air–fuel mixture remains constant during pre-combustion reactions and putting $\frac{c_v}{n} = C_v$

$$q = \left(\frac{C_v}{R} + 1\right)\int_1^2 pdv + \frac{C_v}{R}\int_1^2 vdp \quad (10)$$

When the limits of integration correspond to the point of injection and the point of ignition, q, represents the difference between the heat of reaction and the heat loss to the engine walls between these points. As the heat loss varies with compression ratio, this quantity can be evaluated either by assuming a polytropic compression and constructing a theoretical pressure curve, or by using a motoring pressure curve obtained at the corresponding compression ratio. The latter method was used in this work, as these conditions approximate more nearly those obtaining in the engine prior to injection. The motoring and firing pressure curves were made to coincide at or before the point of injection, and the difference in pressure between these curves is then attributable to pre-combustion reactions.

After converting the pressure–time curves to a

z

pressure–volume basis, the values of the integrals pdv and vdp were obtained by graphical integration using either the point of injection or −40° CA as the lower limit and the point of hot flame arrival as the upper limit of integration. The results of these integrations for fuel D_1 at an injection setting of −15° CA and various compression ratios using limits point of injection and hot flame arrival are given in Table III.

TABLE III

Variation of Pre-flame Heat Release with Compression Ratio

(Fuel D_1. Injection −15° CA. Integration between −15° CA and flame arrival)

Compression ratio	$\left[\left(\frac{C_v}{R}+\frac{1}{J}\right)\int pdv\right]\left[\frac{C_v}{R}\int vdp\right]$ [difference between firing and motoring curves]		Pre-flame heat release, cal	% Heat liberated
	cal	cal		
30	2·7	20·0	17	7·1
28	3·2	22·5	19	7·9
26	3·1	28·0	25	10·8
24	3·0	26·0	23	9·6
22	2·9	36·0	33	13·8
20	2·7	31·0	28	11·7
18	2·6	39·0	36	15·0
16	2·3	38·0	36	15·0
14	2·1	44·0	42	17·5

The heat released by the fuel increases as the compression ratio decreases, falling from 19 cal at a compression ratio of 28 : 1 to 42 cal at a compression ratio of 14 : 1. However, as the compression ratio is decreased the compression work done on the charge also decreases. Calculations assuming isentropic compression indicate the difference in compression heat between these two compression ratios to be 10 cal. Calculations using the data presented in Figs 10–17 are complicated by the variable heat loss to the engine walls and by the lack of information concerning the amount of heat supplied to the air from the engine walls during the early stages of the compression stroke if the engine has been running hot. These calculations indicate a heat leak of approximately 19 cal at 28 : 1 CR and 10 cal at 14 : 1 CR. However, it appears that the total energy change of the charge between fuel injection and flame arrival is roughly constant. At high compression ratios the pre-flame heat release from the fuel necessary to lead to ignition is less than at low compression ratios. There is some relationship between the energy change of the charge and ignition delay as shown in Table IV, the rate of energy change being roughly constant at 14–15 cal/millisec.

The effect of injection timing on the pre-flame heat release has also been investigated at a constant compression ratio of 20 : 1. The heat release between the point of injection and flame arrival has been calculated (Table V), and as would be expected shows a marked increase in the pre-flame heat release from the fuel at early injection settings.

TABLE IV

Rate of Internal Energy Change

(Fuel D_1. Injection −15° CA. Integration as in Table III)

Compression ratio	Internal energy $\left[\frac{C_v}{R}\cdot\int vdp\right]$ difference between firing and motoring curves, cal	Delay to flame arrival		Rate of energy change, cal/millisec
		° CA	Millisec	
30	20·0	7	1·30	15·4
28	22·5	9	1·66	13·5
26	28·0	10	1·85	15·1
24	26·0	11	2·03	12·8
22	36·0	13	2·41	14·9
20	31·0	12	2·22	14·1
18	39·0	15	2·77	14·1
16	38·0	15	2·77	13·7
14	44·0	15	2·77	15·8

TABLE V

Variation of Heat Release with Injection Timing

(Fuel D_1. Compression ratio 20 : 1. Integration between injection and flame arrival)

Injection, ° CA	$\left[\left(\frac{C_v}{R}+\frac{1}{J}\right)\int pdv\right]\left[\frac{C_v}{R}\int vdp\right]$ [Difference between firing and motoring curves]		Pre-flame heat release, cal	% Heat liberated
	cal	cal		
−35	6·7	93·5	87	36
−30	6·2	78·5	72	30
−25	4·9	52·0	47	19·5
−20	4·4	45·0	41	17·0
−15	2·7	31·0	28	11·7
−10	1·6	24·0	22	9·2

These results show that the delay period is influenced by the temperature and pressure at the point of injection. At high compression ratios and late injection settings the heat necessary to cause ignition is available in the hot compressed charge and requires only a small contribution from the pre-flame heat released by the fuel. As the point of injection is advanced, the percentage heat released by the fuel increases corresponding with an increase in the delay period.

CONCLUSIONS

The rate of burning of a fuel droplet has been examined by a variety of workers (Spalding,[14] Penner,[15] etc.), and the sequence of events following injection of a fuel spray into an operating diesel engine has been described by Elliott and Rogers.[16] The present work enables the sequence of events to be examined in more detail. After the fuel droplet has been injected into the hot turbulent air stream, the physical state may consist of four zones; the inner zone of unvaporized fuel surrounded by the second zone of fuel vapour unmixed with air, this being sur-

rounded by a fuel–air mixture of variable fuel concentration, and finally a zone of fuel free air. The energy available as heat in the compressed air prior to injection is used to vaporize the fuel droplet, the amount of heat and swirl determining the relative volumes of the four zones. The initial chemical reaction takes place in the gas phase in the oxygen-rich outer zone and commences almost immediately after injection, leading to the production of the pre-flame intermediates reported in previous work. The heat released by these reactions, together with the heat of compression, is sufficient to raise the temperature of the fuel–air mixtures to the spontaneous ignition temperature.

Three distinct reaction sequences occur. First, the gas phase oxidation by a peroxide free radical process will continue, the rate of oxygen attack upon the fuel molecule increasing with the rise in temperature. Secondly, the further oxidation of the fuel molecule and oxidation intermediates to give the ultimate products of combustion will take place in zones of suitable fuel–air mixtures. Thirdly, the cracking of the fuel molecules will occur in the fuel-rich zone, the endothermic heat of reaction being supplied by the combustion reaction. The rapid rise in temperature after the initial appearance of the flame indicates that the gas phase combustion reactions provide sufficient heat for the endothermic cracking of the fuel and for vaporization of the rest of the fuel droplets. If conditions in the engine are within certain limits the combustion of the fuel fragments continues to supply the heat necessary to vaporize fresh fuel as it is injected and to complete the pyrolysis of the fuel without any marked drop in temperature of the gas mixture until the expansion stroke is reached. If, however, the conditions are not within these limits, and at the point of initial flame appearance there is a large amount of vaporized fuel in the engine, the heat absorbed by the pyrolysis reaction may exceed that supplied by the oxidation reactions—either because the latter can only proceed in part due to limited oxygen availability at the fuel–air interface or because the mass of unmixed fuel vapour receiving radiant heat from the flame is very great. In this case the gas phase temperature will fall until the balance of reaction rates is restored. In the case of late injection, for instance, this balance may not be restored, and carbon as soot and unburnt fuel will be emitted in the exhaust smoke.

At optimum injection settings and with appropriate compression ratios, the heat of compression is sufficient to raise the temperature of the fuel–air mixture to the spontaneous ignition temperature of the fuel in the course of a few degrees crank angle, so that the pre-flame reactions are of little importance and pre-flame intermediates are found only in small concentrations. With very high compression ratios it appears that the whole of the pre-flame heat requirements are supplied by the compression heat.

With early injection the temperature of the air is too low to lead immediately into spontaneous ignition, so that time is available for low temperature pre-flame reactions, resulting in large concentrations of intermediate oxidation products, accompanied in certain circumstances by cool flames. During this prolonged pre-flame period the continued injection of fuel results in the accumulation of unburnt fuel, so that when ignition occurs the radiant heat from the flame front is absorbed by the large mass of fuel, resulting in pyrolysis of the fuel at such a rate that the temperature shows a marked fall from the initial peak value. As combustion proceeds, the temperature again rises and then falls as the expansion stroke is reached. The chemical nature of the fuel is of importance in each of these reaction sequences. In the pre-flame period it is desirable that the oxidation reactions should not result in the formation of large quantities of oxidation inhibitors. A fuel containing hydrocarbons of low spontaneous ignition temperature characteristics is desirable to enable the earliest possible inflammation of the fuel–air mixture, but it is also probable that the nature of the fuel controls the character of the pyrolysis products which are formed in the main fuel vapour mass. Carbon formation during this period is likely to be greater with aromatic fuels than with non-aromatic fuels, by analogy with laminar flame studies,[18] and may result in unburnt soot emitted in the exhaust.

At very high compression ratios with correct injection settings, the character of the fuel is of less significance than at low compression ratios, where the pre-flame energy released by the fuel is of importance.

Under cold starting conditions or under operating conditions where the heat lost to the engine wall may be excessive, the pre-flame energy released by the fuel may be of paramount importance.

References

[1] Garner, F. H., Grigg, G. H., Morton, Frank, and Reid, W. D. *J. Inst. Petrol.*, 1956, **42**, 69–94.
[2] Garner, F. H., Morton, Frank, Saunby, J. B., and Grigg, G. H. *J. Inst. Petrol.*, 1957, **43**, 124–30.
[3] Lyn, W. T. *J. Inst. Petrol.*, 1957, **43**, 25–46.
[4] Rassweiler, G. M., and Withrow, L. L. *SAE Trans.*, 1936, **33**, 185.
[5] Cornelius, W., and Caplan, J. D. *SAE Quart. Trans.*, 1952, **6**, 488.
[6] Walcutt, C., and Rifkin, E. B. *Industr. Engng Chem.*, 1951, **43**, 2844; *cf* also Walcutt, C., Rifkin, E. B., and Betker, G. W. *SAE Trans.*, 1952, **60**, 472.
[7] Saunby, J. B. Ph.D. Thesis, University of Birmingham, 1957.
[8] Hottel, H. C., and Broughton, F. B. *Industr. Engng Chem. (Analyt. Ed.)*, 1932, **4**, 166.
[9] Schack, F. F. *Z. Tech. Phys.*, 1925, **6**, 530.
[10] de Vos, J. C. *Physica*, 1954, **20**, 690.
[11] El Wakil, M. M., Myers, P. S., and Uyehara, O. A. *Trans. Amer. Soc. mech. Engrs*, 1952, **74**, 255; *cf* also Uyehara, O. A., and Myers, P. S. *SAE Quart. Trans.*, 1949, **3**, 178. Uyehara, O. A., Myers, P. S., Watson. K. M., and Wilson, L. A. *Trans. Amer Soc. mech. Engrs*, 1946, **68**, 17; 1947, **69**, 465.
[12] Yu, T. C., Uyehara, O. A., Myers, P. S., Collins, R. N., and Mahadevan, K. *SAE Trans.*, 1956, **64**, 690.

[13] Olsen, D. R., Wentworth, J. T., and Daniel, W. A. *SAE Trans.*, 1954, **62**, 606.
[14] Spalding, D. B. "Some Fundamentals of Combustion," Chap. 4. London: Butterworths Scientific Publications, 1955.
[15] Penner, S. S. "Chemical Reactions in Flow Systems," Chap. 4, p. 67–77. Agardograph 7. London: Butterworths Scientific Publications, 1955.
[16] Elliott, M. A., and Rogers, F. D. *Industr. Engng Chem.*, 1951, **43**, 2854.
[17] DuMond, J. W. M., and Cohen, F. R. *Rev. mech. Phys.*, 1953, **25**, 691.
[18] Clarke, A. E., Hunter, T. G., and Garner, F. H. *J. Inst. Petrol.*, 1946, **32**, 627; *cf* also Thorp, N., Long, R., and Garner, F. H. *Fuel*, 1951, **30**, 266; 1955, **34**, 51.

DISCUSSION

D. Downs (Ricardo & Co., Engineers (1927) Ltd): Almost exactly five years ago I had the pleasure of opening the discussion on Part III of the series of papers from Birmingham on the fundamental combustion in diesel engines. This earlier paper came at a time when little comparable work had been done in the U.K. In recent years, however, the analytical work of the C.A.V. and English Electric teams has been reported, and also the high-speed photographic work by my colleague J. F. Alcock.

Part III was concerned with the chemical aspect of pre-flame combustion; in this most recent paper the physical tools of temperature and pressure have been brought to bear on the problem. Although at first sight this may seem to be an easier approach than the chemical one, it can be seen from this paper that the twin difficulties of experimental uncertainty and uncertainty of interpretation are still with us.

From a wealth of experimental results which are interesting in themselves, Professor Garner and his team have selected two for particular comment.

First, the appearance of two distinct peaks in the flame temperature–time curves; secondly, that the start of the reactions leading to combustion is not accompanied by radiation characteristic of hot ignition. Observation of a large number of high-speed cinematographic records of diesel combustion which have been obtained at Shoreham have accustomed me to the sight of rotating flame fronts in such as the CFR diesel. My first reactions on seeing the two-peak nature of the temperature–time curve is therefore to ascribe it to the swirling of the hot gas in the combustion chamber, leading to two intense flame fronts passing the observation window in succession. The authors consider this possibility but reject it in favour of pyrolysis of the fuel absorbing heat from the gas mixture. I should need more evidence than the authors have yet put forward to convince me.

In quite a number of the records shown, in Figs 10 to 33, it seems to me that the fall of temperature occurs when combustion is virtually complete, as judged by pressure rise. I should like to know whether the authors have examined this question quantitatively, and have tried to equate heat release and fuel delivery, after the analytical method used by Dr Austin and his co-workers, and by the authors themselves, in their examination of pre-flame heat release, to try to decide whether the fall of temperature observed could be explained quantitatively by pyrolysis among burnt fuel.

As far as the second point is concerned, that start of the reactions leading to combustion precede observation of the hot flame, I am very ready to believe this, but I do not think that the authors have proved it. There is a very limited field of vision at their window, and it would be very easy for the first occurrence of flame to be unobserved, and for the flame not to be detected by the photo-multiplier until several crank degrees later.

I was going to ask Professor Morton a question concerning the repeatability of the temperature traces shown in Figs 8 to 24 and 25 to 32. It seemed to me that these include a high degree of repeatability of the temperature traces and I wondered how typical that was. But in his verbal presentation of the paper, Professor Morton was rather frank about the repeatability of some of these temperature curves and so perhaps he need not pursue that point.

The very fact that the authors have carried out their experiments in an engine, rather than in a piece of laboratory apparatus, shows that they are not merely interested in hydrocarbon combustion as such, but in combustion as it affects the performance of engines. Those of us who are concerned with practical problems of engine operation, as well as having an interest in fundamental combustion, might have wished that the authors had given us more information on the performance of the engine under the conditions used for the experiments. I wonder whether, for the benefit of the engineer, who might want to consider the significance of these results as far as the performance of the diesel engine is concerned, the authors can add information on such things as the rate of fuel injection and its duration, and on the power of the engine and its economy.

This is the fifth paper to come from the Birmingham team and I hope that the work will continue in the laboratory. There is little enough fundamental work being done on engine combustion to-day, but we must be careful that such work is related to the real problem of the engine. Combustion problems in the diesel engine to-day are concerned not only with power output and economy but also with cold starting, high-speed misfiring, noise (particularly at idling), exhaust smoke, and multi-fuel operation, to mention only a few of the problems. Might I suggest, for the consideration of the Birmingham team, that for their future work they angle their investigation on one or another of these very pressing practical problems, thus giving an extra edge and purpose to their experiments and putting the engineer even further in their debt.

Professor Frank Morton: Mr Downs' comments are, as usual, much to the point. On the general question of engineering data, etc., and the future work at Birmingham, we can only hope that additional investigators will follow the wider aspects suggested by Mr Downs.

The reason for the observed fall in temperature after the initial peak temperature may well be the passing of distinct flame fronts, and we accept the suggestion that the flame may start at different points in the combustion chamber. Nevertheless, it is believed that the differences observed in flame temperatures with the two fuels under similar operating conditions are a function of fuel composition and related to the pyrolysis reactions of the fuel.

That the reactions leading to combustion are not accompanied by radiation characteristic of hot ignition follows from a consideration of the sampling experiments in conjunction with the present flame temperature measurements (1·2). We agree that the flame might begin at some point in the chamber unobserved by the

window, but it is unlikely that the delay in observing the radiation we have assumed to mark the onset of hot ignition would be as long as that observed between the first appearance of aldehydes and peroxides in the engine gases and the appearance of flame as recorded by the photo-multiplier.

Dr Maund may be able to comment upon the degree of repeatability of the flame traces. In our experience the trace would be repeatable for three or more successive cycles in the same operation, but it might be difficult to obtain an identical trace when repeating the runs at a later date.

Dr J. K. Maund (Birmingham University): May I explain that I worked with Dr Saunby during his final year at Birmingham and then continued the diesel work for a further two years, finishing in 1959.

I agree in principle with Professor Morton, but would not go so far as to say that repeatability is very good. As he said, very similar traces are frequently obtained during the same run, but occasionally quite anomalous results appear. The engine often runs steadily for a long time but for a few cycles it misfires, and then takes some time to settle back to steady conditions. Although one hopes that the engine is running correctly when the oscillograms are taken, it is impossible to photograph one particular chosen cycle. Also, because of the delay during the development of the film and its interpretation, it may be weeks before it becomes apparent that a particular oscillogram is not typical. It is then difficult and time-consuming to repeat the run.

J. F. Alcock (Ricardo & Co., Engineers (1927) Ltd): At Ricardo's we have for some years been filming diesel combustion in colour through large windows in the cylinder head, at 15,000 frames/sec. Much of our work has been done on a cylindrical pre-chamber similar to that in Fig 3, the main differences being: (1) the fuel is injected near-tangentially, instead of axially; (2) only half the air charge was in the pre-chamber, the rest being in the cylinder; (3) the throat member is heat-insulated and runs much hotter than does that in the authors' engine.

Comparing our experiences with those given in this paper, the following points seem relevant.

1. *Dip in the Temperature Curve. Fuel Pyrolysis*

The film shown confirms the authors' view that pyrolysis occurs; dense clouds of soot can be seen. In our case these are not at the time or place which the authors' argument suggests, but this may be due to our different fuel spray direction.

We do find, however, a marked oscillation in the flame going down the throat, just about the time that the authors' temperature dip occurs. They may be connected.

We have measured the light emission from the flame and found a similar dip when viewing the pre-chamber only, but not when viewing the whole combustion space, including the part in the cylinder.

2. *Flame Temperatures*

By comparing the flame colour shown on our film with that of a tungsten filament of known temperature, photographed at the same exposure, we estimate our peak flame temperature to be about 2700° K, much higher than the authors' 2200°–2300° K. Much of this difference may be due to our crude method of estimation, but some may be due to the authors' narrow window not covering the hottest zone.

3. *Reaction before Visible Flame*

We have tried doping our fuel with copper to give non-luminous flame a green colour. With normal delay we usually see very little green during early combustion, and the initial flame nucleus has always been white, except with long delay. However, our latest film, with normal delay, shows considerable green pre-flame, so our ideas on this point are in a state of flux, or even flap.

I doubt, however, whether these green flames are cool ones; various indications suggest that their temperature is about 2000° K. In any case I doubt whether a cool flame would be luminous enough to be photographed with our exposure of $\frac{1}{40000}$ sec.

Professor Frank Morton: Mr Alcock and his colleagues are to be complimented on a very remarkable film. We believe the film demonstrates the rapidity of the pyrolysis reactions behind the flame front, and indicates large amounts of carbon formed in the early stages of combustion. In our opinion such a high degree of pyrolysis in the vapours following the flame front across the inspection window would account for the observed fall in temperature, and the extent of the carbon formation would depend upon the fuel characteristics.

J. G. Withers (BP Trading Ltd): In several places in the paper the suggestion is made that the diesel engine is particularly susceptible to cyclic variations in the indicator diagram, although this was partly contradicted in the presentation. The diesel engine is, of course, much less susceptible to cyclic pressure variations than the gasoline engine, and I think that on the whole the authors' work shows that the pressure and temperature cycles are reproduced fairly accurately.

On p. 183 it is stated that the rate of temperature rise is higher for the lower compression ratios, and the conclusion drawn by the authors is that this accounts for the engine running hot at the lower compression ratios, the rapid rate of temperature rise allowing less time for the heat to be dissipated. I do not think this can be a general conclusion. In most engines it is likely that the optimum *brake* thermal efficiency is obtained at a compression ratio of about 13 : 1.

I am not convinced that the double peaks on the temperature diagrams are unconnected with variations in the rate of fuel delivery during injection. The initial rate of fuel delivery is usually high because the pressure required to lift the injector needle is higher than that required to keep it open. That injection timing and compression ratio influence the position and the extent of the temperature peaks could well be because the rate of energy release and the rate of fuel injection are not in phase with one another and the amount by which the energy release lags behind the amount of fuel injection is clearly influenced by both compression ratio, injection timing, and, of course, fuel ignition quality.

I am not clear why the maximum temperatures are lower with the low cetane fuel when the maximum pressures are higher. The maxima in both diagrams occur at much the same position in the cycle. Surely temperature and pressure must be related at a given volume if the number of molecules in the gas phase remains the same, and this cannot vary very greatly. Part of the difficulty is clearly that neither the pressures nor the temperatures represent the average conditions in the combustion space, nor do the temperature and pressure measurements necessarily correspond to the same part of the combustion space.

I do not agree that in Table II the 10 lb pressure rise method for indicating commencement of combustion

agrees with the method based on start of radiation. The 10 lb pressure rise method shows a steady reduction in ignition delay with rising compression ratio, whereas the start of radiation method flattens off at the higher compression ratios. On the other hand, the flame arrival method shows a steady reduction in ignition delay with compression ratio, but at a much higher rate than the 10 lb pressure rise method. There must be some significance attached to this, and I should be glad to have the authors' comments.

In my view the commencement of combustion can be best defined by the point in the cycle at which the falling rate of pressure rise on the compression stroke begins to rise again. This is equivalent to saying that commencement of combustion is defined as the point in the cycle where the second differential of the pressure rise changes sign. The BP–ASTM ignition delay meter is based on this principle. When using this instrument or this method, there is no problem in deciding where combustion starts even at the higher compression ratios.

The authors' subsequent analyses of heat release are based on ignition delay as defined by hot flame arrival. That this does not coincide with ignition delay as normally understood must be borne in mind.

No account seems to have been taken of the heat required to raise the injected fuel to the prevailing gas temperatures and evaporate some of it, and this is by no means negligible. Some tests that I made a number of years ago on an engine with a 13 : 1 compression ratio showed a fall in preasure below the compression line when fuel was injected. This started from the point of fuel injection, and at the point of commencement of rapid pressure rise the pressure was still well below the normal compression pressure. In these tests the motoring compression line was always within close limits of that obtained when the engine was firing right up to the point of commencement of injection. Some energy might have been released by the fuel, but it was obviously less than the heat required to warm it up. I think that the authors' calculations could be improved by allowing for the heat required to bring the fuel up to gas temperatures, although since the system is never in equilibrium, this might be difficult.

I should also like to see the heat releases calculated for the ignition delay based on the 10 lb pressure rise to see how this would affect the conclusions reached.

Professor Frank Morton: The question of differences between motoring and firing curves and the suggestion that the temperature rise is higher for lower compression ratios will be answered later by Dr Maund. In the present work the motoring curves were not obtained at the same time as the firing curves—when the actual experimental work was being carried out the full significance of this was not realized. Dr Maund has since reported work with the motoring curves being determined during the same period, *i.e.* with a hot engine, and he has noted, as has Dr Lyn, that there is an effect of fuel vaporization. This effect is also shown in the curves given by Mr Burt later in this discussion. The actual heat requirement for vaporization of the fuel is small compared to the total heat released, but is sufficient to alter the firing pressure curve at and just after injection. In our calculations this has been neglected, but will no doubt be included in subsequent publications by Garner and Maund.

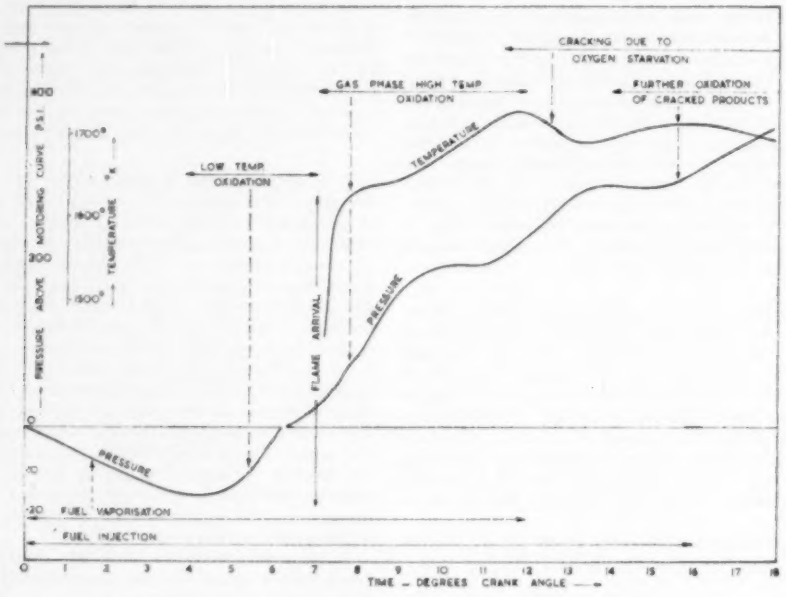

FIG A

SUMMARY OF EARLY REACTIONS

Dr J. K. Maund: It was a little unfortunate that in the present work the motoring pressure diagram was not taken at the same time as the firing diagram. Thus the engine was possibly operating at a different temperature and also, the CFR being what it is, it is possible not to have precisely the same compression ratio. This I think explains the difference between the firing pressure curves

and the motoring pressure curves in the present publication. It will be noticed that in some cases the firing curve is above the motoring curve before injection of fuel, and in some cases below the pressure curve. I think probably Fig 37 illustrates this best. The motoring curve, which is the continuous black line, runs right through the middle of the firing curves. Since this work was completed, I have done, as Professor Morton says, some work on measuring this pre-combustion pressure change, on the CFR engine. I took a firing pressure diagram, and then switched off the fuel, taking a motoring diagram immediately afterwards. This was then repeated. I found that in these conditions the motoring and firing pressure curves did correspond before fuel injection.

As in Mr Withers' experiments, a measurable pressure drop was noticed between fuel injection and flame arrival.

Fig A shows the conclusions following a series of runs on the Crossley engine. The pressure curve is the difference between motoring and firing diagrams and, therefore, represents the pressure effects of the fuel, no engine compression being included. (Note the difference in scale below and above the zero pressure line.)

Fuel injection starts at zero on the time scale and continues for 16° crank angle.

As soon as liquid fuel enters the combustion chamber it commences to vaporize under the influence of the high temperature of the compressed air. This vaporization requires the transfer of the latent heat from the hot gas, which produces a cooling effect, shown by the drop in pressure. This process continues until the concentration of fuel vapour and oxygen is adequate for the first chemical reactions. These reactions occur at low temperature and are usually without light emission.

Previous workers at Birmingham have noticed low intensity pre-flames in this part of the cycle and have shown that they are accompanied by high aldehyde and peroxide concentrations. The first stage is, therefore, a low temperature gas phase peroxidic oxidation.

This type of reaction is exothermic and, therefore, produces a rise in temperature and, therefore, pressure, which rapidly overtakes the pressure fall effect due to vaporization. The rise in temperature increases the reaction rate until a hot flame is initiated in which the fuel vapour is burned direct to carbon dioxide. This process continues while the concentration of fuel vapour and oxygen is sufficient, but with the entry of more liquid fuel into the combustion chamber the immediate availability of oxygen decreases and the high temperatures existing produce cracking of the fuel. These cracking reactions are endothermic and produce the drop in temperature observed by Dr Saunby and myself.

Considering a single droplet of fuel, the oxygen concentration rises from almost 100 per cent some distance from the droplet, to zero at the liquid surface. The oxidation will take place in the intermediate zone, where fuel vapour and oxygen are mixed, but as the reaction continues, using the oxygen and producing a " blanket " of carbon dioxide and water vapour, the oxygen concentration around the fuel droplet will decrease and, under the influence of the high temperature, cracking will take place. The heat necessary for the cracking reactions is taken from the gas surrounding the fuel droplet and gives rise to the fall in the temperature trace.

Professor Frank Morton: Did you calculate the actual energy required to vaporize your fuel—the number of calories?

Dr J. K. Maund: This is very difficult to do because it is not known how much of the fuel is vaporized.

(Since the discussion, calculations have shown that for a cycle such as that shown in Fig A, the energy required for the total vaporization of the fuel is just under 2·0 calories. The pressure drop in the figure represents 0·2 calorie, or 10 per cent of the necessary vaporization energy.)

Professor Frank Morton: The Crossley engine uses more fuel per cycle, 26 ml/min, as against 13 ml/min for the CFR engine. We have calculated that the maximum heat required to vaporize the fuel in the CFR would be less than 1·0 calorie and, whilst this is not negligible, it does not greatly affect the pre-flame heat release calculations given.

R. Burt (" Shell " Research Ltd): Most of our knowledge of the diesel combustion process has been derived from a study of the pressure changes which occur in the engine. In this series of papers, the authors and their co-workers have shown how a better understanding of the diesel combustion process can be obtained from data derived from more sophisticated measuring techniques.

This paper gives us some of the results of yet another valuable analytical technique and the authors must be congratulated in their successful application of a " two-colour " method to the determination of flame temperatures in an engine.

One of the most interesting observations in the paper is the presence of the two peaks in flame temperature with no corresponding pressure variation. It is important to keep in mind the difference between flame temperature and pressure in the engine. The pressure is a homogeneous phenomenon and, in the CFR engine, will be uniform throughout the combustion chamber. The front of the turbulent diffusion flame is distributed non-uniformly through the combustion chamber. Thus there is no reason to expect an exact correlation between the pressure and the flame temperature observed at one position in the combustion chamber.

The authors have suggested that the drop in flame temperature is caused by the absorption of heat from the flame by cracking reactions. The pyrolysis reactions of hydrocarbons at high temperatures are only mildly endothermic, and it is unlikely that they could account for the observed effect. High-speed photography of the flame in a swirl chamber engine * has shown that the flame front moves with the air swirl. The combustion chamber of the CFR engine is designed to give a swirling motion to the air, and it seems likely that the variation in temperature arises from the movement of the flame round the chamber. If it is assumed that the minimum time between the temperature peaks represents the time for one complete rotation a figure for the air velocity of about 120 m/sec is obtained, a reasonable value.

The results show that the two fuels give different temperature profiles under conditions of identical compression ratio and injection timing. The degree of mixing during the delay period will not be the same for the two fuels as a result of the difference in ignition delays. This change in the mixing of fuel and air will produce a corresponding change in the flame pattern and temperature distribution in the combustion chamber.

The authors have observed that with a fixed compression ratio the total burning time is decreased as the injection point is retarded towards tdc. This is in agreement with our measurement of the influence of

* Nagao, F., and Kakimoto, H. *Motortech. Z.*, June 1959, 183–6; Aug 1959, 303–5.

temperature on the burning rate of fuel sprays in a constant volume combustion bomb.

The results of the experiments on the relation between pressure rise and flame arrival are extremely interesting. For example, Japanese workers * are using a photo-electric technique to define the ignition point when carrying out cetane number determinations on the CFR engine. The results we have heard throw valuable light on the relevance of this criterion of ignition. The delay between the commencement of rapid pressure rise and flame arrival is most probably due to ignition occurring in some part of the chamber outside the field of view of the optical system. It is significant that this difference increases as the compression ratio decreases, since the length of the combustion chamber of the CFR engine increases by five times when compression ratio changes from 30 to 14.

A valid criterion of the point of ignition is of great theoretical and practical importance. Some information on the nature of the processes between the beginning of injection and the rapid rise in pressure following ignition can be obtained using the " hot motoring " technique.†

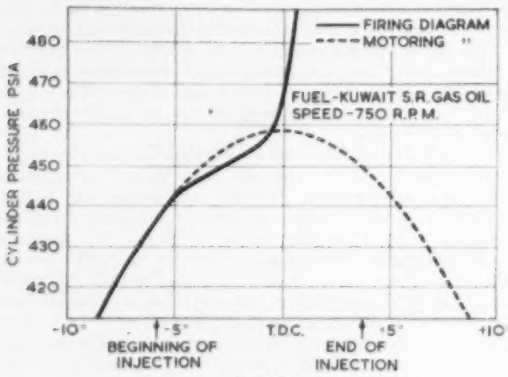

Fig B

Fig B shows the " hot motoring " diagrams and the firing diagram obtained from a single-cylinder direct injection engine. It is clear that a value of 10 lb pressure rise above the compression curve would not indicate the ignition point accurately. A more exact definition of the point of ignition would be when the firing pressure becomes equal to the " hot " compression pressure.

The very fact that the most appropriate criterion of ignition in a diesel engine can still be a matter for discussion is an indication of our lack of exact knowledge of the various processes during the injection and combustion of fuel in diesel engines.

Professor Frank Morton: Mr Burt's suggestion that the observed drop in temperature after the first peak may by due to the flame front passing the window a second time—and this time at a distance from the window so that the observed temperature would be lowered by absorption of energy by the combusted gases—may be the correct explanation. We had considered this, but believed that if this were the explanation we would expect to find similar peaks and troughs for both fuels at all conditions. The differences between the observed temperature traces for the two fuels suggest that in part at least the explanation involves consideration of the fuel quality.

The discussion on ignition delay period suggests that whilst our proposal may not be the best solution, the whole problem needs critical review.

Dr W. T. Lyn (C.A.V. Ltd): I would like first of all to raise a point of detail about the emissivity. The authors quoted that I had established that the spectral emissivity of diesel flames is constant for the wavelengths which they used in their temperature measurement, whereas really my work was confined to the infra-red range of from 1 micron upwards. This does not mean that I do not believe that for the two particular wavelengths which they have chosen the emissivity is in fact the same. But what surprised me was that the measured temperatures check quite well with the results from Uyehara and Myers, who had assumed that the emissivity changes with wavelength, according to the results from Hottel and Broughton for atmospheric flame. Is it because the effect on temperature of the discrepancy in the assumption of emissivity is small? Perhaps the authors will give an indication.

The second point I would like to raise is the " two-peak " nature of the temperature curve. Recent combustion work at C.A.V. shows that there is a peak in rate of heat release at a crank angle corresponding to the rapid rise of pressure (see Fig C). This is followed by peak pressure. Still later the mean temperature (which is calculated from mass of gases, volume, and pressure) attains its peak value. Our interpretation of the two-peak temperature curves obtained by the authors is therefore as follows. At the time of maximum heat release the mean temperature is still relatively low because the total heat released up to that point is quite small; but the very high *rate* of heat release involves high local temperatures which are registered by the authors' method. Later on, when the total heat released is getting quite large and relatively little heat has been lost as work done, the mean temperatures make a peak, which the authors' method also registered. The dip is due to the fall-off of heat release as the pre-mixed part of the fuel burns up. This interpretation helps to explain the results obtained by the authors that low cetane fuel and early injection timing are accompanied by a high first temperature peak and a large dip in the temperature curve. Low cetane fuel and early injection both result in long ignition delay and high rate of heat release initially. This provides for the high first temperature peak which the authors observed, and also the reason for the large dip afterwards. The effect of a high cetane fuel would be just the opposite. This is not to say that the mechanism proposed by the authors—the absorption of heat by cracking reactions—is not operative. But the amount of heat so absorbed is likely to be small compared with the quantities involved in burning and expanding.

Coming to the calculations shown in Tables III to V, I think the formula used to calculate the internal energy in Table IV represents only part of it. The correct formula should, of course, include the $\frac{Cv}{R}\int p\,dv$ term.

I am also rather disturbed to find from the revised Table V that as much as 36 per cent of the heat supplied was released in the " pre-flame " period. This is entirely contradictory to our own experience, in which the whole combustion chamber is in view. Our results invariably showed that the appearance of the flame, as recorded by high-speed photography, coincides with the point of rapid pressure rise to within the order of a degree crank angle. As a matter of fact, we have not been able to

* Tsuge, M., and Okamoto, Y. *JSME*, 1958, **1**, 411.

† Yu, T. C., *et al.* SAE Preprint 633/55, Nov 1955.

observe any flame very much prior to the rapid pressure rise. The apparent late appearance of flame in the authors' case could be due to the limited view of their chamber as well as to the loss of light through their optical system. This is particularly probable, since, as we know, the first phase of combustion is essentially pre-mixed in nature with a rather low luminosity flame. I do not regard this merely as a matter of definition, but a matter of fundamental importance, for if it is really true that as much as 36 per cent of the total heat is released before the appearance of flame, then the mechanism of the reaction ought to be investigated. If, on the other hand, the point of arrival of flame depends on how the measurement is made, then much of the results and discussion on p. 187 lose their significance. In this respect, I would like to point out that the pressure expanding. It is, however, probably a local or point effect, and hence does not result in appreciable cylinder pressure changes. We have made calculations of the heat absorbed and released, but in view of the doubts concerning the relation between the motoring and firing pressure curves would prefer not to comment further on this point until the work of Maund is published.

We do not consider the figure given in Table V that 36 per cent of the heat available is released in the pre-flame period when injection is at −35° CA to be extraordinary or even unexpected. Our earlier work has shown that with very early injection considerable chemical reaction occurs, frequently accompanied by cool flames. Other workers have also observed similar effects, figures as high as 60 per cent of the total heat available being released before ignition. The actual

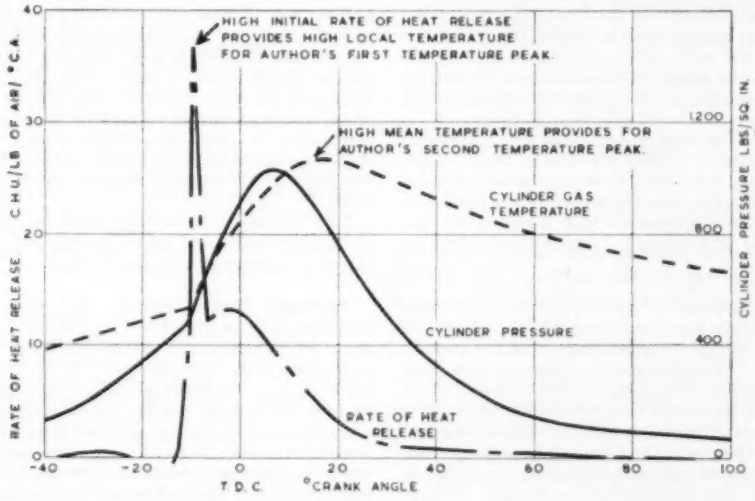

FIG C

CYLINDER PRESSURE, TEMPERATURE, AND HEAT RELEASE DIAGRAMS

diagram in Fig 38 causes some concern. Our own experience showed that the compression curve without injection always lies above the firing curve during the early part of the delay period, due to the heat lost to fuel evaporation. This is not so in Fig 38, which raises doubt on the accuracy of these diagrams for this particular purpose. The situation will be clearer if the authors show a plot of heat release against time or crank angle during the delay period, instead of just the final integral as given in the tables. In my opinion the only way to do this sort of experiment is to obtain the reference compression curve in the successive cycle, as had been done by Myers *et al* of Wisconsin.

Professor Frank Morton: The factors affecting the accuracy of the two-colour optical pyrometer are discussed by Uyehara, Myers, Watson, and Wilson [11] and by Saunby.[7] The assumption of constant emissivity over the wavelengths employed at the slit widths used would not in our opinion affect the accuracy of the temperature measurement by more than a small amount well within the limit of experimental error.

Dr Lyn's explanation of the temperature curves is reasonable, but we do not accept that the amount of heat absorbed in the dissociation of the fuel is small compared with the quantities involved in burning and value may be in error, but the relative magnitude of this effect is correct.

Dr W. E. Malpas (Caltex Services Ltd): I was very glad that Mr Downs introduced a note of controversy early in the evening, and I would like to return to that. I would like to say more about the explanation for the drop in temperature, following the initial peak temperature in the engine cycle, shown by this work. This is a very significant feature of the work reported, and I believe it is worth further discussion.

This evening we have had three explanations for this drop in temperature. First, the authors propose that it is due mainly to the absorption of heat by the endothermic nature of the hydrocarbon cracking reactions which are predominant at this stage in the engine cycle. Secondly, Mr Downs proposed that the successive temperature peaks are due mainly to the arrival of successive flame fronts at the point of observation. Thirdly, it has been proposed that the variations in temperature shown by the authors are due to the swirl of hot gases in the combustion chamber irrespective of the movements of flame fronts within the mass of hot gases.

I would like to say something first of all on the second of these proposals, *i.e.* the suggested arrival of successive flame fronts at the point of observation. First, we should

attempt to define what is meant by a flame front. It could be defined as a zone of hot reacting molecules moving into a cooler mixture of fuel and air. Therefore, one would expect the arrival of a flame front at the point of observation to be accompanied by rapid changes in the chemical analyses of the gases at the point of observation. I would like to refer to a diagram which appeared in a previous paper in this series (*J. Inst. Petrol.*, 1952, **38**, 319, Fig 13). This diagram shows what happens to the chemical analyses of the gases when a flame front passes the sampling valve located at the wall of a combustion chamber. If a number of successive flame fronts were arriving at the point of observation (in this case the sampling valve), then one would expect the chemical analysis curves for O_2 and CO_2 to have a similar shape to the temperature curves reported by the authors of tonight's paper. In fact, the chemical analysis curves do not have the same shape as the temperature curves. The shape of the oxygen and CO_2 curves shown in the diagram is consistent with the postulation of a single flame front passing the point of observation. Therefore, I believe that the second of the proposed explanations can be discarded.

As regards the third suggestion, that the successive peaks in the temperature curve are due to swirl in the combustion chamber, this seems to be a possible explanation. It may be that the true explanation is a combination of this and the explanation put forward by the authors. I wonder if Professor Morton would like to comment on this?

Professor Frank Morton: The reference by Dr Malpas to the gas analysis data previously published is welcome; we had overlooked this in our examination of the present experimental work. We agree that the evidence available does not rule out Mr Burt's suggestion of a second view of the same flame front as it swirls around the chamber. More detailed examination of the Ricardo film might be helpful, but it does suggest that once the flame has become established the whole mass of gas contains areas, or volumes, of dark carbon-rich gas surrounded by flames. Whilst the possibility that the temperature curves observed may be due to physical effects related to window position and flame position, etc., the occurrence of two temperature peaks, the differences between temperature records for different fuels, and the visual evidence provided by Mr Alcock's film support the view that a highly endothermic cracking or dissociation reaction occurs behind the initial flame front.

C. G. MacKenzie ("Shell" Research Ltd): I should like to suggest to Professor Morton that he gives some thought to the mass of fuel in the combustion chamber at any instant. I think many people have said that the rapid rise of gas temperature at the beginning of combustion occurs because of the rapid combustion of premixed air and fuel.

Another thing to bear in mind are the results obtained at the Karlsruhe Institute of Technology, which showed that very high rates of burning could also take place in mist systems.

A further point is that Dr Lyn has shown that the highest rate of heat release takes place immediately after ignition. However, following the first peak in his heat release curve there is a second and smaller peak. This second peak could presumably be smaller, because although there is possibly less fuel in the combustion chamber, the burning rate could be very high. All I am suggesting is that one should take into account the ignition quality of the fuel, the rate of fuel injection, and the state of the air–fuel mixture at various stages in the cycle.

I do not know at the moment how possible variations in burning rate could affect the radiation from the flame, but it is a point worth considering.

Professor Frank Morton: We have considered the question of mass of fuel and its quality. Detailed calculations are perhaps not justified at this moment, but we do suggest that the difference in the temperature traces between the two fuels is due to the quality of the fuels. For fuel D_1, a high cetane fuel, the amount of fuel in the chamber at ignition is much less than with fuel D_6, a low cetane number fuel. Hence the extent of cracking reaction and heat absorbed is greater with fuel D_6 than with fuel D_1. More detailed calculation would require experimental measurement of rates of fuel injection, etc.

The meeting then closed with a unanimous vote of thanks to the authors.

MECHANISM OF OXIDATION OF TRANSFORMER OILS *

By V. PRABHASHANKAR † and D. J. BADKAS †

SUMMARY

The effect of the test procedure of BS 148 and the proposed IEC test on the oxidation of transformer oils has been studied. The poor repeatability of these tests is explained as being due to the test methods adopted, as well as to the inherent qualities of the oil. It is concluded that with both the tests as they are being conducted at present it is not possible to improve their limited utility. It is suggested that by obtaining the oxidation products *v.* oxygen absorption curves, accelerated aging tests may be more realistic.

Symbols

a = capillary constant
a_s = area of the surface of the oil in the flask
a_i = area of the surface of the bubble
A = acidity mg KOH/g
$A_1 \cdot A_4$ = collision constants
A_v = area of the surface of the bubble of volume V
A_n = area of the surface of volume V_n.
B = constants corresponding to activation energy
c_x = the concentration of the oxygen in the section of the oil at distance x from the bottom of the flask
d = depth to which the inlet tube is immersed in the oil
e = natural logarithmic base
g = acceleration due to gravity
h = maximum pressure necessary to break off the bubble
k, K = various constants
L = concentration of the oil vapour in the air space
n = no. of small bubbles
O_a = oxygen concentration in air space
O_b = oxygen concentration in the body of the oil
O_{dA} = oxygen diffusing from air space to oil
O_{dx} = oxygen diffusing from bubble to oil
O_r = total oxygen reacting with oil
O_{ra} = oxygen reacting with oil in the air space
O_{rb} = oxygen reacting within the body of the oil
O_{rs} = oxygen reacting at the bubble surface
O_s = oxygen concentration at the bubble surface
O_{xs} = oxygen concentration in the bubble
p = clearance between the inlet tube and the bottom of the flask
$p_1 \cdot p_n$ = constants
R = radius of the bubble in cm
R_f = the radius of the flask
R_n = radius of the bubble of volume V_n
R_v = radius of the bubble of volume V
s = distance of bubble travel from the end of the inlet tube
S = sludge expressed as % by weight of oil
t = time in seconds
t_a = the time during which the oil is aged
t_1 = time taken by the bubble to travel to the surface
t_f = time of bubble formation
t_n = time taken by the bubble of volume V_n to rise to the surface
t_v = time taken by the bubble of volume V to rise to the surface
T = oxidation temperature in degrees absolute
v = number of bubbles formed in time t_1
v' = number of bubbles formed per second
V = volume of each bubble after the main bubble has broken down to n small bubbles of equal volume
W = weight of the bubble formed
x = distance of a section of the oil from the bottom of the flask
x_1 = distance of the surface from the bottom of the flask
X = an empirical constant
α = the rate of air flow in ml/sec, or l/sec
β = a constant
γ = surface tension of the air–oil interface, dynes/cm
η = viscosity, poises
μ = kinematic viscosity, stokes
ρ = density of the oil in g/ml
ρ_0 = density of air in g/ml
θ, ϕ, ψ = functions of . . .

INTRODUCTION

MINERAL oils are used in transformers for purposes of cooling the windings and for providing electrical insulation. These oils deteriorate in service,[12,15] giving rise to products such as peroxides, acids, water, etc.,[12–14] which are typical products obtained when mineral oil is oxidized.[7] It may be said that oxidation is the prime cause for the deterioration of transformer oils in service.

Among the important acceptance tests performed on transformer oils is the so-called " sludge " test, which measures the oxidizable propensity of the oil. The value of these tests would be enhanced if the results could indicate the behaviour of the oil when placed in service in addition to determining its acceptability. Unfortunately, the test results published so far show that all the oxidation tests that have been proposed have a very poor repeatability and a poorer reproducibility.[10,16]

A sub-committee of the International Electrotechnical Commission (IEC) has been working on certain tentative proposals for an artificial aging test for transformer oils. The repeatability of the proposed test is also no better than that of the older tests. It has been found that with some oils the repeatability is worse than with others, which fact has led to the belief that " certain oils are inherently liable to give inconsistent results."[10] It is difficult to accept the validity of this belief in view of the fact that transformer oils are a homogeneous mixture of mineral oil fractions. It could be that there are various factors in the test procedure that are conducive to inconsistencies in the results and that these factors are operating to different extents with different oils.

* MS received 14 September 1960.

† Indian Institute of Science, Bangalore.

The BS oxidation test is, in all essential factors, except reflux temperature, similar to the IEC test (Fig 1 (*a*) and (*b*) and Table I). The conditions

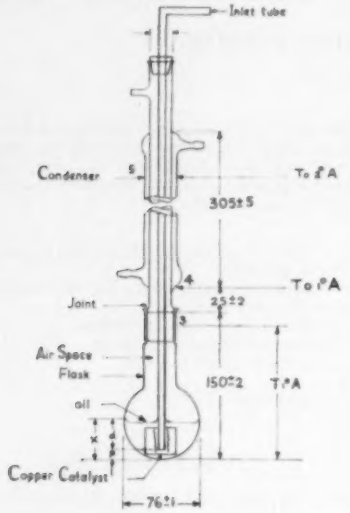

FIG 1 (*a*)

THE OXIDATION SYSTEM IN THE BS 48 SLUDGE TEST

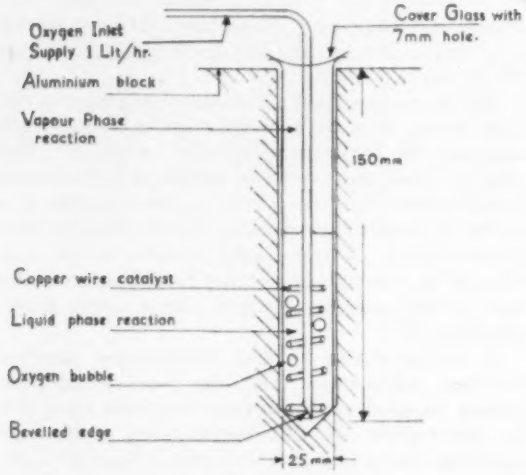

FIG 1 (*b*)

APPARATUS PROPOSED BY THE IEC FOR OXIDIZING TRANSFORMER OIL

in the BS 148 test are better controlled than in the IEC test. Extensive experimental work has been conducted by Massey [10] for studying the effect of the test parameters involved in the sludge test (BS 148). A study was made of the mechanism of the oxidation of oil in the BS 148 oxidation test in the hope that some information could be obtained regarding the reasons for the poor repeatability of this as well as other oxidation tests prescribed by different standards institutions.

The BS oxidation test is carried out at 150° C, while the IEC test is carried out either at 100° or at 110° C.

TABLE I

Comparison of the BS 148/59 and the Proposed IEC Oxidation Test Procedures

Test method	BS 148/59	IEC
Oxidizing agent	Air is bubbled through the oil at 2 l/hr	Oxygen is bubbled through the oil at 1 l/hr
Test vessel	See Fig 1 (*a*) (flask)	See Fig 1 (*b*) (test tube)
Quantity of oil	100 g	25 g
Catalyst	Copper foil, 51 mm × 32 mm	Pure electrolytic copper wire 1·016 mm dia, 30·5 cm long (ASTM catalyst)
Oxygen inlet tube	Id 4 ± 0·02 mm Od	Id 3 mm (min) Od 4·5 mm (max) 60° bevelled edge
Clearance of the inlet tube from vessel bottom	3 mm	As fixed by the edge
Condenser temp	19°–21° C (inlet)	Condenser not specified
Test temp	150° ± 0·5° C	100° C
Test duration	45 hr	164 hr

A considerable proportion of the reaction occurs in the vapour phase in both cases. The reactions that take place are:

(1) Oxidation in the vapour phase, in the air space.

(2*a*) Oxidation in the body of the liquid due to the oxygen that has dissolved in the oil.

(2*b*) Oxidation at the surface of the air bubbles as they rise to the surface of the liquid.

(3) Reaction of the oxidation products with the copper foil or other catalyst.

(4) Catalytic action of the copper or other metal catalysts.

The parameters that affect the test results are given below:

(1) The rate of air or oxygen flow (x).

(2) The depth to which the inlet tube is immersed in the oil (d).

(3) The size of the inlet tube.

(4) The leaks at the joint of the condenser and flask. If a leak is present here, the composition of the oil will be altered when the oil vapours escape, thus changing the viscosity and oxidizability of the oil in the liquid phase. This is of

particular importance in the BS 148 test, since the temperature at the joint will be very close to 150° C.

(5) The condenser temperature in the BS 148 test and the room temperature in the IEC test, since this affects the mean temperature of the vapour phase reaction.

(6) The volume of the air space, and hence the mean temperature of the vapour phase reaction.

(7) The partial pressure of the oxygen in the atmosphere. In the IEC test this has no significance.

(8) The flash point of the oil or the fractional distillation curve of the oil, since this property of the oil determines the proportion of the oil that will be in the vapour phase at the test temperature.

(9) The duration of the test. This will affect the ratings of oils if the shape of the oxidation products *v.* time curves varies from oil to oil.

(10) The temperature of the oil, since this may, in addition to enhancing the rate of reaction, change the course of the reaction.

(11) Nature of the catalyst and its concentration or area.

(12) The effect of the oil volume (V_o).

The amount of sludge and acids formed during the course of the oxidation will be the sum of that produced in the air space, due to the vapour phase reaction and that produced in the body of the liquid. The effect of the different parameters on the vapour phase reaction and the liquid phase reaction will be discussed separately, and the effects of the reactions in both the vapour and liquid phase taken together will be analysed.

THE REACTION IN THE AIR SPACE

1. *The Effect of the Rate of Air Flow* (α)

When the rate of flow exceeds the rate of consumption of oxygen by the oil, then the concentration of the oxygen at the site of the reaction will be constant, and any further increase in the rate of flow will not affect the rate of oxidation. Since the rate of consumption of oxygen varies with the oil that is being tested, the critical rate of flow above which the reaction rate is not affected varies from oil to oil. The maximum rate of oxygen consumption is of the order of 100 ml/100 g of oil/hr.[11] Thus, if the rate of air flow is greater than 0·5 l air/hr, the vapour phase reaction rate will not be affected by the rate of flow.

2. *The Effect of the Depth of Immersion of the Inlet Tube A*

When the tube A (Fig 1 (*a*)) is in the air space above the liquid surface, the concentration of oxygen at the walls of the flask will be less than at the sides of the inlet tube. When the tube is placed below the liquid surface the air bubbles burst at the surface, distributing the oxygen throughout the air space. Thus, when the tube is placed in the air space the amount of products formed is very small. As the tube is immersed into the liquid surface the vapour-phase reaction rate increases until it becomes constant after a certain depth has been exceeded. This critical depth will be a function of the rate of flow (α), the area of cross-section of the flask, and the area of cross-section of the inlet tube.

3. *The Effect of the Tube Diameter*

Changing the diameter of the inlet tube A while keeping the rate of flow constant will alter the bubble radius (Appendix C). However, since the bubbles break up at the surface of the oil, this change in the radius should not affect the rate of the reaction in the air space.

4. *The Effects of Leaks*

The products formed in the air space are condensed and returned to the body of the liquid. The rate of oxidation of the oil is dependent on the composition of the oil. The effect of the overall reaction rate is not additive.[2] Further, the effect of the components on the overall viscosity is also not additive. The viscosity of the oil determines the time taken by the bubbles to reach the surface, and thus the extent of the reaction that occurs at the bubble surface. Therefore, if the vapour fractions escape through the leaks in the condenser flask joints, the composition of the oils will change and the rate of reaction in the liquid phase will be affected in a fashion that is unpredictable. All other factors being the same, the rate of reaction in the vapour phase will, apparently, decrease, since the products of oxidation that are lost will not be taken into account. (See Tables VI and VIII, Ref. 10, Pt III.)

In the IEC test a leak is provided by the hole in the cover glass. Certain fractions of the oil which are of low boiling point escape. This will affect the rate of oxidation of the oil. Further, this effect will depend not only on the particular components that are lost but also on their specific effect on the other components in the oil. It will also depend on the distribution of the various fractions as obtained from the distillation analysis.

5. *The Condenser Temperature*

When the condenser outlet temperature is increased the mean temperature of the vapour phase reaction will be increased. This effect may be seen from equation (7), Appendix B. The extent to which the vapours condense from the cover glass depends on the room temperature. However, the effect of variation in the room temperature on the formation of oxidation products could be well within the wide

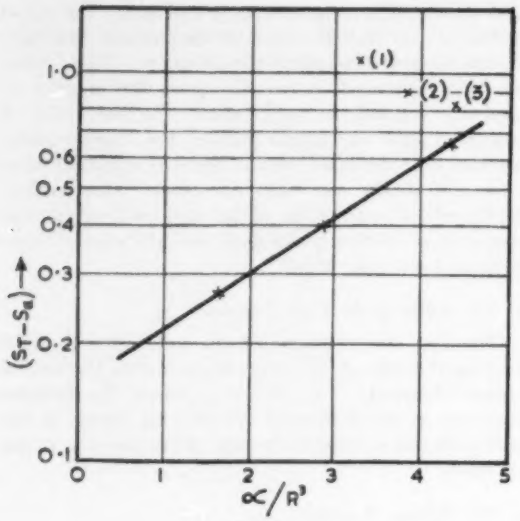

FIG 2

RELATIONSHIP BETWEEN $(S_T - S_a)$ AND α/R^3

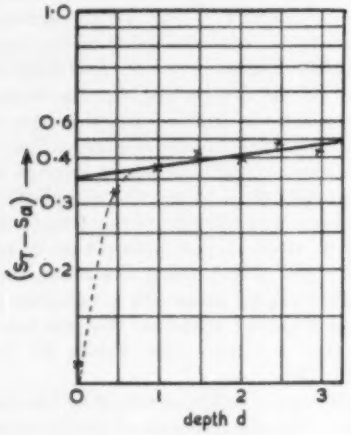

FIG 3

RELATIONSHIP BETWEEN $(S_T - S_a)$ AND DEPTH d

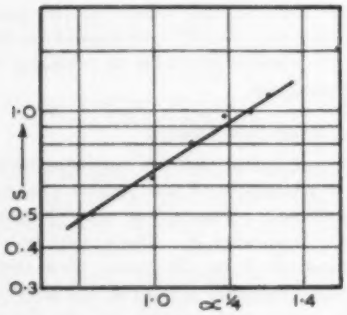

FIG 4

RELATIONSHIP BETWEEN SLUDGE S AND $\alpha^{\frac{1}{4}}$

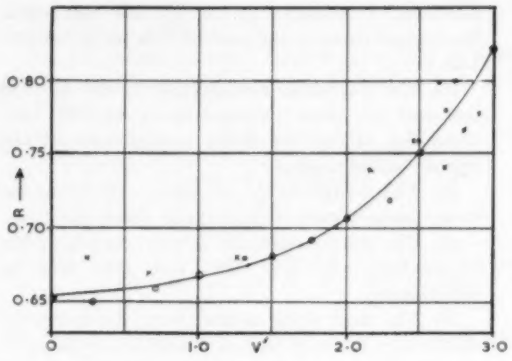

FIG 5

RELATIONSHIP BETWEEN R AND V'

× 4 cm depth ○ 2 cm depth
● 3 cm depth + 1 cm depth

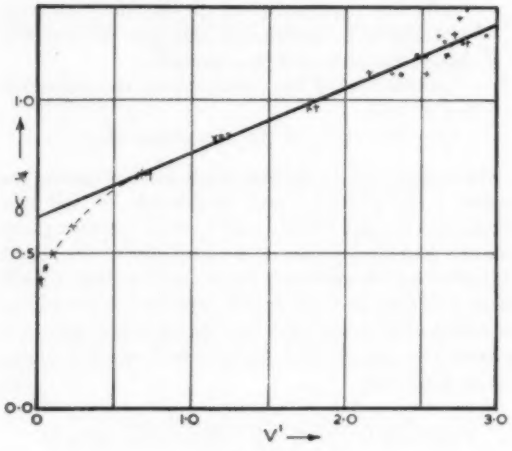

FIG 6

RELATIONSHIP BETWEEN $\alpha^{\frac{1}{4}}$ AND V'

× 4 cm depth ○ 2 cm depth
● 3 cm depth + 1 cm depth

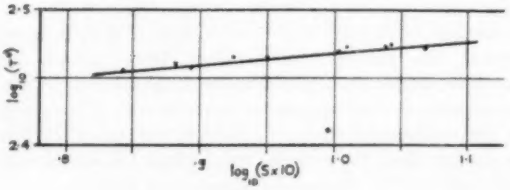

FIG 7

EFFECT OF THE CONDENSER TEMPERATURE ON THE SLUDGE VALUE

T Condenser temperature, ° abs
S Sludge, per cent

Values taken from Ref 17, *J. Inst. Petrol.*, 1446, **32**, 17, oil A in Table I

tolerance permitted by this test. Gossling and Romney [17] have studied the effect of condenser temperature on the test results, and the present analysis (Appendix B, equation (14(*b*)) agrees with their results (Fig 7).

6. *The Effect of the Air Space Volume*

During the course of the BS sludge test the temperature of the condenser walls is kept constant by adjusting the rate of flow of the cooling water. The temperature of the flask will be that of the bath up to the lips of the flask. The temperature then falls in two stages, up to the commencement of the cooled portion of the condenser, where it attains an intermediate value, and from there to the room temperature at some point within the condenser. Assuming, for simplicity of calculation, that the temperature varies linearly as the distance along the length of the condenser, it may be shown that

$$\log_e S = A_2 - A_2(V - V_o) \quad \text{(eqn (14), Appendix B)}$$

where S is the sludge produced in the air space. Thus the sludge (and acid) produced in the air space is proportional to the air space volume.

7. *The Partial Pressure of Oxygen*

This is of importance in the atmosphere, since it will determine the concentration of oxygen at the site of the reaction but, as explained earlier, if the rate of flow is fixed well beyond the critical rate of flow, any differences in the partial pressure do not matter. In the IEC test the oxygen is obtained from liquid air, and with the present arrangement is obtained from oxygen cylinders. So in this particular case the partial pressure of the oxygen in the atmosphere is of no significance.

8. *The Effect of the Flash Point*

The fraction of the oil present in the vapour phase during the course of the reaction will decrease as the flash point of the oil increases. Thus, with an oil having a low flash point the effects of leaks will be very pronounced. Also, the oxidation products of the vapour phase reaction will form a greater part of the total amount of oxidation products (see Table III, ref. 10, Pt III).

The parameters 9, 10, and 11 will be discussed later in the paper.

THE REACTION IN THE LIQUID PHASE

The reactions in the liquid phase will occur in the body of the oil, due to the oxygen present there and at the surface of air bubbles. The concentration of the oxygen in the body of the liquid may be expected to be substantially constant, since oxygen will diffuse into the body of the oil from the surface of the bubbles, as well as from the surface of the liquid. Thus, the variation in the rate of reaction is determined mainly by the reaction occurring at the surface of the bubble.

In the IEC test the area of the surface to depth ratio is very much less than in the BS 148 test (1 : 2 as compared to 11·4 : 1). Hence the reaction at the surface of the bubbles is of greater significance in the IEC test.

The rate of reaction occurring at the surface of the bubbles is proportional to the total area of the surfaces. If a fixed volume of gas is distributed in the form of small bubbles the total area of the bubble surfaces would be greater than if the same volume of gas was enclosed in one large bubble. So with smaller bubbles a higher rate of reaction will occur. Thus, if the inlet tube is not placed axially with respect to the copper cylinder or the inlet tube is too close to the bottom of the flask, a larger number of bubbles will be formed than is normal, giving rise to "rogue" values for sludge and acid which are always higher than the calculated value.

1. *Effect of the Rate of Flow* (α), *Depth of Immersion* (d), *and Inlet Tube Diameter*

The reaction rate depends mainly on the value of the bubble radius. So the variation of the reaction rate with the rate of flow will depend on the relation between the rate of flow and the bubble radius. Harkins and Brown[3] have shown that the minimum diameter of the bubble is a function of the surface tension and the tube diameter. This minimum diameter is attained when the bubble is formed very slowly, say for a period longer than 3 minutes. When the bubble is formed faster the volume of the bubble, and thus the radius, is always larger than this minimum value.

Sugden[4] has shown that a certain maximum pressure is necessary to break the bubble from the tube. This pressure is dependent on the surface tension.

However, it may be seen that if the rate of flow is kept constant the effect of the surface tension is compensated by the extra pressure that is required to detach the bubble from the tube (Appendix A).

After the bubble is detached from the tube it remains in contact with the liquid till it reaches the surface. The extent of reaction is proportional to the product of the area of the bubble surface and time (t_1) for which it is in contact with the oil. This time depends on the radius of the bubble and on the viscosity of the liquid.

The discussion above is regarding the rate of oxygen absorption of the oil. A detailed analysis of the experimental results published in literature [5–9] shows that the acids (A) and the sludge (S), formed at the end of a fixed time interval (t) are related to the total

oxygen absorbed by the oil (O), as given in equations (1) and (2)

$$\log_e A = \phi_1 0 + \phi_2 \frac{do}{dt} + \phi_3 \quad . \quad . \quad (1)$$

$$\log_e S = \phi_1 0 + \phi_2 \frac{do}{dt} + \phi_3 \quad . \quad . \quad (2)$$

The oxidation occurs in the vapour phase, in the body of the oil, and at the oxygen or air bubble surface. If S is the total sludge and A the total acids as measured at the end of the test period, and S_T and A_T the sludge and acids produced in the vapour phase reactions, then $(S - S_T)$ and $(A - A_T)$ will be the sludge and acids formed due to the reactions at the bubble surfaces. The oxygen reacting at the bubble surface is given by

and $0 = k'_4 \alpha = O_{05} k'_5 \alpha \frac{d}{R^3} t_o$ (from eqn (26), Appendix A) . . . (3)

where $k'_5 = (9/4) k k_2 \mu$ . . . . . (3*a*)

From equations (1–3) are obtained for the sludges and acids formed at the bubble surfaces the expressions

$$\log_e (S - S_T) = \phi_4 \alpha \frac{d}{R^3} + \phi_3 \quad . \quad . \quad . \quad (4)$$

$$\log_e (A - A_T) = \phi_4 \alpha \frac{d}{R^3} + \phi_3 \quad . \quad . \quad . \quad (5)$$

The value of S_T and A_T will be constant under the usual conditions of test. (See Appendix A.)

The effect of the depth of immersion (d) is also governed by equation (4). Thus, as the depth increases the total sludge increases, the increase being due to the increase in the rate of sludge formation at the surface of the bubbles (equation (45), Table D, Appendix A).

2. *Effect of the Oil Volume* V_o

On the basis of arguments given in Appendix B, it may be shown that the total oxygen absorption value is given by

$$0_o = A_6 + A_7 x_1 - P_2 x_1^2 + P_3 e - P_4 x_1 - A_1 V_o$$

(Appendix B, eqn (37)

where x_1 is the depth of the oil in the flask and V_o is the volume of the oil.

It may be seen from Fig 1 that as V_o increases x_1 also increases. Nevertheless, the total oxygen consumed will be reduced. Therefore, as the volume of the oil increases the percentage of the oxidation products formed will decrease (Ref 10, para 2, p. 370).

3. *Effect of the Tube Diameter*

Experiments carried out here showed that the radius of the bubble is a function of the tube diameter.

Inlet tube diameter = 0·59 cm ($R = 0{\cdot}00871\ V' +$

$0{\cdot}645 = 0{\cdot}76$ cm ($R = 0{\cdot}0087\ V' + 0{\cdot}720$)

Thus the tube diameter will affect the amount of oxygen taken at the surface of the bubble — O_{os}. As the bore of the tube increases the sludge value should decrease. This tendency may be noticed in the results given by Massey (Table V, ref 10, Pt III).

THE COMBINED VAPOUR PHASE AND LIQUID PHASE REACTIONS

1. *Effect of Temperature*

That optimum aromacity[2] and optimum refining[18] is essential is well known. This indicates that the oxidation of the oil is affected by its composition. When the oil is heated the composition of the liquid phase will be altered, depending on the temperature adopted for the test, as well as on the relative distribution of the components of various boiling points. Thus an oil with a larger percentage of low boiling point fractions will give less reproducible results than the oil having a lower percentage of low boiling point fractions. This statement holds for both the BS 148 and IEC tests. In fixing up the maximum permissible temperature, the composition of the oil should be borne in mind. The present specifications for the flash point and viscosity govern this to some extent.

In the BS 148 apparatus a joint is provided between the flask and the condenser. At this point the temperature of the vapour is approximately equal to the bath temperature. If a leak should occur at the joint a considerable amount of vapour will escape. This could affect the oxidation, depending on the nature of the oil. In fact, Massey[10] has said that a $\frac{2}{1000}$-inch opening has considerable effect on some oils. This criticism is true of the IEC test to a greater extent. In the IEC test an opening is provided at a point where the temperature would be about 10 per cent less than the test temperature. Whereas it is possible that with great care a leak may be prevented at the flask–condenser joint of the BS apparatus, it is impossible to do so with IEC apparatus.

2. *The Duration of the Test*

It has been found by many workers[1,10,11] that the shapes of either the acidity, sludge, or oxygen absorption *v.* time curves vary with both the catalyst concentration and the temperature. It is due to the fact that whatever the time interval and catalyst concentration selected, some oils are liable to be wrongly rated. Since the shapes of the curves are also altered, obtaining the entire curve of oxidation products with respect to time is not of much value. This difficulty seems to be inherent in the very nature of the oils that are used.

However, one fact has been noted by some workers[19-21] while studying the oxidation of lubricating oils. For example, Boozer and Fenske[19] have stated that " for a given hydrocarbon oxidized to the same extent, the amount of oxygen reacting per mole of hydrocarbon oxidized and the amount of products formed appeared to be independent of temperature and catalyst," agreeing with the opinion of Fenske *et al.* Thus, the products formed are a function of the amount of oxygen absorbed by the oil irrespective of the mode by which the oxidation has been affected. If this is true of the oxidation of all the mineral oils a way might be found out of the present difficulty. The oxygen absorption, acidity, peroxide, and sludge values could be determined for different intervals of time. The value of these products as related to the oxygen absorbed would give characteristic behaviour curves for the oil. Perhaps sludge values would not be very useful, since different oils precipitate different amounts of the copper into the sludge. Until this fact is verified for a large number of oils there does not seem to be any solution to the present problem of fixing a proper duration for the test or for fixing the concentration of the catalysts. Selecting a fixed time interval does not give as much information as obtaining the acidity or sludge *v.* time of oxidation curves. The IEC test may be conveniently adopted to determine the concentration of the oxidation products with time.

CATALYSTS

The products of oxidation, as well as the metals added to the oil, act as catalysts. That this is so is well known and a detailed analysis of the experimental results published in refs[5-9] has led to postulations P1 and P2 (Appendix A). This study also indicated that the copper seemed to act as a catalyst by enhancing the activity of " A." Copper has been used both in the form of foil or in the form of a copper salt soluble in the oil. In both forms the rate of oxidation has been found to be enhanced. Thompson[1] has shown that homogeneous catalysis occurs. Apparently the copper goes into solution, and when in solution it acts as a catalyst, since he found that the reaction proceeds at the same rate at which it was progressing even if the foil is removed during the middle of the experiment.* With the same oil the sludge/acid ratio depends on whether a solid catalyst or a soluble catalyst is used.† However, invariably the amount of acids formed with the solid catalyst is less than with a soluble catalyst. For example, when solid copper and soluble copper were used, the graphs given by Liander and Ericson [5] show that when 0·2 per cent sludge is formed the corresponding values of acidity for solid and soluble copper are 0·4 and 1·4 mg KOH/g oil, the corresponding sludge/acid ratios being 0·5 and 0·143. Bawn and Moran [22] have shown that the addition of a soluble catalyst in the middle of an experiment causes a sudden rise in the rate of reaction and after some time the original rate is maintained. As Thompson has put it, in the discussion of his paper,[4] " Each oil seems to know how much catalyst it must precipitate in order to retain the ' correct ' amount (for that oil) in solution." Massey[10] has obtained curves which show a peak in the acidity value as the temperature is varied when a copper foil is used as a catalyst. One possible explanation could be that the acids break down at higher temperatures, or the rate of oxygen supply is inadequate.[5]

However, in view of the facts mentioned earlier, it seems more probable that the products of oxidation (A and A′ of postulate P1) react with the copper foil to form catalytically inert compounds which settle down as sludge. The rates of reaction will be enhanced as the area of the copper is increased. Thus the acid to sludge ratio will fall as the copper area is increased, this effect being enhanced by the rise in the test temperature.

Bawn and Moran's results[22] and Thompson's results referred to above show that most of the copper in solution passes into the sludge. Also, normally less than 5 ppm is found in the oil obtained from transformers in service. Yet it has been found possible to enhance the rates of reaction by increasing the copper concentration. This could be possible only if the products of oxidation are catalytic in action. During the interval of time when the extra copper is in solution, large quantities of intermediate products may be formed which maintain the reaction rate even after the extra copper has been deposited in the sludge. The extent of the copper that would be in solution and its effect on the reaction rate would be a characteristic of the oil. This renders it very difficult to select the proper catalyst concentration, since it must suit the character of the particular oil that is being tested. This implies that accelerating the test by increasing the copper concentration cannot give results capable of being extrapolated to service conditions.

It has been discussed that the main reason for this difficulty is because the products of oxidation formed before the copper deposits in the sludge seem to affect the rate catalytically. From the postulate P1 (Appendix A) it may be shown that the acids and the sludges formed are functions of the peroxides formed. The peroxide formed is a function of the oxygen that is absorbed. This once again leads to the conclusion that accelerated tests may be useful for extrapolation if the acidity, peroxide content, and perhaps sludge values are obtained for various quantities of oxygen absorbed.

* Seventh series of experiments, ref 1.

† Second series of experiments, para 4, ref 1.

CONCLUSIONS

From this study it may be concluded that both the BS 148/51–59 as well as the IEC tests have inherent limitations. These limitations are partly due to the test procedures that have been adopted and partly to the complicated effects of the oil composition and catalysts on the process of oxidation.

Some of the limitations of the test may be removed by changing the specifications for the apparatus and the procedure of testing. Thus, for example, a specification should be given fixing the depth of the tube outlet from the surface of the oil and the height to which the oil should be filled up in the tube, rather than fixing the weight of the oil used and fixing the clearance from the bottom of test tube. A condenser with a joint at the proper place should be specified.

The test may be made more useful if the oxygen absorption is obtained and the acid, sludge, and peroxide formation is shown as a function of the oxygen absorption. Perhaps acid and sludge formation given as a function of the peroxide formation would be equally useful.

These conclusions should be verified in the light of extensive experimental evidence. In view of the complicated nature of the test, it is felt this evidence can be obtained only by co-ordinating the work done throughout the world as it is being done at present by the IEC.

ACKNOWLEDGMENT

The authors wish to thank L. Massey, Research Department, Associated Electrical Industries Ltd, Manchester, for his valuable criticisms and suggestions.

References

[1] Thompson, C. N. *J. Inst. Petrol.*, 1958, **44**, 295.
[2] von Fuchs, —, and Diamond, D. H. *Industr. Engng Chem.*, 1942, 933.
[3] Harkins, —, and Brown, —. *J. Amer. Chem. Soc.*, 1919, 499.
[4] Sugden, —. *J. Chem. Soc.*, 1922, 858; 1924, 27.
[5] Liander, H., and Ericson, G. ASTM Special Technical Publication 172, p. 11.
[6] Salomon, T. ASTM Special Technical Publication 172, p. 40.
[7] Ericson, G. ASEA 31, No. 1–2, p. 16 (1958).
[8] Thompson, C. N. ERA Report E/T 73, 1958.
[9] Irving, R., and Bravey, D. W. ASTM Special Technical Publication 172, p. 48.
[10] Massey, L. *J. Inst. Petrol.*, 1952, **38**, 361.
[11] Massey, L., and Wilson, A. C. M. *J. Inst. Petrol.*, 1958, **44**, 336.
[12] Chisholm, T. H. CIGRE Paper No. 104, 1954.
[13] Gossling, P. W. L. *J. Inst. Petrol.*, 1958, **44**, 273.
[14] Call, R. G. ASTM Special Technical Publication 95, p. 21 (1949).
[15] Humoritch, —. *Engineer, Lond.*, 1947, **184**, 608.
[16] Pollitt, A. A. *J. Inst. Petrol.*, 1946, **32**, 414.
[17] Gossling, P. W. L., and Romney, J. *J. Inst. Petrol.*, 1946, **32**, 424.
[18] Doble, F. C. *Elect. Engr*, 1946, 546.
[19] Boozer, E. R., and Fenske, M. R. *Industr. Engng Chem.*, 1952, **44**, 1850.
[20] Fenske, M. R., *et al.* *Industr. Engng Chem.*, 1941, **33**, 516.
[21] Hicks-Bruun, H. M., *et al.* *Industr. Engng Chem.*, 1944, **36**, 562.
[22] Bawn, C. E. H., and Moran, D. P. *J. Inst. Petrol.*, 1958, **44**, 290.

APPENDIX A

Determination of the Oxygen Absorbed by the Oil In the Liquid Phase

$$\frac{dO_b}{dt} = \frac{dO_{dz}}{dt} - \frac{dO_{ob}}{dt} + \frac{dO_{da}}{dt} \quad . \quad . \quad (1)$$

$$\frac{dO_o}{dt} = \frac{dO_{ob}}{dt} + \frac{dO_{ot}}{dt} + \frac{dO_{oa}}{dt} \quad . \quad . \quad . \quad (2)$$

$$\frac{dO_{ob}}{dt} = k \,.\, O_b \,.\, 1 = k_b \quad . \quad . \quad . \quad . \quad (2a)$$

$$\frac{dO_{oa}}{dt} = k \,.\, O_a \,.\, L = k_a'' L = k_a' \quad . \quad . \quad (2b)$$

$$\int_o^t \frac{dO_o}{dt} \,.\, dt = O_1 + \int_o^t \frac{dO_{oa}}{dt} \,.\, dt \quad . \quad . \quad (3)$$

When steady conditions are attained $\frac{dOz}{dt} = o$.

Therefore

$$\frac{dO_{ob}}{dt} = \frac{dO_{ds}}{dt} + \frac{dO_{da}}{dt} \quad . \quad . \quad . \quad . \quad (4)$$

Now $O_{zt} \simeq O_a$, since the partial pressure of the oxygen in the air space and in the bubble are almost identical because the excess pressure required to form the bubble is a very small fraction of the atmospheric pressure at which the experiment is carried out (being of the order of 0·2–0·3 cm Hg).

$$\frac{dO_{da}}{dt} = k_d \,.\, a_a \,.\, (O_a - O_b) \quad . \quad . \quad . \quad (5)$$

$$\frac{dO_{ds}}{dt} = k_d \,.\, a_s \,.\, (O_a - O_b) \quad . \quad . \quad . \quad (6)$$

($a_a \simeq 38{\cdot}5$ sq cm, $a_s \simeq 2{\cdot}0$ sq cm, with the inlet tube dia of 0·6 cm, 2 bubbles/section, 2 l/hr, 10 bubbles/min, 2 cm/sec, gas velocity).

O_b remains substantially constant during the course of the sludge test. The variation in (dO_o/dt) is determined by the variation in the value of (dO_{ot}/dt).

The Determination of O_s

$$\frac{dO_{ot}}{dt} = k \,.\, O_s = k \,.\, a_s \,.\, v \quad . \quad . \quad (7 \text{ \& } 7a)$$

Since the experiment is carried out for a fixed interval of time

$$O_s = k_1 \,.\, a_s \,.\, v, \text{ where } k_1 = kt_o \quad . \quad (8 \text{ \& } 8a)$$

$$(p - dg\rho) = 2\gamma/R \quad . \quad . \quad . \quad . \quad . \quad . \quad . \quad . \quad (9)$$

The volume of each bubble

$$V = (4\pi/3)R^3 \quad . \quad . \quad . \quad . \quad . \quad . \quad . \quad (10)$$

The number of bubbles/sec is

$$v' = 3\alpha/4\pi R^3 \quad . \quad . \quad . \quad . \quad . \quad . \quad . \quad (11)$$

$$v = (3\alpha t_1)/(4\pi R^3) \quad . \quad . \quad . \quad . \quad . \quad . \quad (12)$$

From equations (8) and (12)

$$O_s = kt_o(4\pi R^3)\,(3\alpha t_1)/(4\pi R^3) \quad . \quad . \quad . \quad (13)$$

$$= (3kt_o\alpha/R)t_1 \quad . \quad . \quad . \quad . \quad . \quad . \quad (13a)$$

$$= (3kt_o\alpha)\,(p - d\rho)\,(\tfrac{1}{2}\gamma)t_1 \quad . \quad . \quad . \quad (13b)$$

Calculation of t_1

Retarding force preventing the bubbles from rising

$$= k_2\eta R(ds/dt) \quad . \quad . \quad . \quad . \quad . \quad . \quad (14)$$

Buoyance force is given by

$$(4/3)\pi R^3(\rho - \rho_o)g \quad . \quad . \quad . \quad . \quad (15)$$

$$(4/3)\pi R^3\rho_o(d^2s/dt^2) = (4/3)\pi R^3(\rho - \rho_o)g - k_2\eta R(ds/dt) \quad (16)$$

or
$$\frac{d^2s}{dt^2} = \frac{(\rho - \rho_o)g}{\rho_o} - \frac{3k_2}{4R^2} \cdot \frac{ds}{dt} \cdot \frac{\eta}{\rho_o} \quad . \quad . \quad (17)$$

$$\simeq \frac{\rho g}{\rho_o} - \frac{3k_2}{4R^2} \cdot \frac{ds}{dt} \cdot \frac{\rho}{\rho_o} \cdot \mu$$

and if
$$a_1 = \rho/\rho_o \quad . \quad . \quad . \quad . \quad . \quad . \quad . \quad . \quad . \quad (18)$$

$$a_2 = (3k_2\rho\mu)/(4R^2\rho_o) \quad . \quad . \quad . \quad . \quad . \quad . \quad . \quad (19)$$

$$s = (a_1/a^2_2)t_1 + (a_1/a^2_2)(e^{-a_2t_1} - 1) \quad . \quad . \quad (20)$$

since at $t = 0$, $s = 0$.

The distance travelled by the bubble in time t_1 is d.

$$\therefore \quad d = (a_1/a_2)t_1 + (a_1/a_2^2)\,(e^{-a_2t_1} - 1) \quad . \quad . \quad (21)$$

From equation (19) a_2 is positive and large and so in the first approximation $(e^{-a_2t_1})$ may be neglected.

Therefore
$$d \simeq (a_1/a_2)t_1 \quad . \quad . \quad . \quad . \quad . \quad (22)$$

or
$$t_1 \simeq k_3 \frac{d}{R^2} \quad . \quad . \quad . \quad . \quad . \quad (23)$$

where
$$k_3 = (3k_2\mu)/4 \quad . \quad . \quad . \quad . \quad . \quad (24)$$

Calculation of O_o, O_t, and A and S

Going back to equation (13*b*), be obtain

$$O_t = kt_o\,3\alpha\,\frac{(p - d\rho)}{2\gamma} \cdot \frac{3k_2}{4} \cdot \mu \cdot \frac{d}{R^2} \quad . \quad . \quad . \quad (25)$$

$$= (9/4)kt_ok_2(\mu\alpha d/R^3) \quad . \quad . \quad . \quad . \quad . \quad (26)$$

$$O_o = O_a + O_b + O_t \quad . \quad . \quad . \quad . \quad . \quad . \quad (27)$$

Since O_a and O_b will be a constant for any particular oil sample (see discussion on the air space reaction),

$$O_o = k_4 + (k_5)(\mu\alpha d/R^3) \quad . \quad . \quad . \quad . \quad (28)$$

where
$$k_4 = O_a + O_b \quad . \quad . \quad . \quad . \quad . \quad (28a)$$

$$k_5 = kk_2(9/4)t_o \quad . \quad . \quad . \quad . \quad . \quad (28b)$$

Assuming that any transformer oil may be treated as a homogeneous product capable of being subjected to a kinetic analysis, and that the reactions that occur in the oil may be represented as follows:

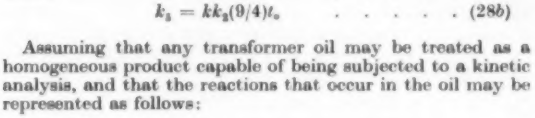

External and internally produced inhibitors react with the free radicals (A') . . . . . (P2)

It can be shown that

$$\log_e S = \phi_1 O + \phi_2(dO/dt) + \phi_3 \quad . \quad . \quad (29)$$

$$\log_e A = \psi_1 O + \psi_2(dO/dt) + \psi_3 \quad . \quad . \quad (30)$$

Equations (29) and (30) have been verified with the experimental results published in refs. 5–9 and found to be justified.

From equations (28) and (29) we obtain

$$\log_e S = \psi_4(\mu\alpha d)/R^3 + \psi_5 \quad . \quad . \quad . \quad . \quad (31)$$

Effect of the Temperature on Acidity

Suppose that the acid reacts with the copper foil to form non-catalytic products:

$$(dA/dt) = (dA_o/dt) - (dA_c/dt) \quad . \quad . \quad . \quad (32)$$

Where (dA_o/dt) is the rate at which the acid is formed from the oil and (dA_c/dt) is the rate at which it reacts with copper.

When $(dA_o/dt) = (dA_c/dt) = 0$ and the acidity does not increase with time. This fact is apparent from the graphs given by Massey.[10]

Assuming that the postulations (P1) and (P2) are justified, it follows that

$$dA_o/dt = k_5A'A \quad . \quad . \quad . \quad . \quad . \quad . \quad . \quad (33)$$

$$\therefore \quad dA/dt = AA_1k_{36}A'e^{-B_3t/T} - AA_2k_{re}e^{-B_rt/T} \quad . \quad (34)$$

$$\log_e A = A_3'\int_o^{t_o} A'dte^{-B_3t/T} - A_4e^{-B_rt/T} \quad . \quad (35)$$

The experimental results given by Massey in Figs 13, 14 and 20 in ref 10, Pt III, have been analysed. The equation satisfying the data is of the form:

$$y = A_1(e^{-B_1x})(A_2e^{-B_2x} - 1) - A_3(e^{-B_3x}) - \quad (36)$$

where
$$y = \log_e (A/e)10^3 \quad . \quad . \quad . \quad . \quad . \quad . \quad . \quad (36a)$$

and
$$x = (1/T)10^3 \quad . \quad . \quad . \quad . \quad . \quad . \quad . \quad (36b)$$

The values of the constants are given in Table A.

Apparently $\int_o^{t_o} A'dt$ is given by $(A_2e^{-B_2/T} - 1)$.

TABLE A

Values of the Constant Pertaining to Equation (36)

Figure No.	Formation of A		Concentration of A'		Copper reaction	
	A_1	B_1	A_2	B_2	A^3	B^3
13	11·3	−4·0	22	−7·48	31·75	−11·25
14	12·07	−4·37	—	—	37·93	−12·07
20	16·5	−6·37	25·9	−9·13	36·6	−13·0

Effect of the Reaction in the Air Space on the Constants Pertaining to Equation (36)

If the heats of activation of the vapour and liquid phases are not identical, an additional term $(-A_4e^{-B_4/T})$ would be present in equation (36). If, on the other hand, the heats of activation are identical and the collision factors differ, then the constant A_4 would merge in the constant A_1 and the equation type would be as is given in (35). From the values given in Table A it seems as if the latter condition is satisfied.

Effect of the Bubble Breaking into Smaller Bubbles on the Reaction Rate

Let a bubble of volume V break up into n smaller bubbles of V_n each.

$$A_o = 4\pi\left[\frac{3}{4\pi}\right]^{\frac{1}{3}} V \quad . \quad . \quad . \quad . \quad (37)$$

$$A_n = 4\pi[3/4\pi]^{\frac{1}{3}}V_n \quad . \quad . \quad . \quad . \quad (38)$$

The time taken by the bubble to rise to the surface is

$$t_v = (3/4)k\mu d(1/R_v^2) \quad . \quad . \quad . \quad (39)$$

$$t_n = (3/4)k\mu d(1/R_n^2) \quad . \quad . \quad . \quad (40)$$

$$\frac{nA_nt_n}{A_vt_v} + n \quad . \quad . \quad . \quad . \quad (41)$$

Therefore, when the bubble breaks up into n bubbles, the oxygen absorbed by the oil increases n times (ref; points 1, 2, 3 in Fig 2).

The Relationship between v' and R

The equations derived earlier were checked against the experimental results published by Massey.[10] Before the results could be checked it was necessary to find the relationship between v' and R. An experiment was conducted by passing air through the standard inlet tube used in the BS 148 sludge test. The depth d was varied from 1 to 4 cm from the surface of the oil. The number of bubbles formed per second was obtained and the rate of flow was also measured. With the aid of these values v' and R were calculated. The values of v' and R did not vary with the depth d so long as the rate of flow α was kept constant. This should be so, since v' and

R depends on $(p - d\rho g)/\gamma$ which remains constant. The experimental results could be expressed by the equation

$$R = 0{\cdot}00871\, e^{\alpha'} - 0{\cdot}645 \quad . \quad . \quad . \quad (42)$$

The values of R were calculated for the corresponding values of α by using the expression given in equation (43).

$$R = \left[\frac{3}{4\pi} \cdot \frac{10^3}{3600}\right]^{\frac{1}{3}} \left[\frac{\alpha}{v'}\right]^{\frac{1}{3}} \quad . \quad . \quad . \quad (43)$$

Effect of α on the Sludge Formation

It has been explained earlier that when α is increased to a value beyond 500 ml/100 g oil/hr, the sludge formed in the air space and in the body of the liquid will be constant. Let this sludge be designated as S_a and the total sludge that is measured in the sludge test as S_t. Then from equation (31)

$$\log_e (S_t - S_a) = \theta_1 + \theta_2(\alpha/R^3) \quad . \quad . \quad (44)$$

The validity of equation (44) is shown in Fig 2 and in Table B.

From Table B it may be seen that as R increases beyond a certain value the rate of reaction should fall, if the bubbles do not break up. If the bubbles break up into smaller ones the reaction rate increases. The space between the inlet tube and the copper foil is about 0·5 cm when the experiment is carried out carefully. If R increases by more than 0·2 to 0·25 cm, the number of bubbles should increase, causing an increase in the reaction rate. This would explain the values obtained for the points 1, 2, 3 in Fig 2.

TABLE B

Calculation of (α/R^3) and $(S_t - S_a)$

v	αl	α	R	R^3	S_t	S_a	$S_t - S_a$	α/R^3
1·0	0·84	0·50	0·670	0·304	0·50	0·23	0·27	1·64
1·5	0·94	0·77	0·685	0·325	0·59	0·23	0·40	2·86
2·0	1·04	1·45	0·712	0·364	0·85	0·23	0·60	4·00
2·5	1·14	1·69	0·729	0·390	0·86	0·23	0·63	4·34
3·0	1·34	2·46	0·822	0·560	1·05	0·23	0·82	4·40
3·5	1·34	3·20	0·926	0·830	1·12	0·23	0·89	3·85
3·9	1·43	4·25	1·066	1·29	1·32	0·23	1·09	3·30

Note. The values of S_t have been obtained from Fig 15, ref 10, pt III, and S_a from Fig 14 of the same reference.

The Effect of the Depth on the Sludge Value

From equation (31) and allowing for the reaction occurring in the body of the liquid and in the air space:

$$\log_e (S_t - S_a) = \theta_3 + \theta_4 d \quad . \quad . \quad . \quad (45)$$

The validity of this equation is checked with the results given in Fig 16 of ref 10 by Massey. These results are given in Table C and in Fig 3.

Effect of Variation in the Tube Bore (An Estimation)

From Table C, θ_3 is 0·111 and θ_4 is −1·9678 in equation (45). The effect of varying the bore between 3 and 4·5 mm does not

TABLE C

Calculation of $(S_t - S_a)$ for Variation in the Depth d

d	S_t	S_a	$S_t - \frac{S_a}{S'}$	$\frac{S_t'}{S_a'}$	$S_t - S_a$ (cal)	S_t (cal)	d
0·0	0·11	0·23	—	—	0·124	0·36	0·0
0·5	0·33	0·23	0·09	—	0·141	0·37	0·5
1·0	0·38	0·23	0·15	—	0·150*	0·38	1·0
1·5	0·41	0·23	0·18	0·835	0·168	0·40	1·5
2·0	0·40	0·23	0·17	1·055	0·178	0·41	2·0
2·5	0·44	0·23	0·21	0·810	0·188	0·42	2·5
2·9	0·42	0·23	0·19	—	—	—	—
(3·0)	—	0·23	—	1·125	0·199	0·43	(3·0)

Note. Average value for S_t'/S_a' is 0·946.

* is the initial value.

produce a very significant change in the test result because of the wide tolerance permitted in the sludge test. However, as the diameter decreases the test results would increase. This tendency may be noted in Table V given by Massey.[10] It would be difficult to assess the acidity values, since the reaction with the copper foil is a significant term in the rate of acid formation.

APPENDIX B

Effect of Temperature on the Air-Space Reaction Rate

In an experiment carried out with boiling water, the temperature in the condenser fell by about 50° C within 30 cm. In the neck it fell by 3·8° C in 7·5 cm. From the neck (points 3 to 4 in Fig 1 (*a*)) it fell by 14° C in 2·5 cm. The flask was in air without a constant temperature bath.

So, with the BS test conditions, it may be assumed that during the sludge test the temperature up to point 3 (Fig 1 (*a*)) is equal to the bath temperature T_1. It may be taken to fall uniformly to a temperature T_{o1} at point 4 and to the temperature T_{o2} within 30 cm length of the condenser. This fall is assumed to be linear with length along the condenser for simplicity of calculation.

$$T = T_1 - \frac{T_1 - T_o}{d_o} \cdot x \quad . \quad . \quad . \quad (1)$$

$$V = a \cdot dx \text{ for the cylindrical portions} \quad . \quad (2)$$

$$V_a = V - V_o \quad . \quad . \quad . \quad . \quad (3)$$

where V_a is the volume of the air space and the volume of the oil is V_o. Between points 3 and 4:

$$(dO/dt) = dV \cdot kz \cdot e^{-B/T} \cdot 1 \cdot 1 \quad . \quad . \quad (4)$$

$$O = \int_o^{x_1} \int_o^{l_o} k_o \cdot dV \cdot e^{-B/T} \cdot dt \cdot dx = k_o l_o a \int_o^{x_1} e^{-B/(m-nx)} dx \quad (5)$$

Therefore

$$O \simeq k_o l_o a x_1 + k_o l_o a (B/n) \log_e (m - nx)/m \cdot \quad (6)$$

where $m = T_1$ and $n = (T_1 - T_o)/x_1$. (7 & 8)

The oxygen in the constant temperature space is given approximately by:

$$k_o l_o (V - V_o)(1' - B/T_1) \quad . \quad . \quad . \quad (9)$$

Therefore the total oxygen consumed will be

$$\simeq k_o l_o [a_1 x_1 + a_2 x_2 + (V - V_o) + B\{(a_1/n_1)\log_e (T_1/T_{o1}) + (a_2/n_2)\log_e (T_2/T_{o2})\} - B(V - V_o)/T_1'] \quad (10)$$

$$\simeq A_1 + A_1(V - V_o) \quad . \quad . \quad (11)$$

$$\log_e S_{oo} \simeq A_2 + A_2(V - V_o) \quad . \quad . \quad (12)$$

Effect of Variation in the Oil Volume

$$\log_e S_{oo} \simeq A_3 - A_4 V_o \quad . \quad . \quad . \quad (13)$$

Effect of Variation in the Condenser Temperature

$$\log_e S_{oo} \simeq A_5' + A_6' \log_e T_o \quad . \quad . \quad (14)$$

Effect of the Reaction in the Liquid Phase

The reaction in the liquid phase will not be affected by the condenser temperature, so a constant term will be added to equation (14*b*), thus altering A_5' to A_5''.

The effect of the oil volume is not so simple, since an increase in the oil volume causes an increase in x_1.

Effect of the Liquid Phase Reaction on the Total Oxidation—Oxygen Consumption in the Body of the Liquid

Let c_x be the concentration of oxygen in a section of the oil at distance x from the bottom of the flask. After equilibrium is attained, the oxygen diffusing into the elemental volume $A_x dx$ will be equal to the oxygen consumed in that section.

$$dO_{ob}/dt_x = k_x c_x A_x dz = (dc/dx) \cdot m \cdot A_x \cdot dx \quad (15, 15a)$$

where $(dc/dx)dx$ is the "concentration potential" across the

layer, m the diffusion constant, and A_x the area of cross-section.

$$O_{ob} = \int_0^{x_1}\int_0^{x_1} k_3 c_x A_x \,.\, dx \,.\, dt = k_3 J_o \int_0^{x_1} c_x A_x \,.\, dx \quad (16, 17)$$

$$dc/dx = (k_o/m)c_x \quad (18)$$

$$\therefore \quad c_x = c_{x_1} e^{(k_o/m)(x-x_1)} \quad (19)$$

$$\text{Now } A_x = \pi(2R_f x - x^2)/R_f^2 \quad (20)$$

$$= -P_o x_1^2 + P_1 x - P_2 + P_3 e^{-P_4 x_1} \quad (21)$$

where

$$P_0 = \pi t_o c_{x_1} m/R_f^2 \quad (22)$$

$$P_1 = 2R_f P_o + (2mP_o/k_o) = 2P_o(R_f + 1/P_4) \quad (23)$$

$$P_2 = 2mR_f P_o/k_o = 2R_f P_o/P_3 \quad (24)$$

$$P_3 = 2P_o/P_4 \quad (25)$$

$$P_4 = k_o/m \quad (26)$$

From equation (26), Appendix A

$$O_{oa} = A_5 \,.\, d = A_5(x_1 - p) \quad (27, 28)$$

where p is the clearance of the inlet tube from the bottom of flask, and $d = (x_1 - p)$ (29)

$$\therefore \quad O_o = O_{oa} + O_{ob} + O_{oa} \quad (30)$$

$$= A_6 + A_7 x_1 - P_o x_1^2 + P_3 e^{-P_4 x_1} - A_1 V_o \quad (31)$$

where $A_6 = (A_1 + A_4 V - P_2 - A_5 p)$ (32)

$$A_7 = P_1 + A_5 \quad (33)$$

$$A_5 = (k_o J_o 9 k_3 \mu\alpha)/4R^3 \quad (34)$$

As V_o increases, x_1 also increases and the total oxygen consumed will be reduced and the percentage of oxidation products formed will decrease. In this matter para 2, p. 370, ref 10 may be cited (180 g oil gives 0·22 per cent sludge and 100 g oil gives 0·85 per cent sludge). So as V_o is increased the percentage of oxidation products fall.

APPENDIX C

Calculation of the Relationship between v, R, and α

An Empirical Relationship

The values obtained from Fig 14 of Ref 10 have been tabulated in Table D and plotted in Fig 4.

$$\log_e S \simeq \theta_5 \alpha^{\frac{1}{2}} + \theta_6 \quad (1)$$

This relationship can be obtained if it is assumed that the radius of the bubble is inversely proportional to the time of the bubble formation.

TABLE D

Relationship between $\alpha^{\frac{1}{2}}$ and S
(from ref 10, Fig 14, of Massey)

L/hr	S	$\alpha^{\frac{1}{2}}$
0·5	0·5	0·84
1·0	0·63	1·00
1·5	0·80	1·10
2·0	0·97	1·19
2·5	1·00	1·26
3·0	1·10	1·31
3·5	—	—
4·0	1·28	1·41

$$R^3 = 0{\cdot}645\alpha/v' \quad (2)$$

In Fig 5 the values of R v. v' obtained from an experiment have been plotted. The curve obtained indicates an equation of the type

$$R = a\,e^{cv} + b$$

The equation of the plotted curve is

$$R = 0{\cdot}00871\,e^{v} + 0{\cdot}645 \quad (3)$$

The tube used was the standard tube used in the BS sludge test, having a diameter of 0·4 cm ± 0·02 cm.

When the tube diameter is altered to 0·76 cm,

$$R = 0{\cdot}0087\,e^{v} + 0{\cdot}720 \quad (4)$$

TABLE E

Experimental Values Obtained for α and v′ using Transformer Oil

Depth	1 cm			2 cm			3 cm			4 cm		
L/hr	v'	R^3	R	v'	R^3	R	v'	R^3	R	v'	R^3	R
2·54	2·76	0·596	0·840	—	—	—	—	—	—	—	—	—
2·16	2·74	0·509	0·70	2·62	0·532	0·81	2·93	0·475	0·78	2·91	0·478	0·78
1·98	2·80	0·456	0·768	2·65	0·481	0·78	2·79	0·457	0·765	—	—	—
1·69	2·47	0·439	0·759	2·49	0·437	0·76	2·51	0·435	0·76	2·67	0·409	0·74
1·36	2·15	0·408	0·741	2·30	0·381	0·72	2·36	0·372	0·72	2·53	0·347	0·70
0·912	1·80	0·326	0·690	1·77	0·332	0·69	1·77	0·332	0·69	1·77	0·332	0·69
0·640	1·34	0·308	0·675	1·31	0·315	0·68	1·30	0·317	0·68	1·28	0·323	0·68
0·320	0·71	0·290	0·662	0·70	0·295	0·66	0·70	0·295	0·66	0·68	0·303	0·67
0·120	0·28	0·276	0·650	0·28	0·276	0·65	0·26	0·297	0·66	0·24	0·323	0·68

A LABORATORY-SCALE HIGH EFFICIENCY VACUUM FRACTIONATION UNIT *

By A. A. MOHAJER †

SUMMARY

In order to carry out the purification of the various intermediates and final products involved in the synthesis of high molecular weight naphthenic hydrocarbons, a vacuum fractionation unit has been constructed.

The column packing is a modified laboratory type of Stedman packing,[1-4] which is reported to have high efficiencies at low pressures, a relatively low liquid hold-up, and a low pressure drop.

For the maintenance of adiabatic conditions, constant pressure, and of constant boil-up rate, suitable automatic or manual devices are incorporated in the unit.

The column has been evaluated at 50 and 10 mm Hg absolute pressures, using the test mixture of *o*-dichlorobenzene and *p*-diethylbenzene.

The HETP of 1·85 cm and 3·27 cm are obtained at the absolute pressures of 50 and 10 mm Hg respectively.

DESCRIPTION OF FRACTIONATION UNIT

The unit is illustrated in Figs 1 and 4. Fig 1 shows a scale drawing of the stillpot and its chamber, reflux meter, the actual column, distillation head, and the multiple-receiver. Fig 4 illustrates the outline of the vacuum system.

Fractionating Column

The column consists of a 20-mm id precision glass tubing, 120 cm long, 116 cm of which is packed with the Stedman packing (153 pairs) of the cup and cone type. The packing is made from stainless steel gauze (25 mesh) and is illustrated in Fig 2, with the liquid and vapour paths shown in Fig 2 (*a*).

To assemble the packing in the column, each unit of packing was first made by pressing lightly together a cup and a cone so that the vapour passage hole in the cone was diametrically opposite to that in the cup. These units were then guided into the glass column by means of a suitable glass tubing in such a position that the hole in the cup of each unit was diametrically opposite to that in the cone of the unit below it.

The mechanism of vapour–liquid contact with this type of packing is stated to be as follows:

During the operation the liquid reflux passing down the column flows alternately to the centre and to the wall of the column, thus ensuring that a continuous film of liquid covers the gauze. Vapour flows into the cup–cone unit through the hole in the cup and out through the diametrically opposite hole in the cone. It then flows round the outside of the cone to the diametrically opposite hole in the next cup above. Vapour–liquid contact is thus restricted almost entirely to that between free flowing vapour and the liquid film, and there is no significant bubbling of vapour through the liquid. Consequently, liquid hold-up and pressure drop with this type of packing are small.

Column Accessories

Fig 1, together with the accompanying key, shows in sufficient detail the stillpot and its chamber, the reflux meter, the distillation head, and the multiple-receiver, as well as the column itself.

Here a few points must be mentioned with regard to the distillation head and the multiple-receiver system, since they are responsible, to a considerable degree, for the ease of operation of the unit.

Distillation Head (Letters A, Fig 1)

This is a total condensation liquid-divider type and has been so designed as to avoid the use of any taps, which tend to stick under reduced pressure.

The take-off line (A6) is normally closed by means of the glass rod (A3) standing on the small conical cup. A one-inch long piece of soft iron is sealed inside the cavity of the upper part of this glass rod. The electromagnet (A4) placed round the outside of the tube in which the glass rod stands is energized at variable intervals (2–50 sec) with a 12-V dc supply by means of an electric timer.

With this timer both the frequency of take-off and the duration of each take-off can be varied as required.

Multiple-Receiver ("*Pig*") (Letters B, Fig 1)

This consists of a 1-litre flask with a B55 neck to which are sealed internally 16 tubes which end in B19 sockets and through which the internally sealed liquid delivery tubes emerge. To these 16 tubes are fitted 16 receivers (B6), each with a capacity of about 40 ml.

To the bottom of the main flask is sealed a vertical glass tube which ends in a glass rod. A "bucket" (B2) with a curved delivery tube sits over this glass

* MS received 13 May 1960.

† British Nylon Spinners Ltd.

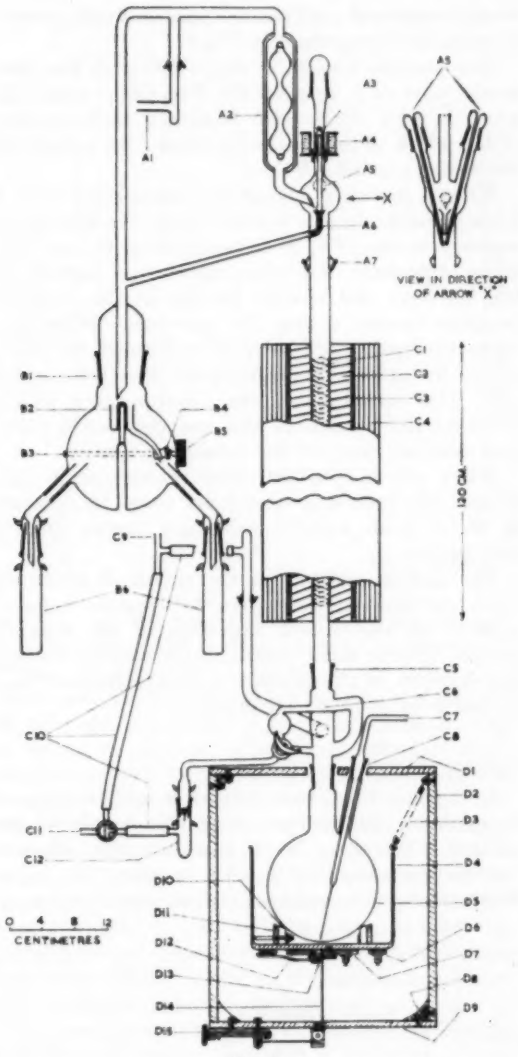

FIG 1

KEY TO FIG 1

A1 The line to the first cold-trap and the vacuum system
A2 Double wall condenser
A3 Glass rod plunger with the iron core sealed inside
A4 Electromagnet (enamelled copper wire, 28G, total resistance 9 ohms)
A5 Thermocouple pockets
A6 Liquid take-off capillary, 2 mm bore
A7 Spherical joints FS 25/40 MS 25/40

B1 B55 ground glass joints connecting distillation head to multiple receiver
B2 Bucket, distributing the distillate to the receivers
B3 Brass strip round which the external magnet slides
B4 Small permanent magnet (2 × 0·4 × 0·4 cm) fixed to the delivery tube of the bucket by means of a piece of Teflon
B5 The external magnet for positioning the delivery tube over the receivers
B6 Receiver bottles, with B19 cones, of which there are 16 altogether

C1 The column proper, precision glass tubing, 20 mm id packed with the Stedman packing
C2 Asbestos tape lagging between the column proper and the jacket heaters
C3 3-inch dia Duralumin pipes which carry the jacket heaters
C4 Corrugated asbestos pipe lagging
C5 B24 ground glass joints
C6 Reflux meter
C7 Nitrogen bleed to assist boiling
C8 B14 ground glass joints
C9 The line to one side of differential pressure manostat (PS)
C10 Rubber tube connexions
C11 The line for venting and evacuation of C12
C12 The receiver for sampling during calibration of column

D1 Sindanyo lid with the rear half fixed and the front half loose
D2 Asbestos cement tubing
D3 Three equally spaced springs keeping D4 centrally suspended in the chamber
D4 Thick-base aluminium saucepan, 7-inch dia with handle removed
D5 Stillpot, 1 litre capacity with B24 neck and B14 side-neck
D6 Main stillpot heater, Bray ring, 300 W, 240 V
D7 Subsidiary stillpot heater, Bray ring, 200 W, 240 V
D8 Asbestos filling to exclude air
D9 Sindanyo base
D10 Soft asbestos ring seating for the stillpot
D11 Duralumin ring, containing D10 between itself and a brass ring and the whole centred in the saucepan by three equally spaced brass rods
D12 Three equally spaced strips, holding D6 to the bottom of D4
D13 Central aluminium block holding D7 to the bottom of D4
D14 Thin Bowden cable with one end carrying a nipple and held in D13 and the other end passing through a hole in the centre of D9, over a pulley and fixed to the travelling screw; when the flask is in position this cable is loose
D15 Knob for lowering or raising the saucepan, in order to remove or replace the stillpot

rod. A small permanent magnet (B4) is fixed to the lower end of the delivery tube and a small, but relatively powerful magnet (B5) can slide round a brass strip (B3) fixed round the outside of the flask. Thus, by careful manipulation of the outside magnet, the end of the delivery tube of the bucket can assume positions over the mouth of each one of the 16 tubes.

Stillpot Heating Chamber

This is shown fairly clearly in Fig 1 (letters D) and the space here will be devoted mainly to the description of the control of the boil-up rate.

The heat to the chamber is supplied by two heaters.

(*a*) Main stillpot heater, Bray ring, 300 W, 240 V, adjusted by means of a Variac.

(*b*) Subsidiary stillpot heater, Bray ring, 200 W, 240 V, in series with a variable resistance.

Boil-up Rate Control

Fairly accurate control of the boil-up rate is achieved by means of the subsidiary stillpot heater (*Hss*) working on an "on–off" basis operated by the pressure drop through the column.

The pressure switch (*PS*) controlling this subsidiary

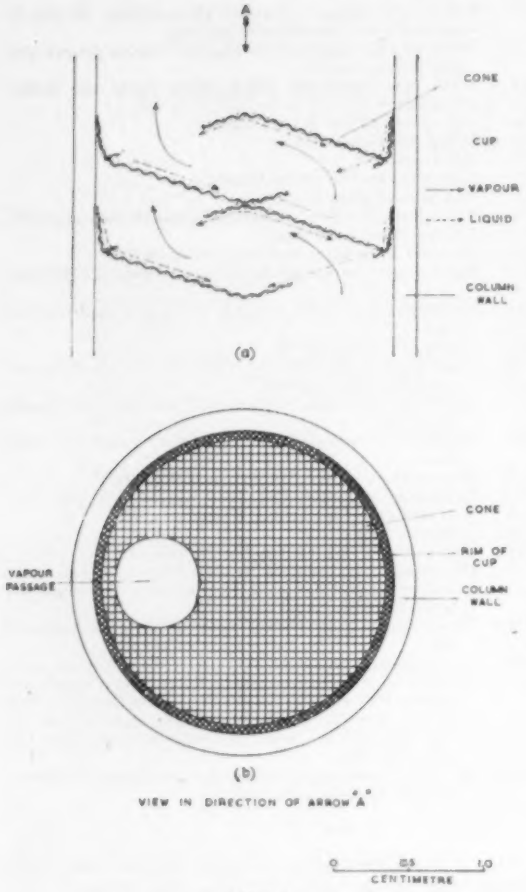

FIG 2

heater consists of a differential manostat with sealed-in contacts of tungsten wire (Fig 3).

This pressure switch, in conjuction with the electronic valve (*V*), operates the Post Office relay (*R*), which in turn switches the horseshoe electromagnet (*EM*), which in turn makes or breaks the contact in the mercury switch (*MS*).

When a particular boil-up rate corresponding to a given pressure drop is decided upon, the amount of mercury in the (*PS*) is adjusted so as to give this value of pressure drop when the level of mercury in the left limb just touches the tip of the sealed-in tungsten contact during the operation. When this contact is made, the current flows through the valve (*V*) to the extent of energizing the Post Office relay (*R*). This switches on the electromagnet (*EM*), breaking the contact in the mercury switch (*MS*) and thus switching off the subsidiary heater.

When the boil-up rate and pressure drop fall, exactly the reverse process takes place, the contact in *MS* is made and the subsidiary heater (*Hss*) is switched on.

The various resistors in the circuit of electronic valve are chosen so as to give the optimum value of current for the smooth operation of the mercury switch. Under these conditions the current through the contacts in the pressure switch is reduced to a workable value of 0·1 milliamp.

Column Heaters

In vacuum fractionation there is a wide range of temperature distribution along the length of the column. Therefore it is essential, for effective column operation, to be able to vary the jacket temperature independently in as many points as

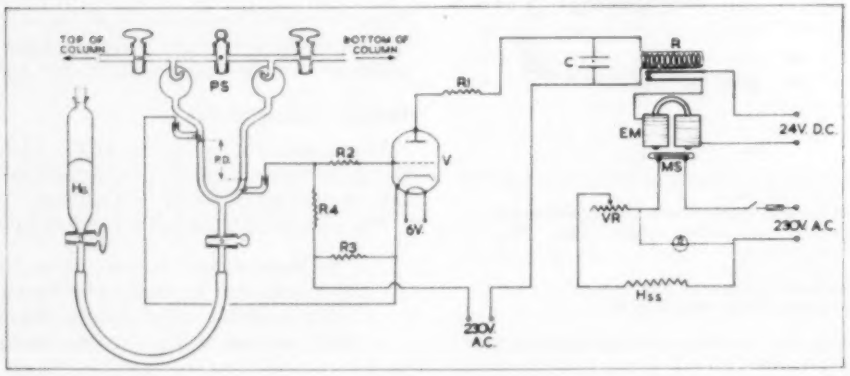

FIG 3

AUTOMATIC CONTROL OF BOIL-UP RATE

PS	Differential manostat	*R4*	250,000 Ω	*MS*	Mercury switch
V	Electronic valve, 6J5 GT/G	*C*	Condenser, 1 OMFD	*VR*	Variable resistance
R1	100,000 Ω	*R*	Post Office relay, 20,000 Ω	H_{ss}	Subsidiary stillpot heater, Bray ring, 200 W, 240 V
R2	250,000 Ω	*EM*	Horseshoe electromagnet		
R3	5000 Ω				

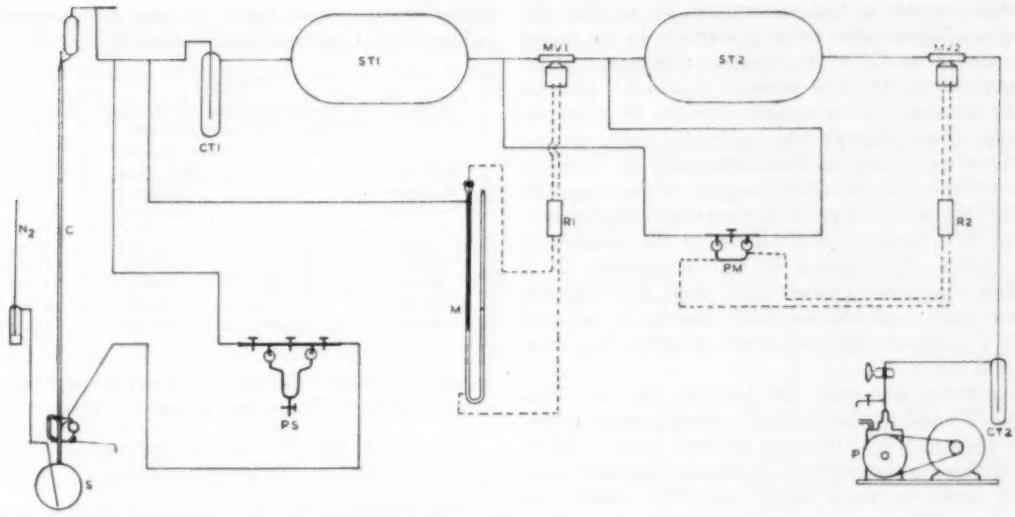

FIG 4

LINE DIAGRAM OF VACUUM SYSTEM

possible. In this case the heating of the column jacket is carried out in four separate sections, each covering approximately a quarter of the column.

Each one of these four heaters consists of a Duralumin tube approximately 1 ft long, 3 inches od carrying the resistance wire 30 G Brightray, 800–900 ohms suitably insulated between layers of silica cement and glass tape. The heat input to these heaters is adjusted by means of four separate Variacs (230 V input from a constant voltage transformer and 0–270 V output). The current to each heater is indicated by means of an ammeter (0–0·5 amp). The space between the glass column and the heater is taken by several layers of asbestos tape (1 inch × $\frac{1}{16}$ inch), and the column is finally lagged on the outside by a 1-inch thick corrugated asbestos pipe lagging.

The heat input to each section is adjusted so as to bring about adiabatic condition, as indicated by the differential thermocouples (see below).

Temperature Measurement and Adiabatic Control

Temperature of the centre of each section of the column and that of the vapour at the top of the column are measured by Chromel–Alumel thermocouples using a potentiometer.

Apart from the temperature-measuring thermocouples, differential thermocouples are made thus:

Chromel——•——Alumel——•——Chromel

One of these two junctions, together with the temperature-measuring thermocouple, is placed next to the column wall in the middle of each section of the column. The other junction is placed at the same level but close to the heater of that section. The two Chromel ends of the differential thermocouples are connected, through a selector switch, to the potentiometer. Any temperature difference between the column proper and the column heater at each section will deflect the galvanometer indicator one way or the other, whereas when there is no difference between these two temperatures, the galvanometer shows no deflection. By this means the column Variacs are so adjusted as to bring about, as far as possible, adiabatic condition throughout the length of the column.

It is usually regarded as preferable to keep the column very slightly wet, *i.e.* the heater side to be very slightly colder than the column side.

Vacuum System

The column is maintained under any desired reduced pressure by means of an electric vacuum oil pump working through two magnetic valves and two surge tanks, all placed in series, as shown in Fig 4.

Previous experience with other types of pressure regulators such as Cartesian manostats had shown them to have for our purposes certain limitations such as significant fluctuations of pressure. It was therefore decided to use magnetic valves operated by manometers with sealed-in contacts, in conjunction with electronic valve and Post Office relays.

The automatic operation of the first magnetic valve *MV*1 is in an exactly analogous manner to that of the control of the boil-up rate (Fig 3), with the magnetic valve replacing the horseshoe electromagnet operating the mercury switch. Also the value of the resistor *R* is a tenth of that in Fig 3.

The absolute pressure of the system is set by the

movable contact of the manometer, M, so that the difference between the levels of mercury in the closed limb and at the tip of the sealed-in platinum contact is equal to the absolute pressure required. As soon as the mercury makes contact with the Pt wire, the current flows through the electronic valve to the extent of energizing the Post Office relay R_1, which in turn switches on the electromagnet of the magnetic valve. Thus no further evacuation takes place. When, as a result of a small rise in the pressure of the system, the contact in the manometer M is broken, the reverse process takes place, the magnetic valve opens, and the required vacuum is restored with a pressure fluctuation of certainly less than 0·1 mm Hg.

A pressure monastat PM between the two surge tanks $ST1$ and $ST2$ establishes a small pressure difference (6–8 mm Hg) between the two tanks. When this difference is disturbed the second magnetic valve $MV2$ opens or shuts similar to $MV1$. Since this pressure difference is only approximate, the Post Office relay R_2 without the electronic valve is regarded as sufficiently adequate.

Thus three regions of pressure are established which, in order of increasing pressure, are:

Region 1: Between the pump and $MV2$.
Region 2: Between $MV2$ and $MV1$.
Region 3: Between $MV1$ and the column.

The pressure difference between the top and bottom of the column which depends on the boil-up rate is set and maintained by the pressure switch PS. The left hand side of this is connected to the vacuum line near the top of the column and the right hand side to the side tube of the reflux meter at the bottom of the column. The details of this have already been explained under "Boil-up Rate Control."

EXPERIMENTAL RESULTS

The column was evaluated at absolute pressures of 50 and 10 mm Hg with a test mixture of *o*-dichlorobenzene and *p*-diethylbenzene. The vapour–liquid equilibria results by Bragg and Richards[5] have been used to calculate the efficiencies.

o-Dichlorobenzene ("purified") as received contained about 25 per cent of the *para*-isomer as the main impurity. It was carefully purified by repeated fractionation.

Pure *o*-dichlorobenzene was obtained with n_D^{20} 1·5518.

p-Diethylbenzene was prepared by reduction (zinc amalgam in acid) of *p*-ethyl acetophenone. The crude product was carefully fractionated in the column at 50 mm Hg absolute pressure to give pure *p*-diethylbenzene with n_D^{20} 1·4950. (*p*-Diethylbenzene, n_D^{20} 1·4969;[5] n_D^{14} 1·4978[6]).

Synthetic mixtures of *o*-dichlorobenzene with *p*-diethylbenzene were made up and their refractive indices at 20° C measured as recorded in Table I. The

TABLE I

Refractive Indices of Synthetic Mixtures of o-Dichlorobenzene–p-Diethylbenzene

Mol % *o*-dichlorobenzene	n_D^{20}	Mol % *o*-dichlorobenzene	n_D^{20}
0·00	1·4950	77·00	1·5355
30·95	1·5092	85·20	1·5409
42·60	1·5154	91·45	1·5452
64·70	1·5279	93·00	1·5465
68·40	1·5300	100·00	1·5518

values of relative volatility, α, were taken from the graphs given by Bragg and Richards;[5] these were:

for 50 mm Hg absolute pressure, $\alpha = 1{\cdot}076$;
for 10 mm Hg absolute pressure, $\alpha = 1{\cdot}128$.

The efficiencies of the column at various boil-up rates, together with the corresponding pressure drops,

TABLE II

Column Efficiencies at 50 mm Hg Absolute Pressure

Boil-up rate, ml/hr	Pressure drop, mm Hg	n_D^{20}		Efficiency theoretical plates
		Overhead	Bottom	
297	35·5	1·5500	1·5295	41·8
270	31·0	1·5509	1·5298	51·1
242	26·0	1·5510	1·5290	53·9
230	24·3	1·5510	1·5290	53·9
224	23·2	1·5513	1·5290	62·7
221	22·2	1·5511	1·5284	57·0
220	21·2	1·5510	1·5283	54·7
203	19·2	1·5512	1·5282	59·0
184	16·0	1·5511	1·5282	57·2
152	12·0	1·5512	1·5281	60·9

TABLE III

Column Efficiencies at 10 mm Hg Absolute Pressure

Boil-up rate, ml/hr	Pressure drop, mm Hg	n_D^{20}		Efficiency theoretical plates
		Overhead	Bottom	
236	39·0	—	—	—
207	35·0	—	—	—
200	34·0	1·5509	1·5275	32·6
188	32·0	—	—	—
174	29·5	1·5507	1·5274	31·2
165	27·0	1·5509	1·5273	32·6
158	25·5	1·5510	1·5269	33·8
142	22·0	1·5511	1·5272	35·4

under equilibrium conditions and total reflux for the two absolute pressures of 50 and 10 mm Hg, are given in Tables II and III respectively.

At 50 mm Hg absolute pressure, with the particular binary mixture employed, the column efficiencies are above 50 theoretical plates for boil-up rates in the range of 270 to 152 ml/hr. The highest value of efficiency in this range is 62·7 theoretical plates at the optimum boil-up rate of 224 ml/hr.

The height equivalent of a theoretical plate (HETP) of the packing (116 cm high) for 62·7 theoretical plates is 1·85 cm.

At 10 mm Hg absolute pressure the column efficiencies are above 30 theoretical plates for boil-up rates in the range 200 to 142 ml/hr. The highest value of efficiency obtained is 35·4 theoretical plates at the lowest boil-up rate recorded, *i.e.* at 142 ml/hr. This corresponds to an HETP of 3·27 cm.

Column Performance in Practice

The performance of the column has been shown to be satisfactory in several fractionations at reduced pressures. Various products of reasonable degree of purity have been obtained. Of these, mention will be made here of only two cases where the degrees of purity were determined. These were:

(1) 4,5-Dimethyl*cyclo*hexene was obtained with a purity of 99·9 (±0·1) per cent from a mixture of its isomers by fractionating at 190 mm Hg absolute pressure.

(2) *n*-Dodecyl alcohol, fractionated at 5 mm Hg, was purified from its lower and higher homologues to a degree of purity of 99·5–99·8 per cent.

Pressure Drop through the Packing

Pressure drop measurements at 50 and 10 mm Hg absolute pressures, using the test mixture, are summarized in Tables II and III respectively. Pressure drop measurements at 50 mm Hg, using pure components, appear in Table IV. Fig 5 shows plots of pressure drops *v.* boil-up rates.

TABLE IV

Change of Pressure Drop with Boil-up Rate at 50 mm Hg Absolute Pressure

o-Dichlorobenzene (unflooded)		*o*-Dichlorobenzene (pre-flooded)		*p*-Diethylbenzene (pre-flooded)	
Boil-up rate, ml/hr	Pressure drop, mm Hg	Boil-up rate, ml/hr	Pressure drop, mm Hg	Boil-up rate, ml/hr	Pressure drop, mm Hg
110	1·0	257	35·0	330	27·5
180	4·0	235	30·0	317	24·5
231	7·0	220	27·5	294	22·5
277	10·0	209	25·5	284	20·8
316	13·0	193	22·7	270	18·5
324	16·0	190	20·5	240	15·0
334	20·0	168	16·4	206	12·0
330	23·0	156	14·0	297	23·2
		145	12·0	321	25·2
		135	10·0		
		125	8·0		

For the pre-flooded column, each plot consists, in the main, of two fairly smooth lines of curves with a sudden break or interruption of smoothness between them. The boil-up rate corresponding to this point is regarded as the loading point of the column, the point at which the column has become completely covered with a thin film of liquid. At this boil-up rate the column is expected to be most efficient, since

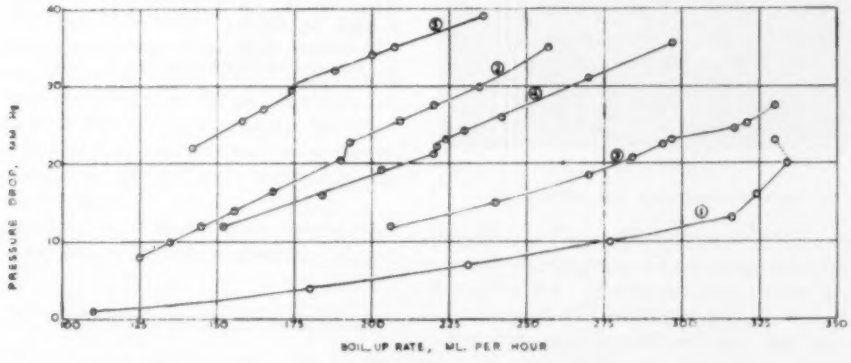

FIG 5

COLUMN PRESSURE DROP *v.* BOIL-UP RATE UNDER VARIOUS CONDITIONS

1. *o*-Dichlorobenzene alone, unflooded, at 50 mm Hg absolute pressure
2. *o*-Dichlorobenzene alone, pre-flooded, at 50 mm Hg absolute pressure
3. *p*-Diethylbenzene alone, pre-flooded, at 50 mm Hg absolute pressure
4. *o*-Dichlorobenzene–*p*-diethylbenzene mixture, pre-flooded, at 50 mm Hg absolute pressure
5. *o*-Dichlorobenzene–*p*-diethylbenzene mixture, pre-flooded, at 10 mm Hg absolute pressure

below it the packing may not be fully wetted and operational, and above it the thickness of the liquid film on the packing may be too high for efficient vapour–liquid contact to take place.

The absolute value of pressure drop at which the sharp rise occurs appears to be independent of the type of liquid distilled (compare curves 2 and 4, Fig 5). It is, however, dependent on the absolute pressure of fractionation, increasing as the absolute pressure is decreased.

DISCUSSION

Using the binary mixture of *o*-dichlorobenzene–*p*-diethylbenzene, the column efficiencies were determined at the two reduced pressures of 50 and 10 mm Hg. These were 62·7 TP and 35·4 TP respectively. The choice of these absolute pressures was determined by the availability of vapour–liquid equilibria data for the particular mixture employed. It must therefore be emphasized that the absolute pressure of 50 mm Hg at which the highest efficiency has been obtained, cannot be regarded as the optimum operating pressures for the column.

The reduced efficiency at 10 mm Hg could be almost wholly attributed to the very high pressure drop which must make the attainment of adiabatic conditions along the length of the column impossible to achieve.

In reduced pressure fractionation appreciable pressure drop (20 to 30 mm Hg) is obtained. This normally depends on the boil-up rate and on the absolute pressure of fractionation, increasing as the former is increased and as the latter is decreased. The boil-up rate at which the sudden change in the smooth pattern of pressure drop/boil-up rate relationship takes place is almost the same as the optimum boil-up rate. This fact could be made use of when the column is employed for fractionations at other reduced pressures, besides those investigated above.

CONCLUSIONS

A laboratory high efficiency vacuum fractionation unit has been constructed with the main features of a no-tap multiple fraction cutter, a high-sensitivity pressure control, an automatic control of the boil-up rate, and with a manual control of the adiabatic conditions along the length of the column.

The packing used in the column is of the Stedman type. The column efficiencies at the two absolute pressures of 50 and 10 mm Hg are found to be 62·7 TP (max) and 35·4 TP (max) respectively.

The pressure drop through the column under optimum operating conditions depends on the absolute pressure of fractionation. It rises as the absolute pressure is lowered.

The study of the pressure drop/boil-up rate diagram may act as a guide in choosing the optimum boil-up rate.

ACKNOWLEDGMENTS

The author wishes to thank Professor F. H. Garner, O.B.E., for his keen interest in this work and for his generous award of a Research Scholarship, Professor S. R. M. Ellis for his advice and encouragement in the presentation of this work, Dr C. R. Porter for his guidance and valuable advice, and Dr E. A. Coulson and Mr Grant of the Chemical Research Laboratories, Teddington, for their general advice on some column accessories and for the grant of the Stedman packing.

References

[1] Stedman, D. F. *J. Amer. Inst. Chem. Engrs*, 1935, **33**, 153.
[2] Bragg, L. B. *J. Amer. Inst. Chem. Engrs*, 1941, **37**, 19.
[3] Carney, T. P. "Laboratory Fractional Distillation," Chap. 9. New York: Macmillan, 1949.
[4] Morton, F. *Trans. Instn Chem. Engrs*, 1951, **29**, 240.
[5] Bragg, L. B., and Richards, A. R. *Industr. Engng Chem.*, 1942, **34**, 1088.
[6] "Handbook of Chemistry and Physics," p. 652. Cleveland: Chemical Rubber Publishing Co., 1947.

FOAM COMPOUNDS FOR USE AGAINST FIRES IN WATER MISCIBLE SOLVENTS*

By P. NASH† and R. J. FRENCH†

FOAM is the only fire-fighting material which can give enduring protection against the re-ignition of fires in flammable liquids, since all other materials, such as dry powders, carbon dioxide, and vaporizing liquids are effective only while their application is being continued. Modern protein-based foam compounds, while very effective against fires in liquid hydrocarbons with fire-points below 100° C, give little or no protection against fires in water miscible solvents, as these cause a rapid breakdown of the bubble-structure of the foam.

During recent years, foam manufacturers have devoted considerable effort to the development of "all-purpose" foam compounds which would be effective against fires in both hydrocarbons and water miscible solvents. This article reviews the types of all-purpose compounds available, and discusses their performance on flammable liquid fires. Hereafter "solvent" will be used as an abbreviation for "water miscible solvent."

TYPES OF COMPOUND

The all-purpose compounds currently available on the market fall into two classes:

(*a*) Those based on normal protein foam compounds with an additive designed to make them solvent-resistant. In one such compound the additive forms a "gel" when it comes in contact with the solvent; this layer of gel acts as a raft on which the foam layer floats, away from further contact with the solvent. In other compounds the additive is a heavy metal salt of a fatty acid which is insoluble in water. When distributed in the bubble walls this solid material has the effect of giving stability in the presence of solvents. The basic foaming agent may be a normal protein-based compound.

(*b*) Compounds of "synthetic" origin, not derived from natural protein materials.

METHOD OF TESTING FOAM COMPOUNDS

The fire performance of foam is measured by the Joint Fire Research Organization by a method illustrated in Fig 1, which is available for application to both hydrocarbon and solvent fires. Foam of the required physical properties is applied gently, through a fixed top applicator, to the surface of the liquid burning in a circular tank. The radiation from the flames is measured by four radiometers, and the time for it to be reduced or "controlled" to a chosen fraction (one-third, one-tenth, etc.) of its original intensity is measured for each rate of application of the foaming solution. A reduction of the intensity of radiation to one-third of its initial value would be described as "two-thirds control," etc. In this way a graph showing the relationship between the "rate of application" of solution and "time to control the fire" may be plotted (Fig 2 (*a*)).

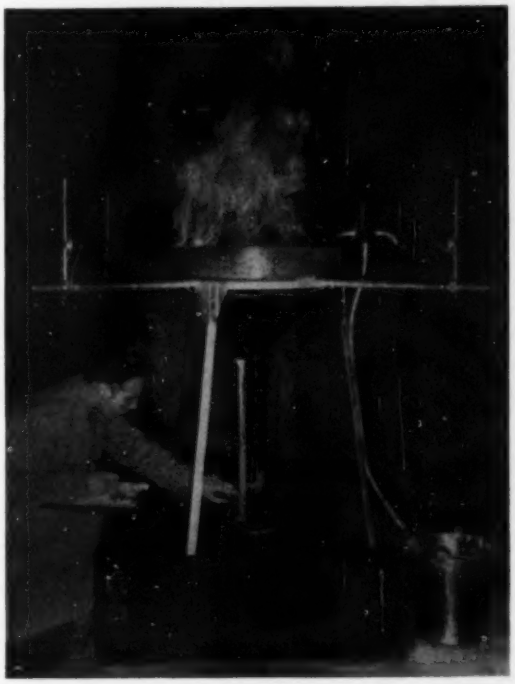

FIG 1
MEASURING THE FIRE PERFORMANCE OF FOAM

Fig 2 (*b*) can be derived from the first, since rate of application × time to control = quantity used to control. These two types of graph form a useful basis for the comparison of the effectiveness of different foams on the same flammable liquid, and for the same foam on different liquids. Both curves

* MS received 20 January 1961.

† Fire Research Station, Boreham Wood, Herts.

exhibit a "critical rate of application" below which the fire cannot be controlled, however long application is continued. At higher rates of application the times to control, or quantities used to control, may be compared. Fig 2 (*b*) often exhibits a minimum

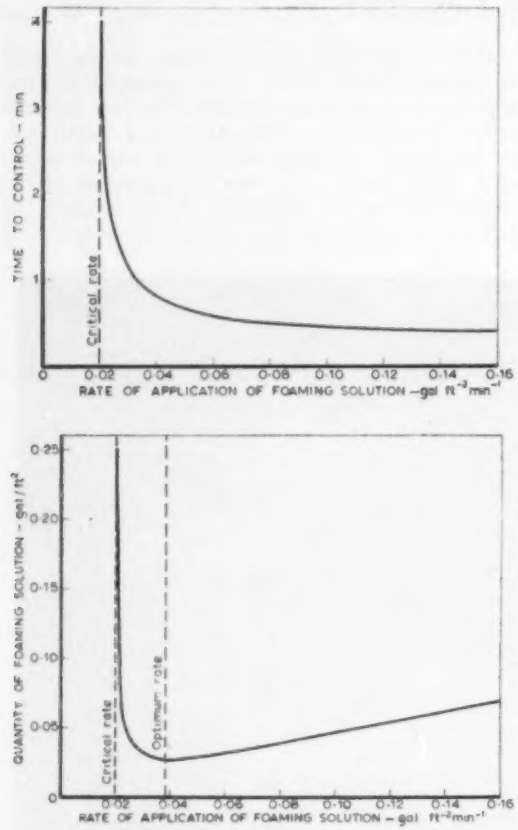
TIME TO CONTROL – min
Critical rate
RATE OF APPLICATION OF FOAMING SOLUTION – gal ft⁻² min⁻¹
QUANTITY OF FOAMING SOLUTION – gal/ft²
Critical rate
Optimum rate
RATE OF APPLICATION OF FOAMING SOLUTION – gal ft⁻² min⁻¹

FIG 2

CONTROL OF FLAMMABLE LIQUID FIRE BY FOAMING SOLUTION

value, showing a most economical or "optimum" rate of application. In cases where the foam solution is not miscible with the flammable liquid under test the rate of drainage of water from the foam may be measured directly from the volume of water separated out in the glass cylinder, shown in Fig 1.

PERFORMANCE OF FOAMS ON VARIOUS FLAMMABLE LIQUIDS

Table I compares the critical rates of application of foaming solution, for foams produced from the various compounds, when applied gently to the surface of different flammable liquids. The foams were produced in a laboratory foam generator to give the same physical properties as they would have in a standard branchpipe. The foams are denoted by the following code letters:

A—Normal protein-based compound (no additives)

B_1—Solvent-resisting (protein base with raft-forming additives)

B_2—Solvent-resisting (protein base with raft-forming additive and additional iron salts)

B_3—Solvent-resisting (protein base with raft-forming additive and additional sodium salts)

C_1—Solvent-resisting (protein-base with bubble-wall stabilizer)

C_2—Solvent-resisting (protein-base with bubble-wall stabilizer made by a different manufacturer)

The solvent-resisting foam compounds C_1 and C_2 require special arrangements whereby the compound and stabilizer are metered into the water supply some 3–10 sec before the foam is made. Premixing of the solution is not possible.

It will be seen from Table I that all the solvent-resisting foams give an adequate performance on MEK, with the exception of B_1. This foam was later replaced by B_2 and B_3, which gave a very much better performance on this solvent. In general, the solvent-resisting foams on solvents gave critical rates for gentle application in the range 0·02–0·07 gal ft^{-2} min^{-1} according to the type of foam and solvent. This may be compared with the value of 0·02 for a good protein foam on petrol. When foam made from compound C_2 was applied by jet downwards into an MEK fire the foam was broken down rapidly and little appeared on the surface of the solvent, even at a solution rate of application as high as 0·2 gal ft^{-2} min^{-1}. This illustrates the importance of gentle application for all solvent fires. Two of the solvent-resisting foams were tested on petrol; these foams had a normal protein base with additives, and gave critical rates one and a half to five times as great as a protein foam without additive.

Of the solvents, industrial methylated spirits and methanol fires were the easiest to control, while the MEK fire was the most severe. Acetone and *iso*-propyl alcohol fires were intermediate in severity.

It is of interest to compare the quantities of foam likely to be used to control a fire at rates above the critical. This has been done in Tables II (*a*), (*b*), and (*c*) for three different flammable liquids.

CONCLUSIONS

The tests indicate that the "all-purpose" foam compounds can give a reasonable performance both on hydrocarbons and on solvents, provided that they are applied gently to the surface of the burning liquid.

TABLE I

Critical Rates of Foam Applied Gently to Various Flammable Liquids
(measured in gallons of foaming solution per square foot per minute)

Flammable liquid	Petrol	Industrial methylated spirit	Methanol	*iso*Propyl alcohol	Acetone	MEK	Physical properties of foam	
							Expansion, units	Critical shear stress, dyn/cm²
Foam compound		Critical rate—gal ft⁻² min⁻¹						
A	0·02 (3% sol)	Very rapid breakdown. Unsuitable for practical use					7·0	200
B_1	Not tested	0·03 (10% sol)	Not tested	0·07 (12% sol)	0·04 (8% sol)	0·55 (15% sol)	2·8	60
B_2	Not tested	Not tested	Not tested	Not tested	Not tested	0·07 (10% sol)	3·0	40
B_3	0·035 (12% sol)	Not tested	0·025 (10% sol)	Not tested	Not tested	0·065 (12% sol)	3·0	40
C_1	Not tested	0·03 (4% comp, 4% additive)	Not tested	0·05 (4% comp, 4% additive)	Not tested		7·4	660
C_2	0·10 (5% comp and additive)	Not tested	0·02 (5% comp and additive)	Not tested	Not tested	0·055 (5% comp, 5% additive)	2·4	300

TABLE II (*a*)

Quantity of Foam Solution to Control Petrol Fire (Two-thirds Control)

Solution rate of application, gal ft⁻² min⁻¹	0·05	0·10	0·20	0·50
Foam compound	Quantity of solution to control (gal/ft²)			
A	0·03	0·04	0·05	Not measured
B_3	0·2	0·1	0·1	Not measured
C_2	Below critical rate		0·08	Not measured

TABLE II (*b*)

Quantity of Foam Solution to Control Methanol Fire (Two-thirds Control)

Solution rate of application, gal ft⁻² min⁻¹	0·05	0·10	0·20	0·50
Foam compound	Quantity of solution to control (gal/ft²)			
A	Rapid breakdown—not practicable			
B_3	0·15	0·08	Not measured	Not measured
C_2	0·025	0·025	0·05	Not measured

TABLE II (*c*)

Quantity of Foam Solution to Control MEK Fire (Two-thirds Control)

Solution rate of application, gal ft⁻² min⁻¹	0·10	0·20	0·50	1·0
Foam compound	Quantity of solution to control (gal/ft²)			
A	Rapid breakdown—not practicable			
B_1	Below critical rate			0·2
B_2	0·12	0·10	Not measured	
B_3	0·10	0·20	Not measured	
C_2	0·05	0·05	0·08	Not measured

If they are projected into the liquid their performance is likely to suffer badly, and it is probable that the fire will not be controlled. It is most important, therefore, that these compounds are applied as gently as possible to the surface.

For application to petrol fires, a greater quantity of "all-purpose" compound than normal protein compound is likely to be required for control of the fire. The factor of increase is likely to vary between one and a half and ten times as much, dependent upon the compound used and the rate of application of foam per unit fire area. The minimum rate at which the foam can be applied to be effective may also

have to be increased by a factor of one and a half upwards, depending on the foam and the solvent considered.

A normal protein compound is not practicable for control of a solvent fire and an "all-purpose" compound is necessary. The compounds are likely to be fairly economical on solvents, with consumption ranging from one to five times and minimum effective application rates of one to four times that of a normal protein compound on a petrol fire. The actual figures depend again on compound, solvent, and rate of application.

ACKNOWLEDGMENT

The work described in this paper forms part of the programme of the Joint Fire Organization of the Department of Scientific and Industrial Research and Fire Offices' Committee; the paper is published by permission of the Director of Fire Research.

OBITUARY

ROBERT BLYTHMAN KERR, M.B.E.

1904–1961

ROBERT BLYTHMAN KERR, who died on 22 February 1961, was deputy managing director of Foster Wheeler Ltd.

He was born on 15 October 1904 and was educated at Uppingham School between January 1919 and July 1923, where he secured his first M.B. for Cambridge University. He then went on to Cambridge and was a student at Gonville and Caius from October 1923 to July 1925, where he read science and physics.

His industrial career started as an overseer in a Barbados sugar factory in 1926, which was followed with an appointment to Trinidad Leaseholds Ltd as assistant refinery operator and later as assistant to the general manager in Trinidad. It was during this period, as a major in the Trinidad Artillery Volunteers, that he was awarded the M.B.E. His subsequent career led him to Foster Wheeler Ltd, whom he joined in October 1949 as engineer in the Process Plants Division (Contracts Department). In 1954 he was promoted to the position of chief contracts engineer of the Process Plants Division and joined the board of directors in February 1959, subsequently becoming deputy managing director in January 1960.

He was an associate member of the Institute of Petroleum and a graduate of the Institute of Chemical Engineers.

He leaves a widow and a son and daughter.

ERRATUM

IT is regretted that an error occurred in the *Journal* of April 1961, on p. 119 of the paper on "Applied Petroleum Research on a Vehicle Dynamometer". The seventh paragraph should read as follows:

"We have measured the air velocity at the duct outlet and have found it to be *within* 5 per cent of the speed of the car. This is nominally correct, in our opinion, particularly bearing in mind that the air speed is not constant over an outlet of this type."

PETROLEUM PROCESSING PLANTS

CRUDE DISTILLATION

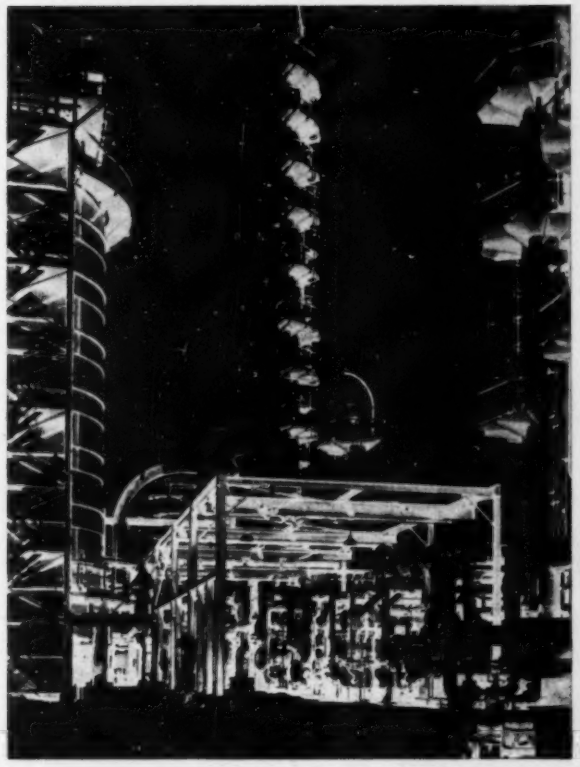

37,200 B.P.D. CRUDE UNIT.

PARSONS POWERGAS have unequalled experience in the design, engineering, procurement, erection and commissioning of complete refineries or processing units for the petroleum industry.

PARSONS POWERGAS

THE RALPH M. PARSONS COMPANY
LOS ANGELES • NEW YORK

THE POWER-GAS CORPORATION LIMITED
LONDON • STOCKTON-ON-TEES

484

15 PORTLAND PLACE LONDON W.1

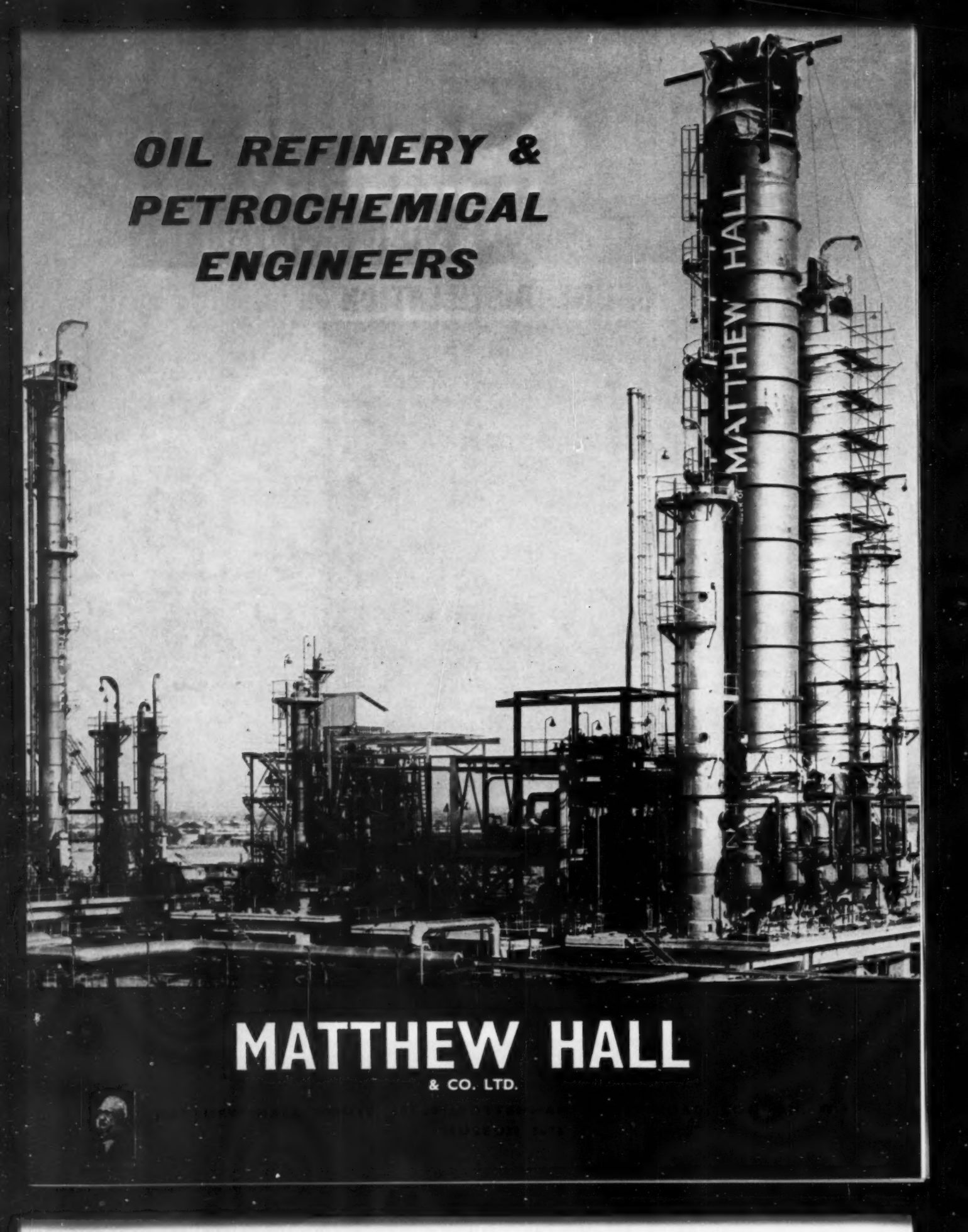
OIL REFINERY &
PETROCHEMICAL
ENGINEERS
MATTHEW HALL
MATTHEW HALL
& CO. LTD.

All kinds of couplings

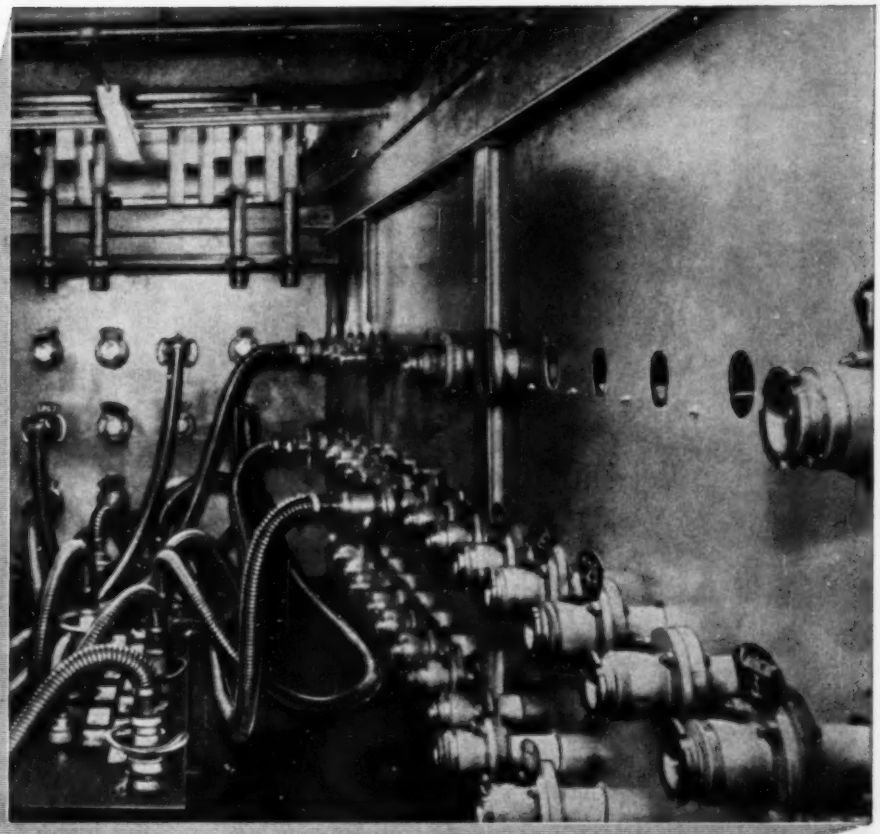

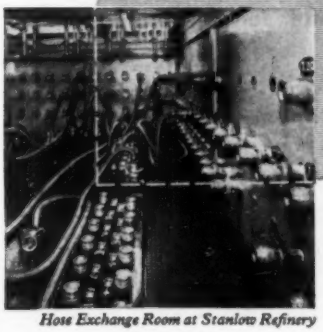

Hose Exchange Room at Stanlow Refinery

Avery Hardoll industrial couplings eliminate wasteful, dangerous spillage. Self-sealing valves prevent flow from starting until the Hose and Tank Units are coupled. On disengagement, the valves return to the self-sealing position before the Units can be uncoupled. Avery Hardoll industrial couplings are widely used for rapid, safe bulk-handling in the petroleum, aviation, and food processing industries. For complete details about the new facility that Avery Hardoll couplings bring to liquid transfer write to:—

Avery-Hardoll
LIMITED

OAKCROFT ROAD · CHESSINGTON · SURREY

Telephone: Elmbridge 5221/7

tank construction is a job for

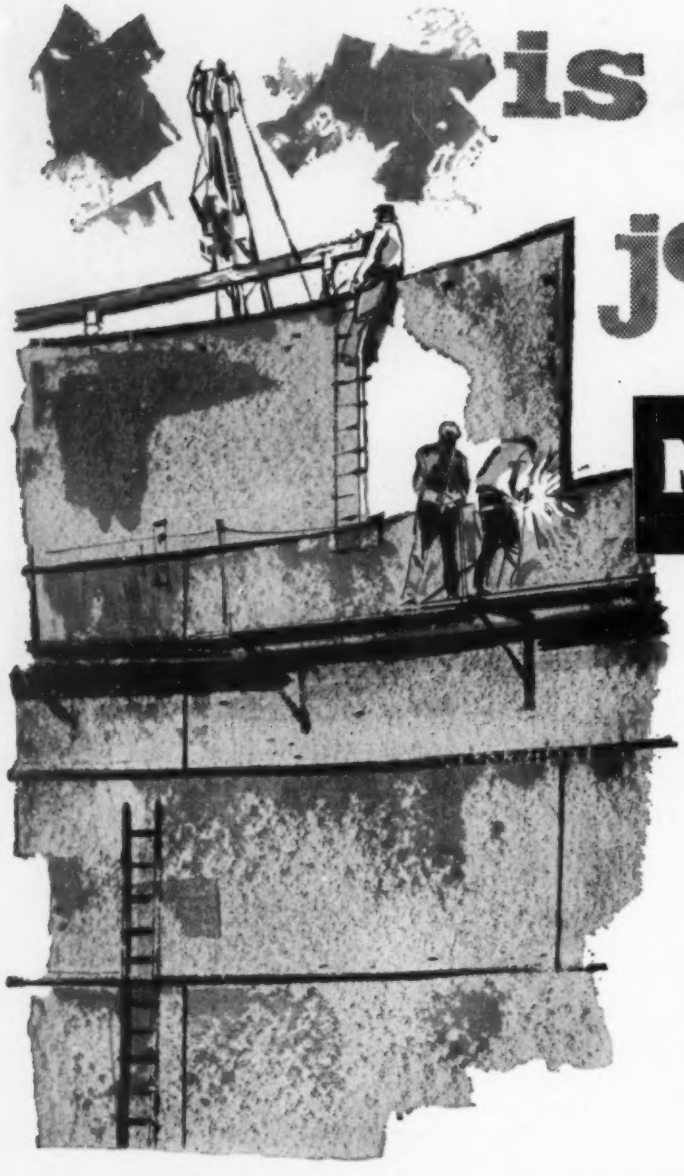

MECHANS LIMITED

Whatever the type of tank, and its size... whatever the liquid or gas to be stored, Mechans can design it, construct it and erect it. Mechans' conservation equipment is found in all parts of the United Kingdom and many parts of the world. Mechans' tanks—and process vessels—are doing a good job for many companies. If your plans include new tankage projects, its a job for Mechans.

MECHANS LIMITED SCOTSTOUN IRON WORKS GLASGOW W 4

Telephone: Scotstoun 2211

BETTER PERFORMANCE WITH AEI HEAT EXCHANGERS

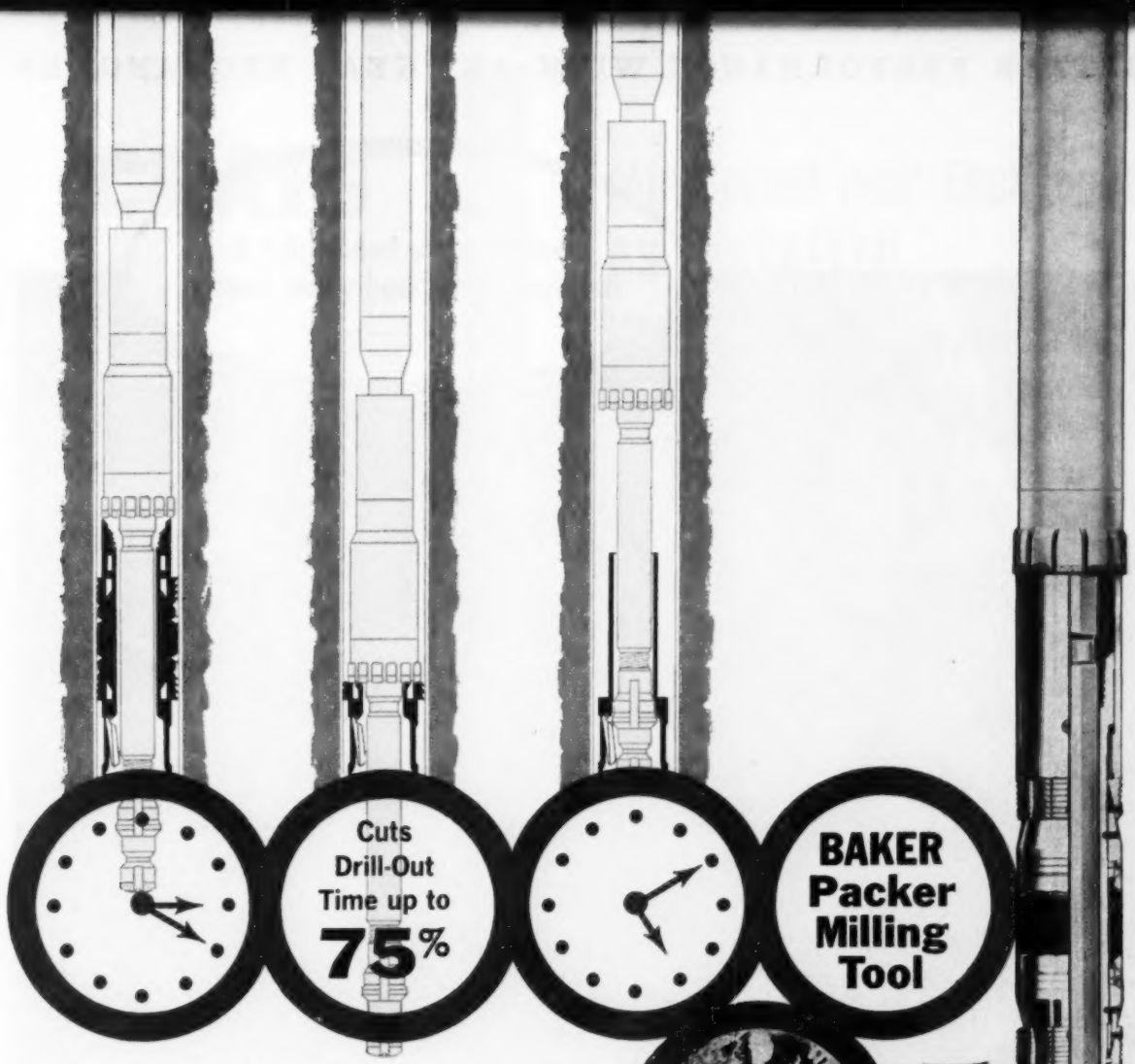

THAT'S RIGHT... rock bits require 8 to 16 hours to drill-out drillable Production packers—but the new Baker Packer Milling Tool does the job in 2 to 4 hours.

Why does this new tool reduce the time so drastically? Because Baker engineers designed it to perform this one job efficiently. It is not an all-purpose milling tool. Hence, it does not mill up the entire packer, but *only* those elements that hold the packer in a set position against the casing.

Another important factor is the sustaining, self-sharpening action of the milling shoe and bottom sub. These cutting areas are dressed with special Baker Milling-Carbide Compound. Hundreds of carefully selected carbide chips are bonded in a matrix, and so distributed that an efficient milling action is always maintained.

During milling the tool is stabilized in the casing by its lower portion which rotates inside the packer body. A simple spring-loaded *catch sleeve* expands below the packer so that when the tool is retrieved, the remaining portion of the packer can be brought to the surface. This catch sleeve also provides a positive emergency release.

In addition to Baker production packers, the milling tool may be used for other drillable packers of similar design.

Set at 19,425 feet in 7-inch casing, this Retainer Production Packer was milled over in two hours and fifty minutes, and the cast-iron body and bottom of packer retrieved without damage to 4½-inch liner just below it.

PRODUCT NUMBER 747-C

BAKER OIL TOOLS, INC. • HOUSTON • LOS ANGELES • NEW YORK

BETTER PERFORMANCE WITH AEI HEAT EXCHANGERS

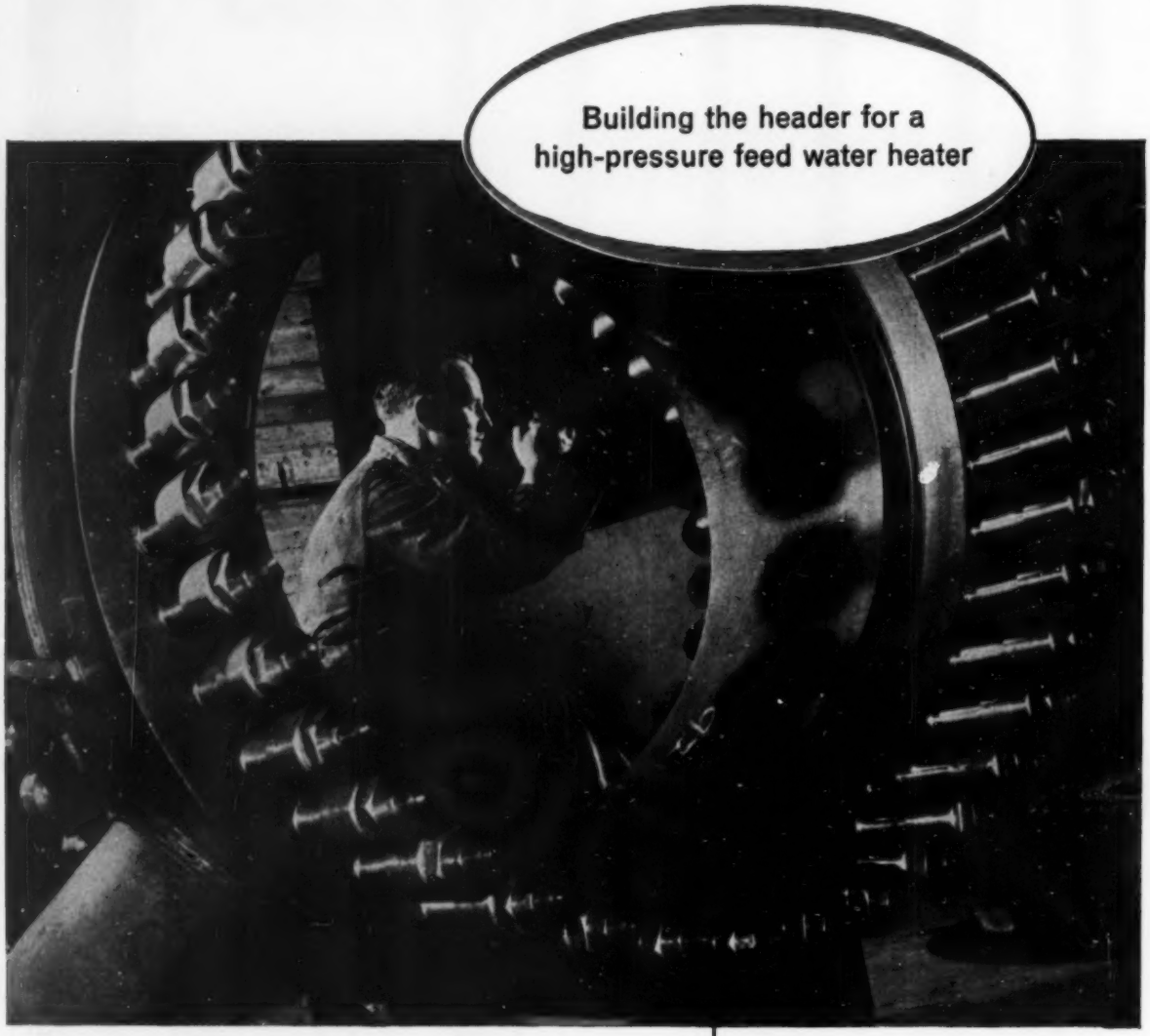

Here in a specially-equipped works of AEI, a craftsman is working on a water header for a high-pressure feed heater to withstand a working pressure of 2700 p.s.i.g.

The AEI Turbine-Generator Division's Petershill Works in Glasgow manufactures all types of heat exchange and auxiliary equipment including a wide range of pressure vessels for general industrial applications. AEI experience and skill could solve your heat exchange problems

For further information write to the AEI Turbine-Generator Division at Trafford Park, Manchester 17, or to your local AEI office.

Products include:
DEAERATORS · SURFACE CONDENSERS
HEAT EXCHANGERS
LARGE STEEL PLATE FABRICATIONS
STORAGE TANKS · EVAPORATORS

AEI **Associated Electrical Industries Ltd.**

Turbine-Generator Division

TRAFFORD PARK, MANCHESTER 17

WORKS AT: MANCHESTER · RUGBY · GLASGOW · LARNE

B/A004

CRAIG

Solo-aire

HUDSON

(Air Cooled Heat Exchangers)
AS INSTALLED IN FAWLEY AND WHITEGATE REFINERIES

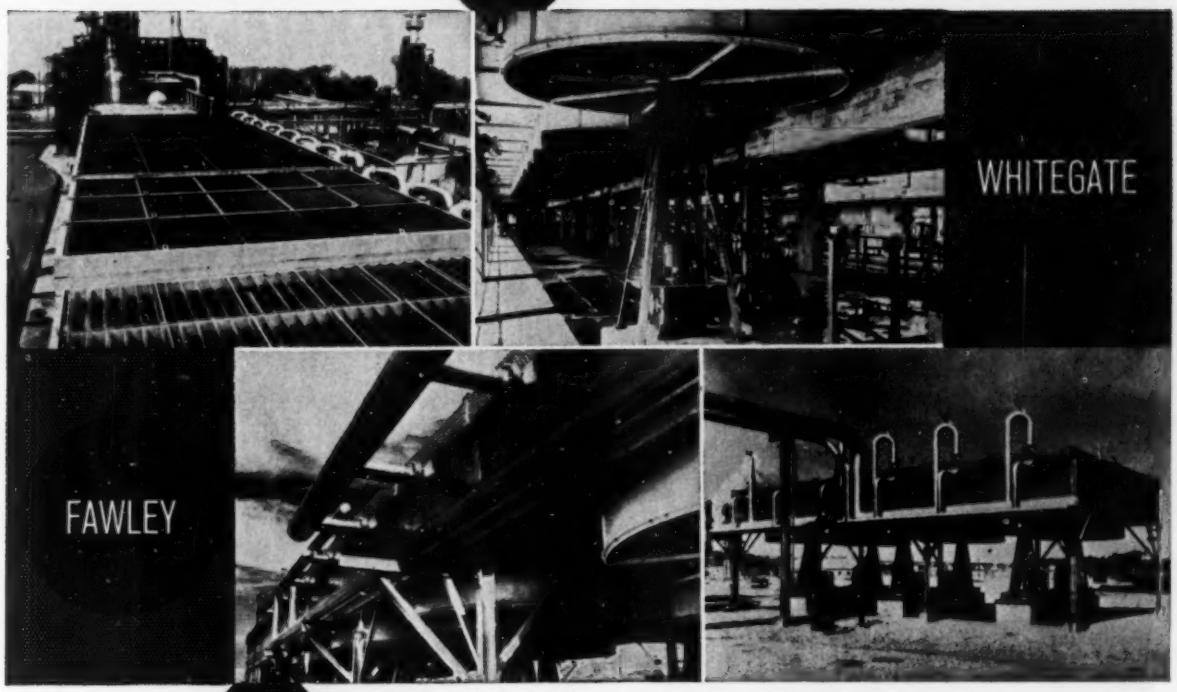

'SOLO-AIRE' Exchangers are part of the range of air cooled equipment for which A. F. CRAIG & CO. LTD. of Paisley, Scotland, are licensed by the HUDSON ENGINEERING CORPORATION of Houston, Texas, U.S.A., to manufacture for sale throughout the world.

ENQUIRIES :—
A. F. Craig & Co. Ltd., Caledonia Engineering Works, Paisley, Scotland
Tel: Paisley 2191

LONDON :—
727 Salisbury House, London Wall, E.C.2.,
Tel: NATional 3964

Better temperature measurement transmission with the new

FOXBORO

M/12A Pneumatic

TEMPERATURE TRANSMITTER

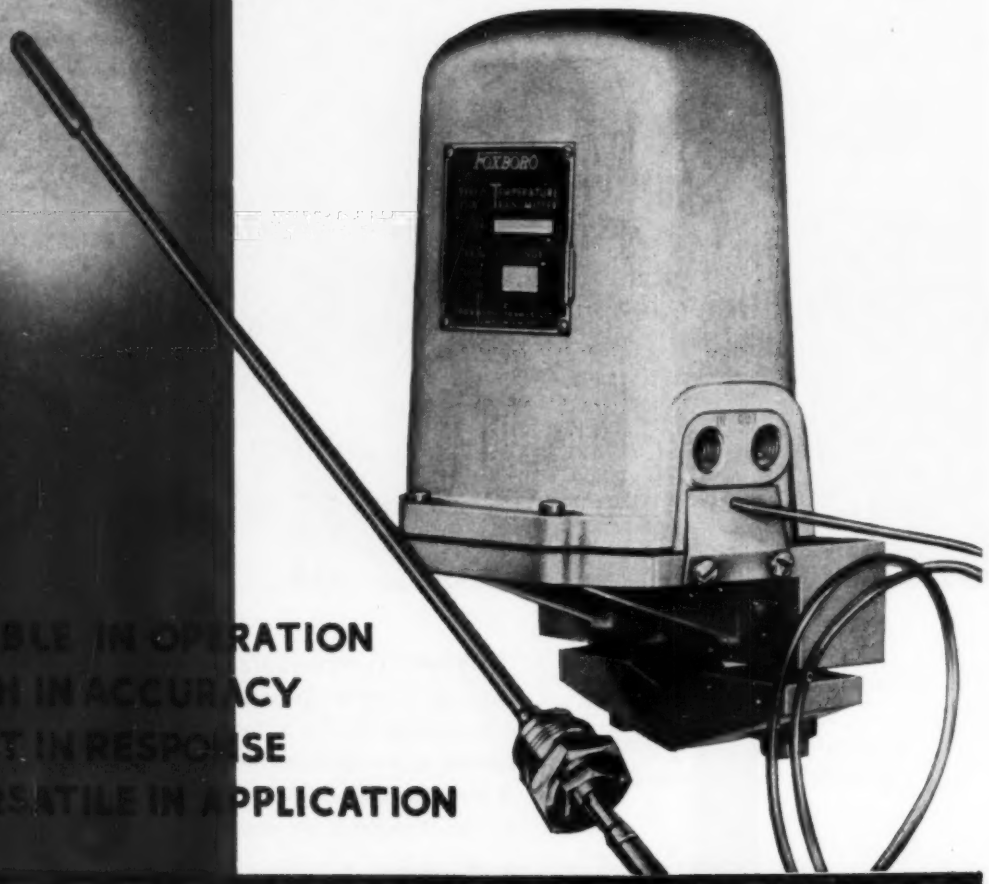

- STABLE IN OPERATION
- HIGH IN ACCURACY
- FAST IN RESPONSE
- VERSATILE IN APPLICATION

FOXBORO-YOXALL LIMITED

REDHILL SURREY ENGLAND

. . . on-stream ahead of schedule

Maintaining schedule during the construction of a processing unit requires the precise co-ordination and timing of a series of design, engineering, procurement and construction details. But to complete ahead of schedule requires the extras in experience . . . in judgement, that save minutes and days. A right decision . . . a proper procedure . . . a new technique, these are the *experience factors* that help PROCON build better and on time.

Procon completed this "HF" Alkylation unit, built for Midland Cooperatives, Inc., days ahead of schedule. Midland located in Cushing, Oklahoma, uses the high octane alkylate to supplement its premium gasoline.

Turnaround, unit revamping, one unit or a complete refinery from the ground up . . . whatever your requirement you can trust the entire job to PROCON.

PROCON*

* Registered Trademark PROCON Incorporated

WORLD-WIDE CONSTRUCTION FOR THE PETROLEUM, PETROCHEMICAL, AND CHEMICAL INDUSTRIES

PROCON (*Great Britain*) LIMITED
BUSH HOUSE, ALDWYCH, LONDON, W. C. 2, ENGLAND

PROCON INCORPORATED, DES PLAINES, ILLINOIS, U. S. A.
PROCON INTERNATIONAL S. A., CHICAGO, ILL., U. S. A.
PROCON (CANADA) LIMITED, TORONTO, CANADA
PROCON PTY. LIMITED, SYDNEY, AUSTRALIA
PROCOFRANCE S. A. R. L., PARIS, FRANCE
PROCON LIMITADA, SAO PAULO, BRAZIL
PACIFIC PROCON LIMITED, MANILA, P. I.
VICAPROCON, S. A., CARACAS, VENEZUELA

HEAT AND CORROSION RESISTING STEEL CASTINGS

for refineries to all British Standards and American grades. Special materials include "NIMOCAST" and ALL HIGH NICKEL base alloys. Shell moulded castings. Sand castings up to 2½ tons. Centrifugal castings up to 12 feet long and 36" diameter.

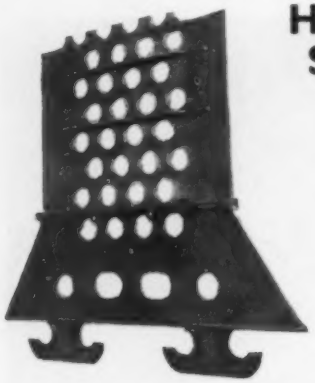

Heat resisting alloy steel tube supports.

32 feet long Catalytic Hydrogen Reformers. Completely fabricated from CENTRIFUGALLY cast tubes in 25/20 Cr/Ni Alloy.

Stainless Steel Weld Neck, Slip-on and Blind Flanges Centrifugally cast.

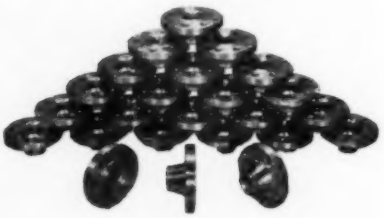

SHEEPBRIDGE ALLOY CASTINGS LTD.

(One of the Sheepbridge Engineering Group)

SUTTON-IN-ASHFIELD · NOTTS. · ENGLAND

Telephone:—Sutton-in-Ashfield 590. Telegrams:—"Centrifugal" Sutton-in-Ashfield, Notts.

Methods for Assessing Performance of Crankcase Lubricating Oils —Engine Tests

(Part 3 of IP Standards for Petroleum and its Products)

Contains five engine test methods for lubricating oil and a method for rating engine cleanliness and wear

54 pages Illustrated
Price **30s. 0d.** post free

Obtainable from

The Institute of Petroleum
61 New Cavendish Street
London, W.1

METHODS FOR SAMPLING

(Part IV of IP Standards for Petroleum and its Products)

This book contains details of the apparatus and procedures for sampling petroleum and its products which comprise IP Method 51.

44 pages Illustrated

Price **10s** post free

Obtainable from

The Institute of Petroleum
61 New Cavendish Street
London, W.1

Efficient Economic KELLOGG Catalytic Reformers

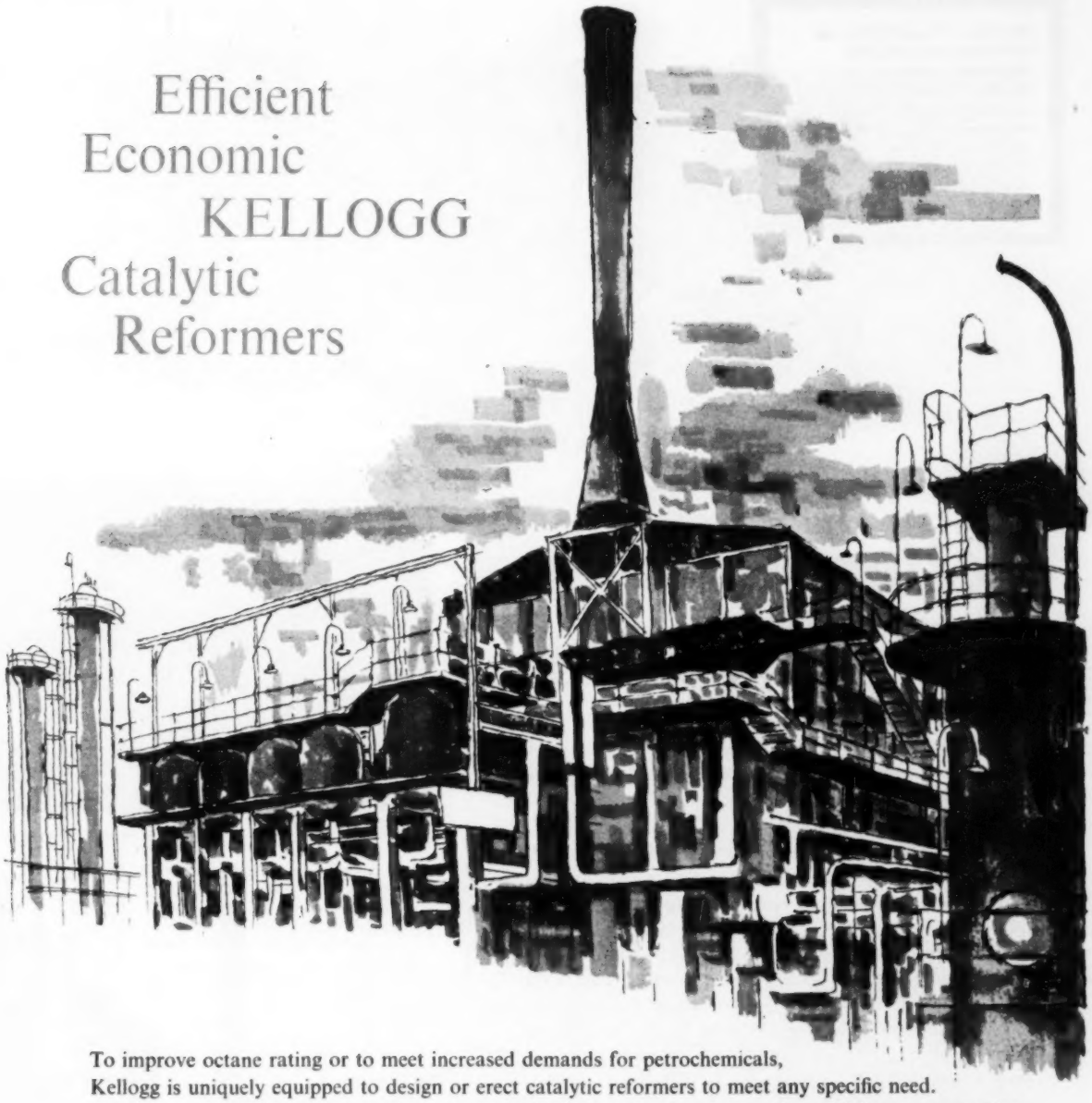

To improve octane rating or to meet increased demands for petrochemicals, Kellogg is uniquely equipped to design or erect catalytic reformers to meet any specific need. Combined with Kellogg-designed hydrotreating facilities, cat reforming produces high octane gasoline of superior quality. The reformate is also a rich source of aromatics for petrochemical production. Feedstocks reformed include light, heavy and full-boiling virgin naphthas as well as thermally and catalytically cracked stocks which have been selectively pretreated. Products include aromatics such as benzene, toluene, and xylenes plus isobutane and hydrogen.

Kellogg International Corporation has extensive experience in catalytic reforming, drawn from a total of 40 commercial installations having a combined throughput of close to 350,000 B.P.D.

For further information send for the booklet "Regenerative Catalytic Reforming".

M KELLOGG W

Kellogg International Corporation

KELLOGG HOUSE · 7-10 CHANDOS STREET · CAVENDISH SQUARE · LONDON W.1

SOCIETE KELLOGG · *PARIS* · THE CANADIAN KELLOGG COMPANY LTD · *TORONTO*
KELLOGG PAN AMERICAN CORPORATION · *BUENOS AIRES* · COMPANHIA KELLOGG BRASILEIRA · *RIO DE JANEIRO* · COMPANIA KELLOGG DE VENEZUELA · *CARACAS*

Subsidiaries and affiliates of THE M. W. KELLOGG COMPANY NEW YORK

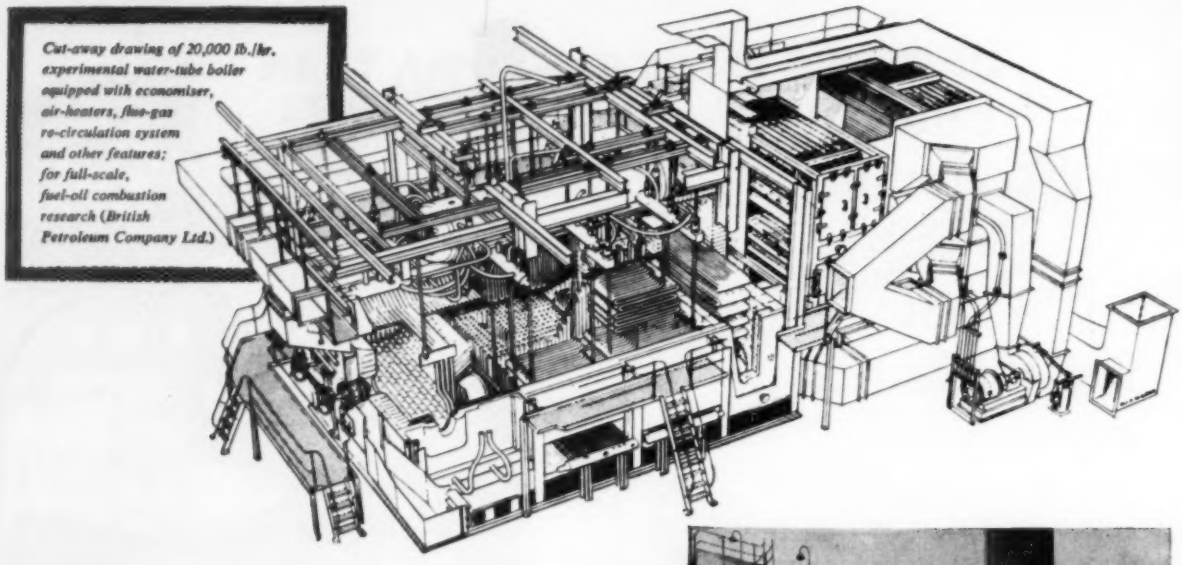

Cut-away drawing of 20,000 lb./hr. experimental water-tube boiler equipped with economiser, air-heaters, flue-gas re-circulation system and other features; for full-scale, fuel-oil combustion research (British Petroleum Company Ltd.)

Tailor-made or "off-the-peg"

The special experimental boiler shown above has been designed and built by Babcock to British Petroleum Company specifications, for research—at a new B.P. combustion laboratory—into the methods and effects of burning liquid fuels under full-scale operating conditions.

It was Babcock also that designed and built the special 300,000 lb./hr. CO boiler (below, right) at the Esso Fawley refinery, to utilize the steam-generating potential of the exhaust gases from a catalytic cracker.

In refineries and chemical plant the world over, conventional Babcock boilers of all types and sizes, fired with a wide variety of fuels and in both indoor and outdoor installations are, reliably and economically, supplying steam for heating, processing and power production.

So it is that Babcock is serving the oil and chemical industries with a wide range of plant—tailor-made to special requirements or built to established, "off-the-peg" Babcock designs.

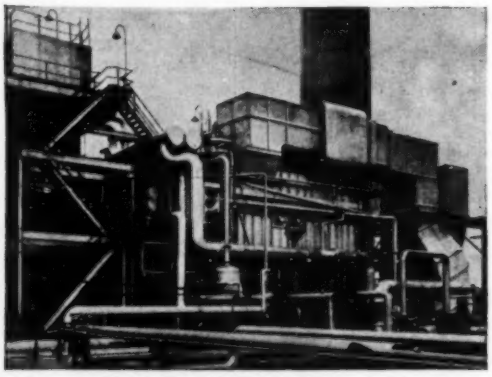

Type FH oil-fired Integral Furnace boiler in an outdoor installation; (Esso refinery, Fawley).

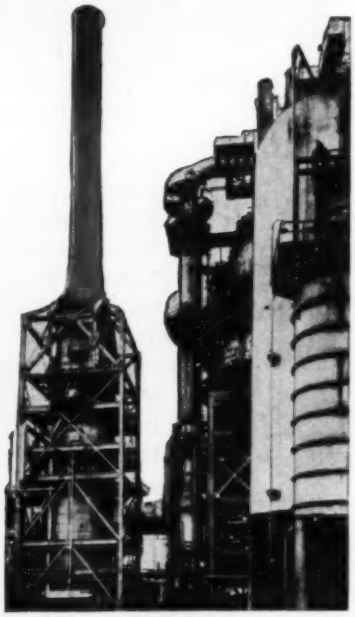

300,000 lb./hr. CO boiler, operating on "waste" gases from a catalytic cracker; (Esso refinery Fawley).

BABCOCK *service to the oil and chemical industries*

COMPLETE STEAM-RAISING PLANTS, SEPARATELY-FIRED SUPERHEATERS, HEAT-EXCHANGERS, Equipment for the UTILIZATION OF WASTE HEAT, TREATING TOWERS, MANIFOLDS and other PRESSURE VESSELS, in mild-steel or clad plate.

BABCOCK & WILCOX LIMITED, BABCOCK HOUSE, 209 EUSTON RD., LONDON, N.W.1

FOSTER WHEELER

ANNOUNCE THEIR REMOVAL

TO NEW

PREMISES

The London address of the world-wide Foster Wheeler organisation is now :—

FOSTER WHEELER HOUSE, CHAPEL STREET, N.W.1.

Increasing commitments have necessitated the expansion of all departments embracing the design, engineering, fabrication and construction of :—

Single units and complete refineries for the oil and chemical industries.

Land and marine boilers and ancillary equipment for power generation.

Complete reactor coolant circuitry for nuclear power.

Foster Wheeler also offer every facility for research and development including co-operation on heat transfer, fluid flow and kindred problems of nuclear power.

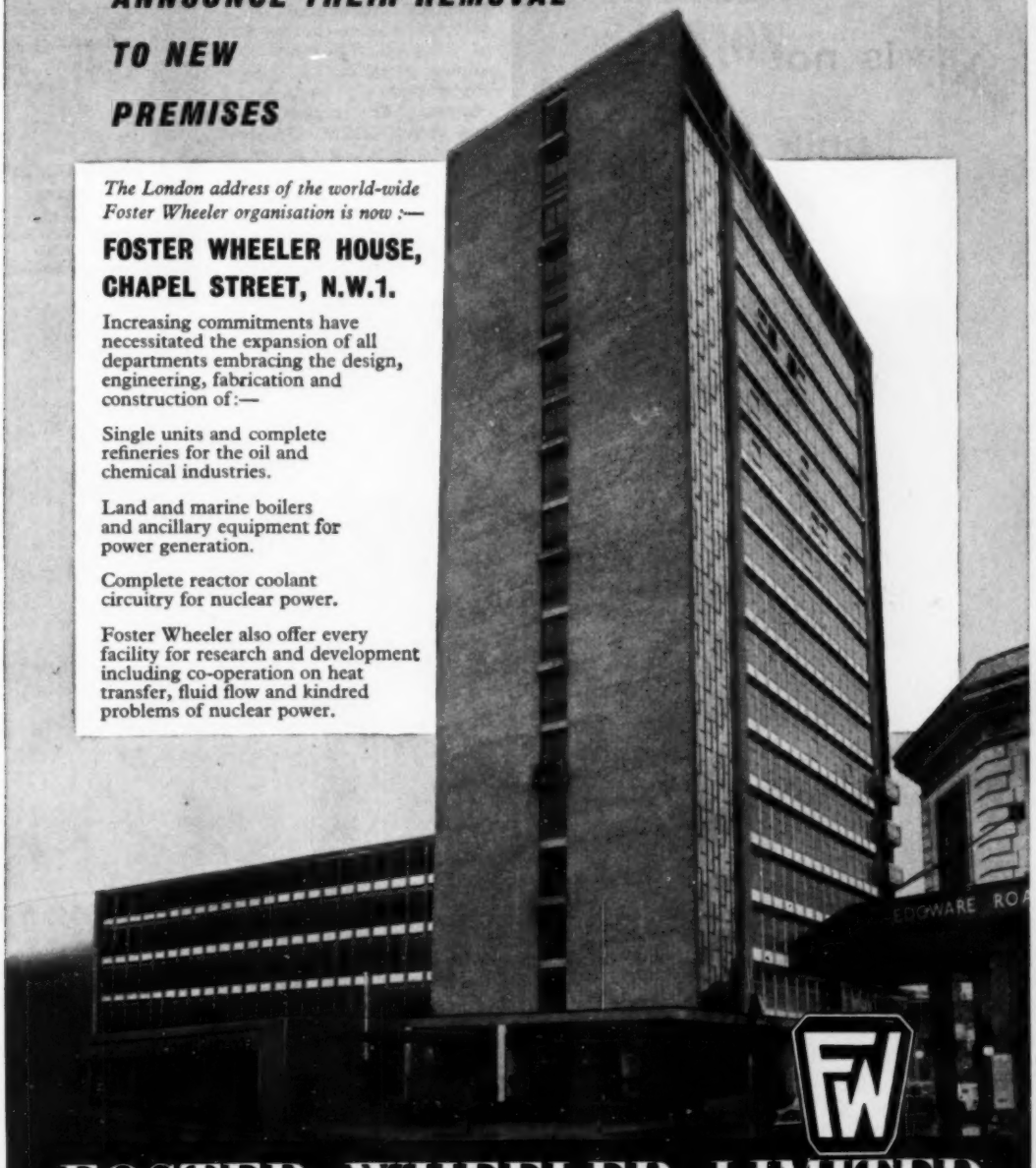

FOSTER WHEELER LIMITED

FOSTER WHEELER HOUSE, CHAPEL STREET, LONDON NW1. Telephone PADdington 1221

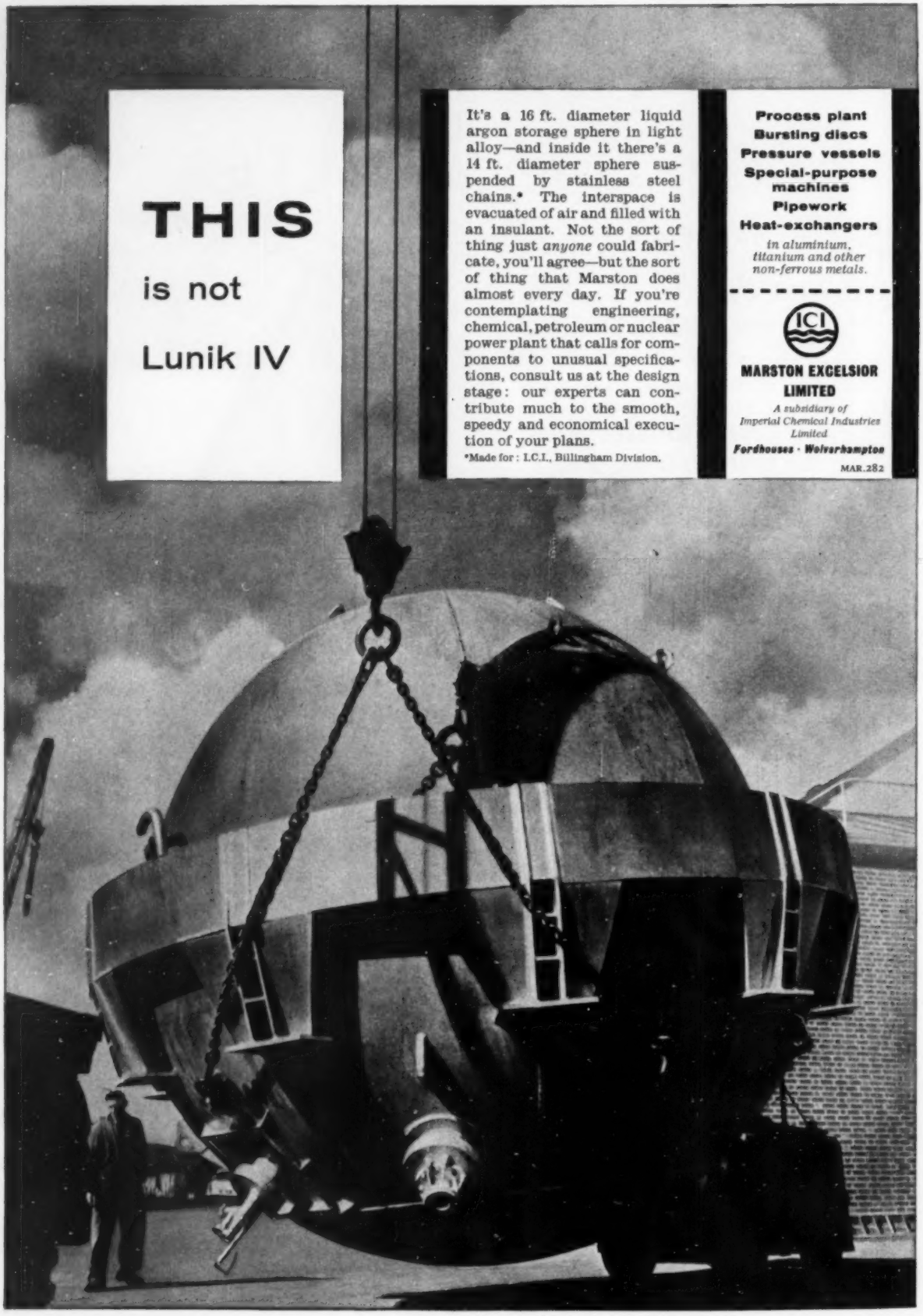
THIS
is not
Lunik IV
It's a 16 ft. diameter liquid argon storage sphere in light alloy—and inside it there's a 14 ft. diameter sphere suspended by stainless steel chains.* The interspace is evacuated of air and filled with an insulant. Not the sort of thing just *anyone* could fabricate, you'll agree—but the sort of thing that Marston does almost every day. If you're contemplating engineering, chemical, petroleum or nuclear power plant that calls for components to unusual specifications, consult us at the design stage: our experts can contribute much to the smooth, speedy and economical execution of your plans.
*Made for: I.C.I., Billingham Division.
Process plant
Bursting discs
Pressure vessels
Special-purpose machines
Pipework
Heat-exchangers
in aluminium, titanium and other non-ferrous metals.
ICI
MARSTON EXCELSIOR LIMITED
A subsidiary of Imperial Chemical Industries Limited
Fordhouses · Wolverhampton
MAR.282

The GENEFAX GROUP *for everything in Refractories*

GR

FIREBRICKS, INSULATION and PLASTIC REFRACTORIES for the OIL INDUSTRY

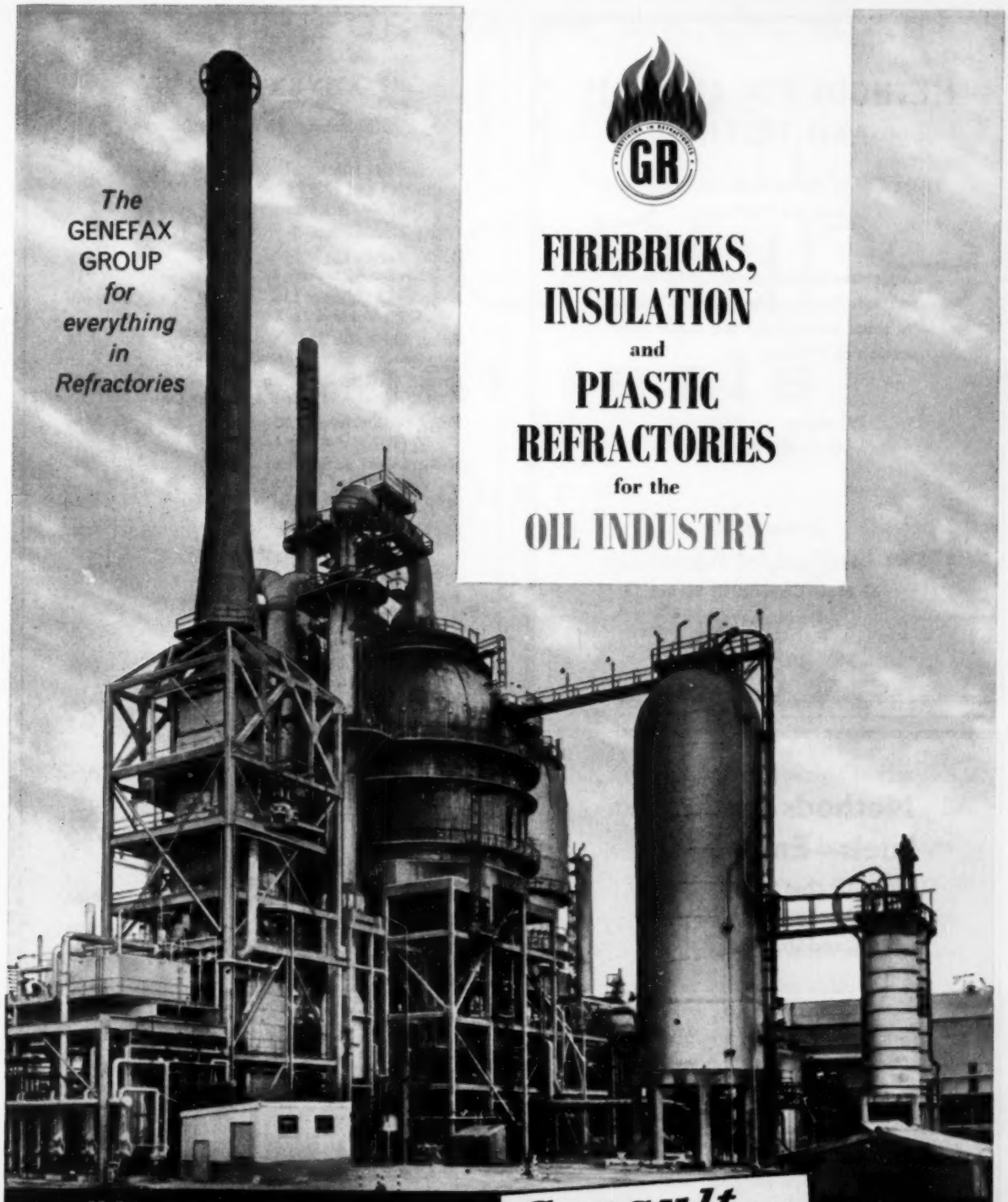

C.O. Boiler with capacity of 300,000 lbs steam per hour at Esso Refinery, Fawley, by courtesy of Messrs. Babcock & Wilcox Ltd.

Consult...

GENERAL REFRACTORIES LTD

GENEFAX HOUSE SHEFFIELD 10 ENGLAND

Telephone: 31113 (6 lines)

Telegrams: 'Genefax' Sheffld, Telex

METHODS FOR ANALYSIS AND TESTING

(Part I of IP Standards for Petroleum and its Products)

Comprises all the general laboratory methods, including certain small scale rig tests, which form the major proportion of IP Standards.

793 pages Illustrated
Price **42s** post free

Obtainable from

The Institute of Petroleum
61 New Cavendish Street
London, W.1

Methods for Rating Fuels—Engine Tests

(2nd Edition)

(Part 2 of IP Standards for Petroleum and its Products)

Contains revised versions of six of the methods published in the first (1955) edition, and details of the new Extended Research Method (IP 172/60T).

134 pages Illustrated

Price **30s. 0d.** post free

Obtainable from

The Institute of Petroleum
61 New Cavendish Street
London, W.1

ADVERTISERS

(Advertising Agencies in Italics)

Associated Electrical Industries (Manchester) Ltd vi
(The TGA Co. Ltd)
Avery-Hardoll Ltd iii
B. W. Valves Co. Ltd xvii
(Sandbrook, Metcalf & Co. Ltd)
Babcock & Wilcox Ltd . . . xii
(S. H. Wright & Co. Ltd)
Baker Oil Tools Inc. v
(John A. Ripley Advertising Inc.)
British Oxygen Co. Ltd, The . . Jan.
(F. C. Pritchard, Wood & Partners Ltd)
Peter Brotherhood Ltd . . . May
(J. Peers & Associates Ltd)
Robert Cort & Son Ltd . . . Jan.
(Granthams of Reading)
A. F. Craig & Co. Ltd . . . vii
De Havilland Propellers Ltd . . Apr.
(Samson Clark & Co. Ltd)
Dorr-Oliver Co. Ltd . . . . Mar.
Foster Wheeler Ltd xiii
(Wm Hopwood & Co. Ltd)
Foxboro-Yoxall Ltd viii
W. J. Fraser & Co. Ltd . . . May
(Technical Advertising Service)
General Refractories Ltd . . . xv
(John Mitchell & Partners Ltd)
Matthew Hall & Co. Ltd . . . ii
Hughes Tool Co. . . . . Apr.
(Foote, Cone & Belding Ltd)
Intermit Ltd . . . . . Apr.
(Sandbrook, Metcalf & Co. Ltd)
Kellogg International Corporation . xi
(Reynell & Son Ltd)
A. & J. Main & Co. Ltd . . . Mar.
(Hannaford & Goodman Ltd)
Marston Excelsior Ltd . . . xiv
(Clifford Martin Ltd)
Mechans Ltd iv
(James Jack Advertising Ltd)
Newman, Hender & Co. Ltd . . xviii
(Adams Bros. & Shardlow Ltd)
Parsons Powergas i
Procon (Great Britain) Ltd . . . ix
(Tobias, O'Neil & Gallay Inc.)
Pyrene Co. Ltd . . . . . Jan.
(Nelson Advertising Service Ltd)
Sheepbridge Alloy Castings Ltd . . x
(T.B.M. Advertising Ltd)
Simmonds Aerocessories Ltd . . May
Solartron Electronic Group Ltd . . Mar.
(P. A. May & Partners Ltd)
Universal Oil Products Co. . . . May
(Tobias, O'Neil & Gallay Inc.)
Henry Wiggin & Co. Ltd . . . Apr.
(Technical & General Advertising Agency Ltd)

FOR WATER, AIR, OIL, GAS, etc

spot tight closure

that lasts

A revolutionary

PIVOTED DISC VALVE

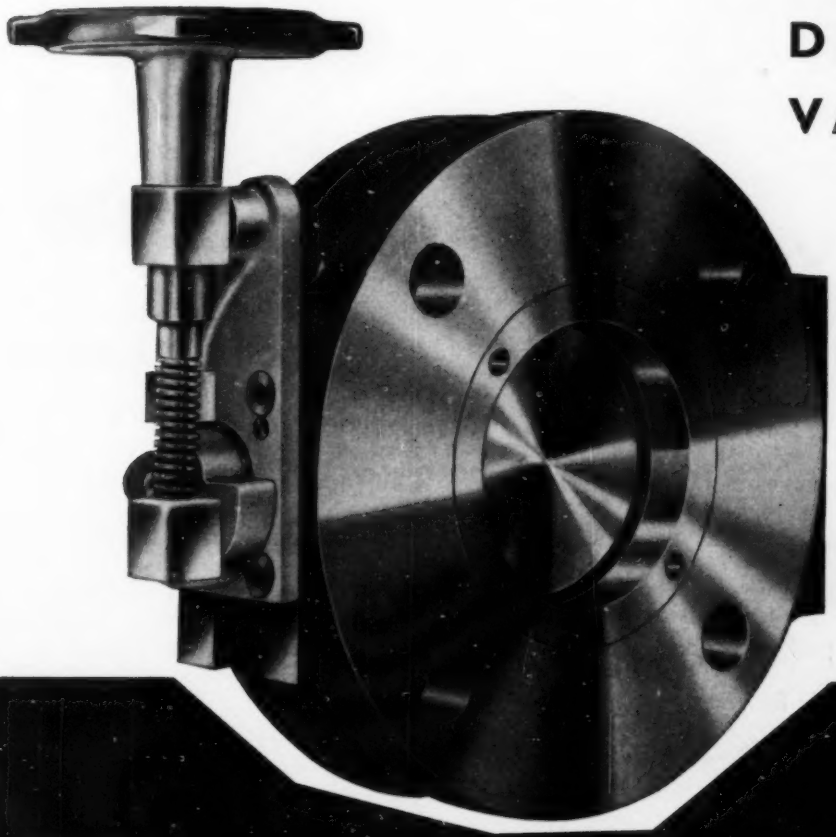

Spot tight closure when a valve is new – is not news. To maintain spot tight closure over long periods of service has been the ambition of makers and users alike.

How this is achieved is fully explained in technical folder W.F.I., which is yours for the asking.

B. W. VALVE CO. LTD

(PROPRIETORS: CHARLES WINN & CO. LTD. BIRMINGHAM 1)

145 GRANVILLE STREET, BIRMINGHAM-1

Telephone: MIDland 7151

The Valve Complex on the Shell-B.P. Petroleum Development Company of Nigeria Limited's discovery well at Oloibiri, Nigeria.

The positive tightness of *Newman-McEvoy* VALVES

Automatic sealing, self-aligning gates and non-distorting seats combine to give unquestionable 100 per cent tightness at all times and in all circumstances. An independent sealing system operated by line pressure on each side of the valve stops leakage as it starts. Stem packings and bearings are easily replaced under full line pressure. Proved under hardest working conditions.

NEWMAN, HENDER & Co., Ltd.

Telephone: Nailsworth 360. Telex: 4375

WOODCHESTER, STROUD, GLOS., ENGLAND.